REPORT NO.
EERC 76-4
SEPTEMBER 1976

EARTHQUAKE ENGINEERING RESEARCH CENTER

EARTHQUAKE INDUCED DEFORMATIONS OF EARTH DAMS

by

NORMAN SERFF
H. BOLTON SEED
F. I. MAKDISI
C.-Y. CHANG

A report on research sponsored by
the National Science Foundation

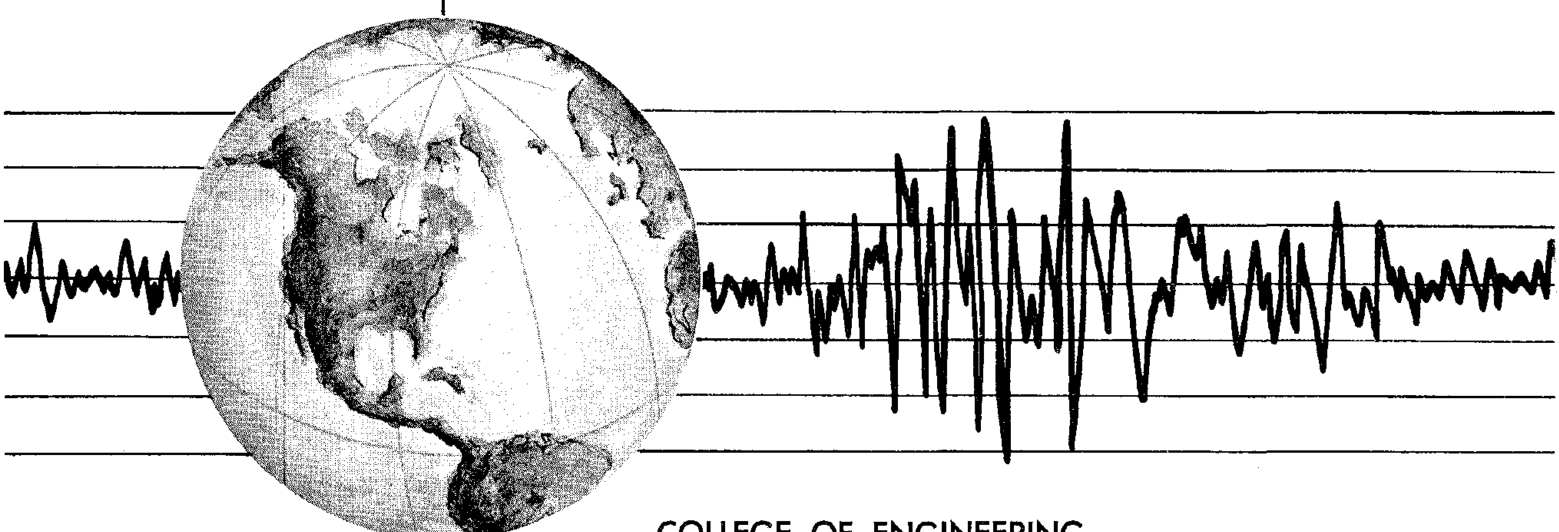

COLLEGE OF ENGINEERING

[illegible]ERSITY OF CALIFORNIA ·

For sale by the National Technical Information Service, U. S. Department of Commerce,

See back of report for up to date listing of EERC reports.

BIBLIOGRAPHIC DATA SHEET	1. Report No. NSF/RA-761770	2.	3. Recipient's Accession No.

4. Title and Subtitle	5. Report Date
Earthquake Induced Deformations of Earth Dams	September 1976
	6.
7. Author(s) N.Serff, H.B. Seed, F.I. Makdisi & C.-Y. Chang	8. Performing Organization Rept. No. EERC 76-4
9. Performing Organization Name and Address Earthquake Engineering Research Center 47th. St. & Hoffman Blvd. Richmond, CA 94804	10. Project/Task/Work Unit No. 11. Contract/Grant No. ENV75-21875
12. Sponsoring Organization Name and Address National Science Foundation 1800 G Street, N.W. Washington, D.C. 20550	13. Type of Report & Period Covered 14.

15. Supplementary Notes

16. Abstracts

A finite element method for calculating the earthquake induced deformations of an earth dam has been developed and applied to a study of the deformations induced in the upper San Fernando Dam during the earthquake of February 9, 1971.

The calculated deformations are in reasonable agreement with the displacements measured after the earthquake, and the calculated stresses and strains explain some of the observed effects of the earthquake on the dam, such as cracking in the outlet conduit and the development of slide scarps on the upstream slope.

The method complements the existing procedure for the dynamic analysis of earth dams proposed by Seed et al (1973), and appears to provide a reasonable basis for determining permanent deformations in earth dams due to earthquake shaking.

17b. Identifiers/Open-Ended Terms

17c. COSATI Field/Group

18. Availability Statement	19. Security Class (This Report)	21. No. of Pages
Release unlimited	UNCLASSIFIED	
	20. Security Class (This Page) UNCLASSIFIED	

Ia

EARTHQUAKE ENGINEERING RESEARCH CENTER

EARTHQUAKE INDUCED DEFORMATIONS OF EARTH DAMS

by

Norman Serff

H. Bolton Seed

F. I. Makdisi

C.-Y. Chang

Report No. EERC 76-4

September 1976

A Report on Research Sponsored by
the National Science Foundation

College of Engineering
University of California
Berkeley, California

Abstract

A finite element method for calculating the earthquake induced deformations of an earth dam has been developed and applied to a study of the deformations induced in the upper San Fernando Dam during the earthquake of February 9, 1971.

The calculated deformations are in reasonable agreement with the displacements measured after the earthquake, and the calculated stresses and strains explain some of the observed effects of the earthquake on the dam, such as cracking in the outlet conduit and the development of slide scarps on the upstream slope.

The method complements the existing procedure for the dynamic analysis of earth dams proposed by Seed et al (1973), and appears to provide a reasonable basis for determining permanent deformations in earth dams due to earthquake shaking.

ACKNOWLEDGEMENTS

The research described in this report was sponsored by the National Science Foundation through Grant No. ENV75-21875 for research on Analysis of the Seismic Stability of Earth Dams. The authors gratefully acknowledge this support.

Appreciation is also expressed to Professor K. L. Lee of the University of California, Los Angeles, and to Professors T. V. McEvilly and W. N. Houston of the University of California, Berkeley, for helpful suggestions during the course of the study.

TABLE OF CONTENTS

TABLE OF CONTENTS cont.

LIST OF TABLES

LIST OF FIGURES

LIST OF FIGURES cont.

Chapter 1

Earthquake Induced Deformations of Earth Dams

Introduction

A possible failure mechanism for an earth dam during an earthquake is the loss of freeboard, and the subsequent overtopping of the dam, caused either by slope failure or settlement of the crest due to strains induced in the dam by seismic inertia forces. Sophisticated methods for assessing the stability of embankment slopes are now available, having progressed from the pseudo-static approach to the currently available comprehensive dynamic analysis which incorporates the varying bedrock acceleration during the earthquake, the change in material properties with the level of strain induced by the earthquake inertia forces, and laboratory tests to determine the resistance of the embankment soils to the cyclic stresses induced by the earthquake motions (Seed et al., 1969, 1973). However, the information gained from such analyses to date has provided only an approximate assessment of the deformations occurring due to seismic force applications (Seed et al., 1973), and while this is all that is required in many cases, it would seem desirable that a general method to predict earthquake-induced deformations be made available to the designer of earth dams.

A comprehensive approach to the determination of earthquake induced deformation of an earth dam must include an analysis of both the initial stresses acting throughout the dam and the superimposed cyclic stresses due to the earthquake, together with a comprehensive program of laboratory testing to determine the strains induced in the soil by the superimposed cyclic stresses. Finally, a system of integrating the strains induced in individual elements to predict the deformed shape of the dam is required.

The initial and simplest approach to this problem was that used by Seed et al. (1973) which simply involved determining an overall average shear strain likely to develop in an extensive zone of an embankment. A second approach was presented by Lee (1974) and applied to the analysis of the deformations of five dams. It involved the concept that seismic deformation of a dam is due to softening of the soil by seismic shaking and the resultant settling of the dam to a new condition compatible with the changed stress-strain properties of the embankment soils.

A different approach is presented in this report. The method integrates the element strains, calculated by the approach advocated by Seed et al. (1973), in a finite element formulation to calculate the deformation of an earth dam due to seismic forces. The method is used to calculate the deformation of the Upper San Fernando dam during the earthquake of February 9, 1971, and shown to give results in reasonable agreement with the measured displacements.

Previous Studies

The earliest analytical technique used to study the dynamic response of earth dams to earthquake ground motion was the vertical shear beam method (Mononobe, Takata & Matamura, 1936; Ambraseys, 1960). Limitations associated with the technique restrict the analysis to dams which can be idealized as homogeneous structures; furthermore only shear mode response is determined, and the effect of the vertical component of the ground motion cannot be included. However, as this analysis considers the dam to be a deformable body, it makes possible the determination of the manner in which the seismic coefficient (representing the earthquake-induced inertia forces) varies with height within the dam as well as with time.

The most versatile analytical tool for dynamic response analysis currently available is the finite element method. It was first applied to the study of the dynamic response of earth dams by Clough & Chopra (1966) and of earth banks by Idriss & Seed (1967). These first studies incorporated a linearly elastic medium with uniform viscous damping. Later modifications of this approach incorporated an equivalent linear analysis, where the shear modulus of the soil and the damping are strain-dependent, and used an iterative procedure to achieve a strain-compatible result (Seed et al., 1973).

Methods of analysis of the deformation of a dam embankment under a combination of sustained and cyclic stresses can be divided into two categories--effective stress analyses or total stress analyses.

In an effective stress analysis the deformation-controlling characteristics of the soil are determined by a suitable program of laboratory tests. These characteristics include the pore-water pressure generation coefficients, the yield stress and the rate of plastic deformation at stresses above the yield stress, and their variation during the earthquake. Incorporating these results in appropriate analytical analysis, the magnitude of the deformation is assessed.

In a total stress analysis, the initial and superimposed cyclic stresses are determined analytically. In the laboratory, samples of the soil in each zone of the dam are consolidated under the initial stress conditions of corresponding elements in the dam, then subjected to uniform cyclic stress histories equivalent to those determined from the response analysis, and the resulting deformations noted.

With either an effective or a total stress analysis, it is necessary to integrate the individual element deformations to obtain the overall deformation of the dam. The results should be the same, whichever method is used, provided the method is correctly applied.

Until recently, methods used by most designers to determine the seismic stability of earth dams employed a limiting equilibrium concept, where the result of the analysis was expressed as a single number, such as a factor of safety against total failure. The effect of the earthquake was simulated by a static force acting on a potential sliding block to represent inertia forces in the dam, and a conventional stability analysis, such as the method of slices, was used to determine the stability of the dam. The procedure was similar to the static stability analysis, though the critical sliding surface was usually different for the two cases. The dam was determined to be stable under the specified loading conditions if the factor of safety was greater than unity. Otherwise, failure was considered total, and no estimate of the actual displacement could be made. The force on the sliding block, which represented the inertia forces, was expressed as a percentage of the weight of the block, and was characterized by a seismic coefficient. The seismic coefficient, which was related to the maximum ground acceleration which could be expected at the site, varied between about 0.05 and 0.15.

This method of analysis assumes that the seismic force on the dam acts in one direction for an infinite time, whereas the actual inertia forces reverse after a short period, approximately 0.25 to 0.5 seconds for most earthquakes, with possibly only minor slumping occurring before the forces reverse, even though the factor of safety may fall below unity for part of the cycle. However, this slumping, cumulative over a number of strong ground motion cycles, could culminate in sufficient loss of freeboard resulting in overtopping of the dam, even though no general slope failure occurs. Thus the deformation of the dam will depend on the duration, as well as the severity, of the ground motion. The time factor cannot be incorporated into limiting equilibrium methods of analysis.

An early attempt to rationalize the pseudo-static approach of applying a static force to simulate earthquake loading was made by Seed & Martin (1966). As a knowledge of the variation of the inertia forces during the earthquake, and the frequency of this variation, would be of more significance to the designer than an equivalent static force, a method to determine these for a given design earthquake was presented.

It was assumed that the random variation of the seismic coefficient could be expressed as a number of uniform cycles at a given frequency. For dams of uniform construction, design curves were presented which gave the characteristics of this uniformly varying seismic coefficient, as a function of the fundamental period of the dam, using the El Centro record as design earthquake.

The technique used to calculate the dynamic response of the dam was the vertical shear beam approach, where the dam is considered as a triangular wedge with linear visco-elastic response characteristics, i.e., the response is controlled by shearing between horizontal slices and the shear stress along any horizontal surface is uniform. This assumption produces shear stresses along a horizontal plane that are an average value, the actual values being higher near the center of the dam and lower near the slopes. The material properties of the dam--the shear modulus, damping and density--were assumed constant throughout. Although the method does not allow for absorption of energy due to plastic deformation, this could be simulated by an increase in the damping ratio of the materials.

A theoretical solution for the fully recoverable horizontal displacement with time was programmed and used to determine the displacement of each element in the dam; from the displacements the shear strain and, subsequently, the shearing force records are calculated.

The calculation of the varying seismic coefficient is simplified by assuming that the sliding mass is a triangular wedge with a horizontal base. The time-varying record of the average value of the seismic coefficient acting over the height of the wedge, for the applied earthquake, is calculated by determining the varying shear force acting on the base of the wedge, then dividing by the mass of the wedge to give the average horizontal acceleration which would produce the same shearing force.

Since laboratory tests are usually performed using uniform stress cycles, the random variation with time of the seismic coefficient thus calculated was represented by an equivalent number of constant amplitude cycles, an equivalent maximum seismic coefficient, and a corresponding predominant period.

It was found that the equivalent seismic coefficient increases as potential sliding wedges at higher elevations within the dam are considered, and decreases, for any given section of the dam, as the height of the dam increases. In the earlier pseudo-static approach, the seismic coefficient was usually taken to be constant for all dams in a given area, and throughout the height of any embankment. Only the horizontal component of the ground acceleration is used in the analysis, a restriction of the shear beam approach, but the effect of vertical acceleration could be included by inclining the direction of the resultant force acting on the sliding mass. This method of approach was subsequently extended to potential sliding masses with other shapes than triangular wedges by Ambraseys and Sarma (1967).

The first method of analysis aimed at calculating the permanent deformations in dams, was proposed by Newmark (1965) and successfully applied by Goodman and Seed (1966) to the analysis of the dynamic behavior of model sand embankments on a shaking table.

Newmark's approach is based on the concept of a yield acceleration, in which no movement takes place along a potential sliding surface until the acceleration of the sliding mass exceeds some limiting value. Using a procedure analogous to that of analyzing the movement of a sliding block on an inclined plane, the time record of acceleration of the sliding mass, which is calculated using a method such as the elastic shear wedge theory, is compared with the yield acceleration. Whenever the acceleration of the mass exceeds the yield acceleration, a process of double integration is used to calculate the progressive down-slope displacement (Fig. 1.1).

Difficulties in applying this procedure may arise in the determination of the yield acceleration for saturated soils. The yield acceleration is a function of the soil strength, which in turn is a function of the effective stress and thus dependent on the transient pore-water pressures generated during the earthquake. At the present time, it is not possible to predict, in general, the variation of the pore-water pressure during an earthquake. However, Martin et. al. (1975) have developed a procedure which allows the calculation of the pore water pressure history for the case where no initial shear stress acts, and this method might ultimately be extended to embankment problems. Furthermore, data from undrained cyclic load tests may be interpreted to determine an effective yield stress for use in this type of analysis.

The concept of deformations caused by accelerations in excess of the yield acceleration (Newmark's method) is primarily applicable to cases where

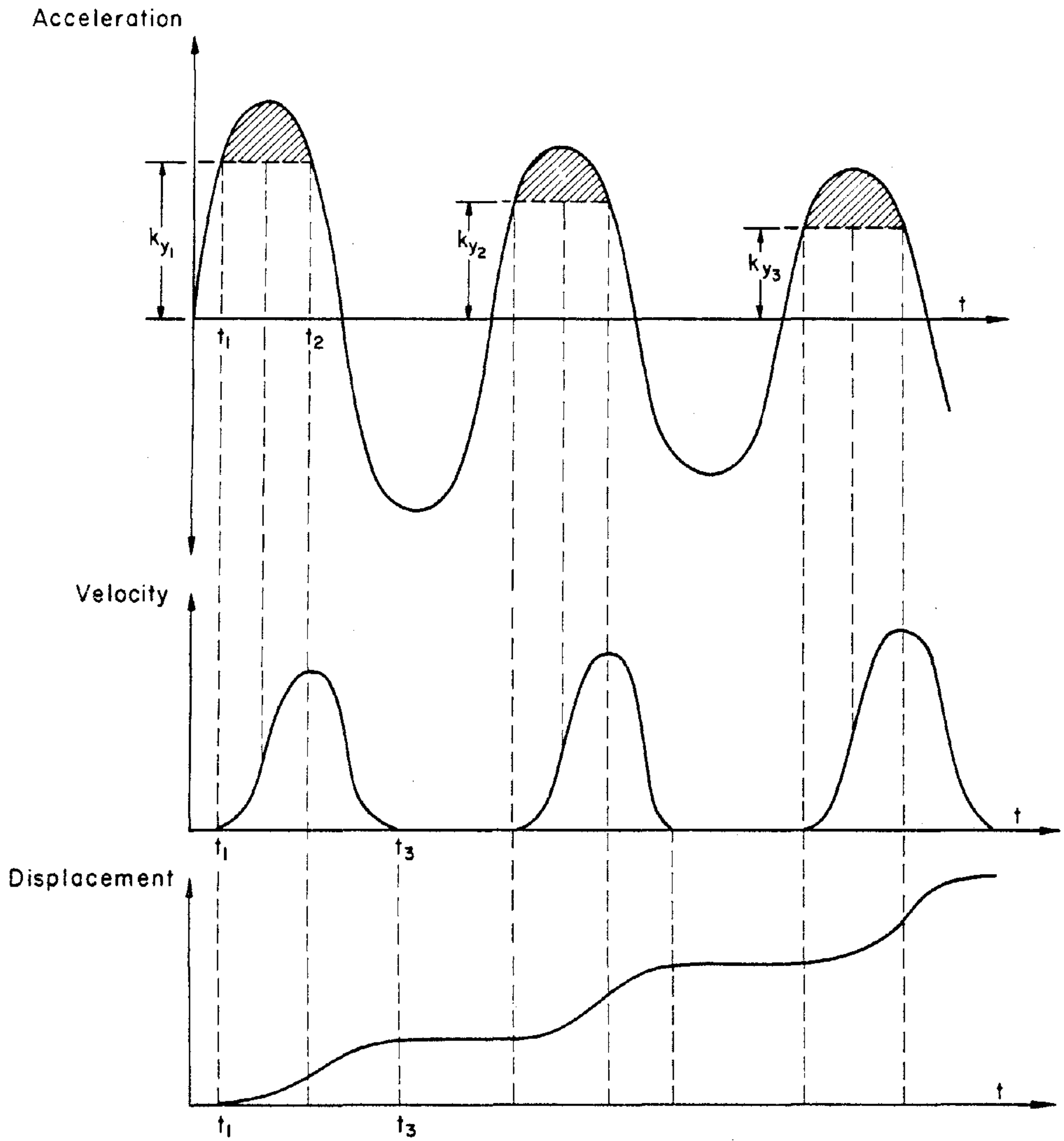

FIG. 1.1 INTEGRATION OF ACCELEROGRAMS TO DETERMINE DOWNSLOPE DISPLACEMENTS

the movement of slopes occurs along well-defined failure zones. Such a failure mechanism occurs in dense, cohesionless soils and in cohesive soils. Experimental evidence has shown (Seed & Goodman, 1964) that in dry, dense, uniform slopes, subjected to a fairly uniform acceleration, failure occurs by mass sliding of a thin surface zone, making it a problem amenable to solution by Newmark's method. Movement downslope occurs during each cycle of acceleration where inertia forces are large enough to cause a temporary instability. Movement stops when the force is reversed, and the overall effect is a progressive downstream movement, causing a flattening of the slope at the toe and settlement of the crest.

Shaking table model tests (of dry sand embankments) were conducted by Goodman and Seed (1966) and deformation was analyzed by Newmark's approach. The mechanism of failure observed was a slide in a thin surface layer, similar to that reported previously. A formula, based on the strength of the soil, was developed to calculate the yield acceleration. By allowing for the decrease of soil strength, and hence yield acceleration, with increasing slope displacement, reasonable agreement was found between measured and calculated displacements.

However, in other soils and particularly saturated cohesionless soils, the shear stress may exceed the yield stress over a large part of the dam, and hence extensive shear zones will exist. In such cases, an analytical approach is required which can determine deformations over a wide zone and integrate them to give the overall deformation of the embankment.

An alternative method for the seismic design of earth dams, which followed the concept first proposed by Newmark (1963) that the stability of an embankment during an earthquake should be assessed on the basis of the deformations produced, was presented by Seed (1966), and has been used to analyze the behavior of the Sheffield Dam in the 1925 Santa Barbara earthquake (Seed et. al., 1969) and the Dry Canyon Dam during the 1952 Kern County earthquake (Lee and Walters, 1973). This method incorporated the consideration of the history of the stresses developed throughout the embankment, and the behavior of samples tested in the laboratory under similar stress conditions. The method is primarily applicable to conditions where drainage cannot occur during the earthquake, such as in saturated fine-grained soils, conditions usually found in the upstream slope of an earth dam.

As a preliminary step, the initial stress conditions acting along the assumed failure surface are determined. The method of slices, using the procedure of Lowe and Karafiath (1959), was used to determine the normal and shear stresses at the base of each slice, using drained soil strength data. From a Mohr circle, the corresponding principal stresses are found. In the laboratory, specimens of soil, compacted at field water content to field density, are consolidated under a range of confining pressures and stress ratios which encompass the range found in the dam.

Cyclic triaxial tests are then performed on the consolidated specimens to find the cyclic deviator stress causing failure. In the tests, only the major principal stress is varied. This test limitation is of minor importance as the confining pressure has no effect on the stress-strain relationship of a saturated soil.

The data from the laboratory tests is presented as a relationship between the cyclic shear stress along the failure plane causing failure and the normal stress on the failure plane before the earthquake. Strength curves are presented for a range of consolidation ratios.

The consolidation ratio and the normal stress on the assumed slip surface before the earthquake are known from the static analysis. Hence, the maximum cyclic shear stress that can be developed at the base of each slice without causing excessive deformation is found from the laboratory data. By a method of analysis similar to that used to determine the initial static stresses, but including the maximum equivalent cyclic inertia force, as determined by an analysis such as that of Seed and Martin (1966), and acting in the direction to cause an increase in shear stress, trial values of a factor of safety are tried until the force system acting on the slices is in equilibrium. Undrained soil strength parameters are used.

The analysis is repeated for a range of potential sliding surfaces until the surface with the minimum factor of safety is found.

For some soils no well-defined failure takes place as strain increases. Strain, and consequently deformation of the dam, increase throughout the earthquake. As no analytical procedure existed at the time to relate axial strain of laboratory samples to deformations in the dam, empirical relationships were required. A discussion of the deformations of the Otterbrook dam, under static loading conditions, and of the corresponding axial strains of laboratory samples was presented (Seed, 1966). Recommendations on the relationship between axial strain of laboratory specimens and maximum tolerable field deformations are presented as an aid to the design engineer.

Subsequently this method of analysis was modified to provide a means for evaluating the strains developed throughout the cross-section of a dam (Seed, Lee and Idriss, 1969; Seed, Lee, Idriss and Makdisi, 1973). The laboratory procedure is similar to that proposed by Seed (1966), but the calculation of stresses is made by the finite element approach, using strain-dependent soil properties. As it is the basis upon which the deformations analysis presented in this report is founded, a full description of the method is given in the following chapter.

Chapter 2

Static and Dynamic Analyses of Earth Dams

Introduction

The design of an earth dam to withstand safely the effects of earthquake ground motions is an important engineering problem in seismically active areas of the world. The ground accelerations during a moderate to strong earthquake can cause large inertia forces throughout the dam. These forces, which reverse in direction with each cycle of ground motion, induce cyclic stresses, and consequently strains, throughout the embankment. The resulting permanent deformation is evidenced by slumping and sometimes cracking of the dam. If the strains are severe enough, or the slumping large enough, the dam may fail due to slope instability or overtopping.

The analysis of the stresses and strains induced in the dam by the earthquake, and the determination of the resulting deformations, is a complex and difficult problem. Before the development of the finite element method (Turner et al., 1956), its subsequent application to the dynamic response of earth dams (Clough and Chopra, 1966), and a means of interpreting the induced stresses in the light of the results of laboratory tests on the soil to give an overall picture of the behavior of the dam (Seed, 1966), no satisfactory solution to the problem existed.

To render the analysis more tractable, a number of simplifying assumptions are generally made. Foremost among these is the representation of the dam, a three-dimensional structure, by a two-dimensional transverse cross-section in which a state of plane-strain exists. For the dynamic analysis of an embankment this assumption is usually necessary for reasons of analysis cost and computer capacity. However, as coupling between transverse and longitudinal motions in the dam is believed to be small, the response calculated by the plane-strain analysis will usually be sufficiently accurate for practical purposes.

In the finite element technique, the dam, a continuous structure, is represented by an assemblage of elements, usually either triangular or quadrilateral, connected only at their nodes. A relationship between nodal displacement and distribution of strain within the element is assumed, and based on this relationship and the stress-strain characteristics of the soil within the element, a stiffness is calculated for each element and then summed to give an overall stiffness for the dam which relates the forces acting within and on the dam to the nodal displacements. These forces, due to gravity, seepage, or inertia, are distributed to act only at the element nodes. From the nodal displacements, element strains and stresses are easily calculated. In a dynamic analysis, the ground acceleration at specific time intervals is used to calculate inertia forces and an analysis is run for each time step to produce stress histories for each node.

For a comprehensive analysis of the response of an earth dam to an earthquake, it is necessary to perform first a static stress analysis to determine the stress distribution throughout the dam before the earthquake; then a dynamic analysis to determine the history of the varying stresses during the earthquake; and finally a laboratory study to determine the behavior of the material of the dam under conditions of cyclic stress. A knowledge of the initial static stresses is required since the behavior of soil under dynamic stresses depends on the stresses under which the soil was consolidated. Cyclic stresses applied in the laboratory are uniform in frequency and amplitude and so the stress histories for the elements of the dam must be converted to an equivalent number of uniform stress cycles in order to estimate behavior of the various elements of the dam from the laboratory tests. The following sections of this chapter discuss more fully the steps of the analysis outlined above, as first proposed by Seed et al, 1969.

Static Stress Analysis

Although it is possible to estimate the static stress distribution in a dam by approximate means (Lee and Idriss, 1975) the ultimate value of the complete stability analysis of the dam will depend on the accuracy with which each step is performed. The best method to date for calculating stresses is the finite element technique, and the most comprehensive approach using the finite element technique is that presented by Ozawa and Duncan (1973) and Wong and Duncan (1974) in which the method of construction of the dam is simulated by a progressive analysis where an additional layer of elements is added at each step. The nonlinear stress-strain properties of soils are also included in the analysis.

The number of layers used in the analysis need not be equal to the actual number of layers used in the construction of the dam. Approximately eight to ten layers are sufficient for a large dam. Though this type of analysis is necessary if an accurate measure of deformations during construction is required, the stresses calculated are not very different from an analysis using only one layer, i.e., a gravity turn-on analysis (Lee and Idriss, 1975). Displacements calculated from an analysis in which the dam is built up in layers are maximum near mid-height on the center line and smaller near the top and base of the dam, similar to the displacement pattern measured in the field. The displacements calculated by a gravity turn-on analysis are a maximum at the top or the dam and smallest at the base (Clough and Woodward, 1966).

The method used (Ozawa and Duncan, 1973) to represent nonlinear stress-strain curves is that proposed by Kondner (1963). The stress-strain curve is assumed to be a hyperbola, expressed as:

$$(\sigma_1 - \sigma_3) = \frac{\varepsilon_a}{a+b\varepsilon_a} \qquad (2.1)$$

where a, b are empirical constants;

ε_a is the axial strain; and

σ_1, σ_3 are principal stresses.

The formulation in Equation (2.1) represents the nonlinear stress-strain curve for the confining pressure of σ_3. In order to determine the values of the parameters 'a' and 'b', the equation is written in the following linear form:

$$\frac{\varepsilon_a}{(\sigma_1-\sigma_3)} = a + b\varepsilon_a \qquad (2.2)$$

The graphical representation of both equations is shown in Fig. 2.1. It can be seen from Fig. 2.1b that the parameters 'a' and 'b' are respectively the intercept and slope of the straight line. It can be seen from Fig. 2.1a that the value of the asymptotic stress difference $(\sigma_1-\sigma_3)_{ult}$ is always greater than the stress difference at failure, $(\sigma_1-\sigma_3)_f$. These two values are related as follows:

$$(\sigma_1-\sigma_3)_f = R_f \, (\sigma_1-\sigma_3)_{ult} \qquad (2.3)$$

where R_f is a factor called the failure ratio. The failure ratio is always less than unity, and is a measure of how well the stress-strain curve for a

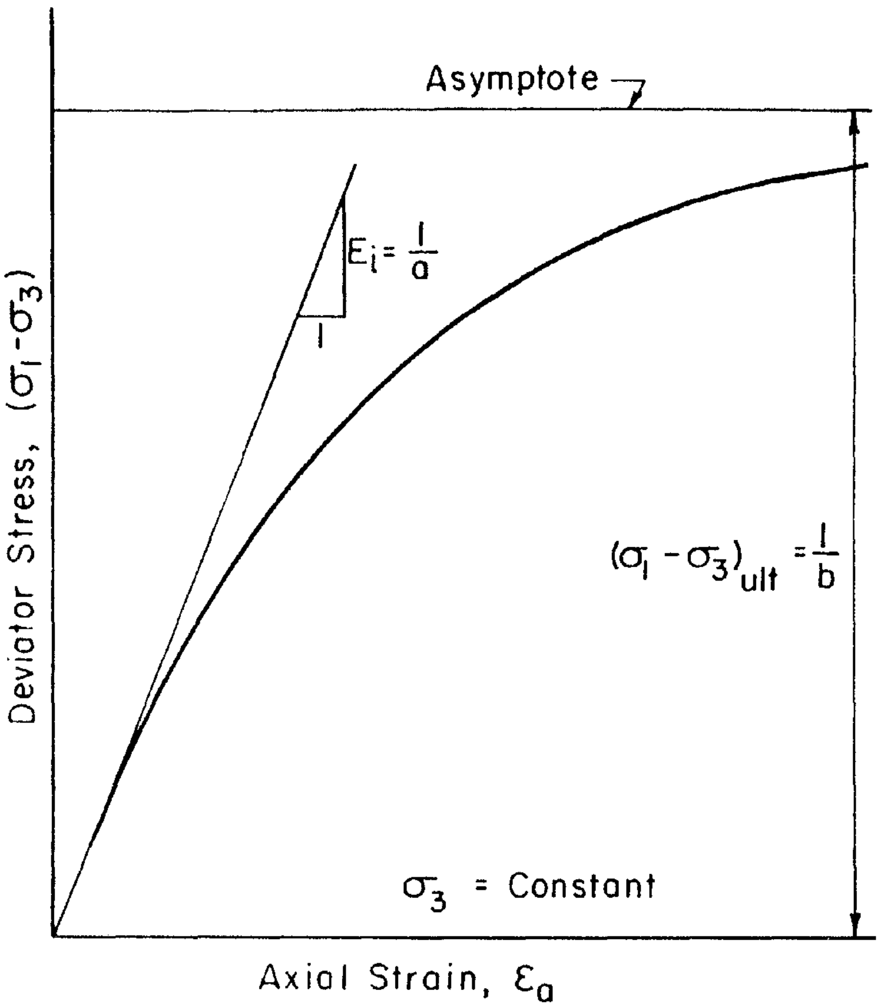

FIG. 2.1a HYPERBOLIC REPRESENTATION OF STRESS-STRAIN CURVE

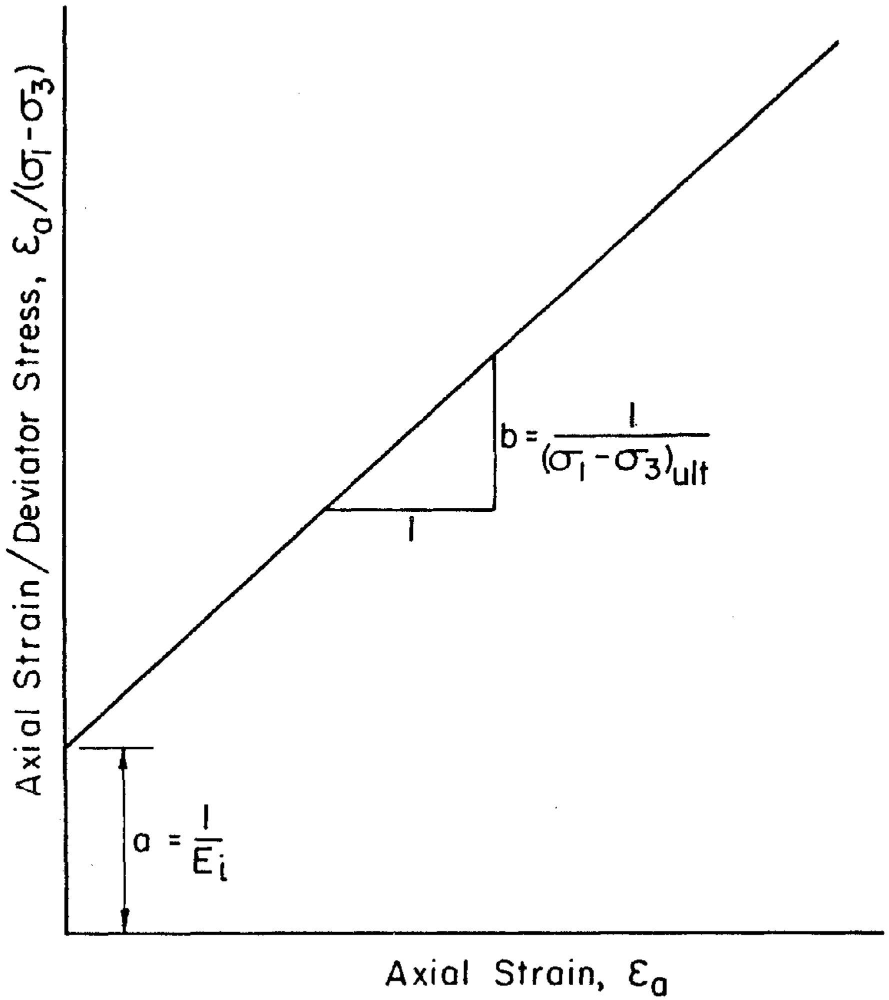

FIG. 2.1b LINEAR TRANSFORMATION OF HYPERBOLIC STRESS-STRAIN CURVE

soil approaches a true hyperbola; a value of R_f equal to unity corresponds exactly with a hyperbola.

As the stress-strain characteristics of a soil depend on the confining pressure (σ_3), the value of the initial tangent modulus, E_i, as shown in Fig. 2.1a, must be related to the confining pressures. The relationship used by Kulhawy et al. (1969) is that proposed by Janbu (1963):

$$E_i = K\, P_a \left(\frac{\sigma_3}{P_a} \right) \tag{2.4}$$

where K is a modulus number;

n is an exponent determining the rate of change of E_i with σ_3 (both K and n are pure numbers); and

P_a is the atmospheric pressure in the same units as σ_3.

The values of K and n are found by plotting the values of E_i, determined from a range of tests at differing confining pressure, against the confining pressure, on a log-log scale (Fig. 2.2) and fitting a straight line to the data.

To calculate the value of the failure ratio, R_f, the strength at failure is expressed as follows (Mohr-Coulomb relationship):

$$(\sigma_1 - \sigma_3)_f = \frac{2c \cos\phi + 2\sigma_3 \sin\phi}{1 - \sin\phi} \tag{2.5}$$

and

$$R_f = \frac{(\sigma_1 - \sigma_3)_f}{(\sigma_1 \ \sigma_3)_{ult}} \tag{2.6}$$

Thus we have a method of relating stress to strain for a given value of confining pressure, using the hyperbolic relationship discussed, by means of the parameters K, n, R_f, c and ϕ.

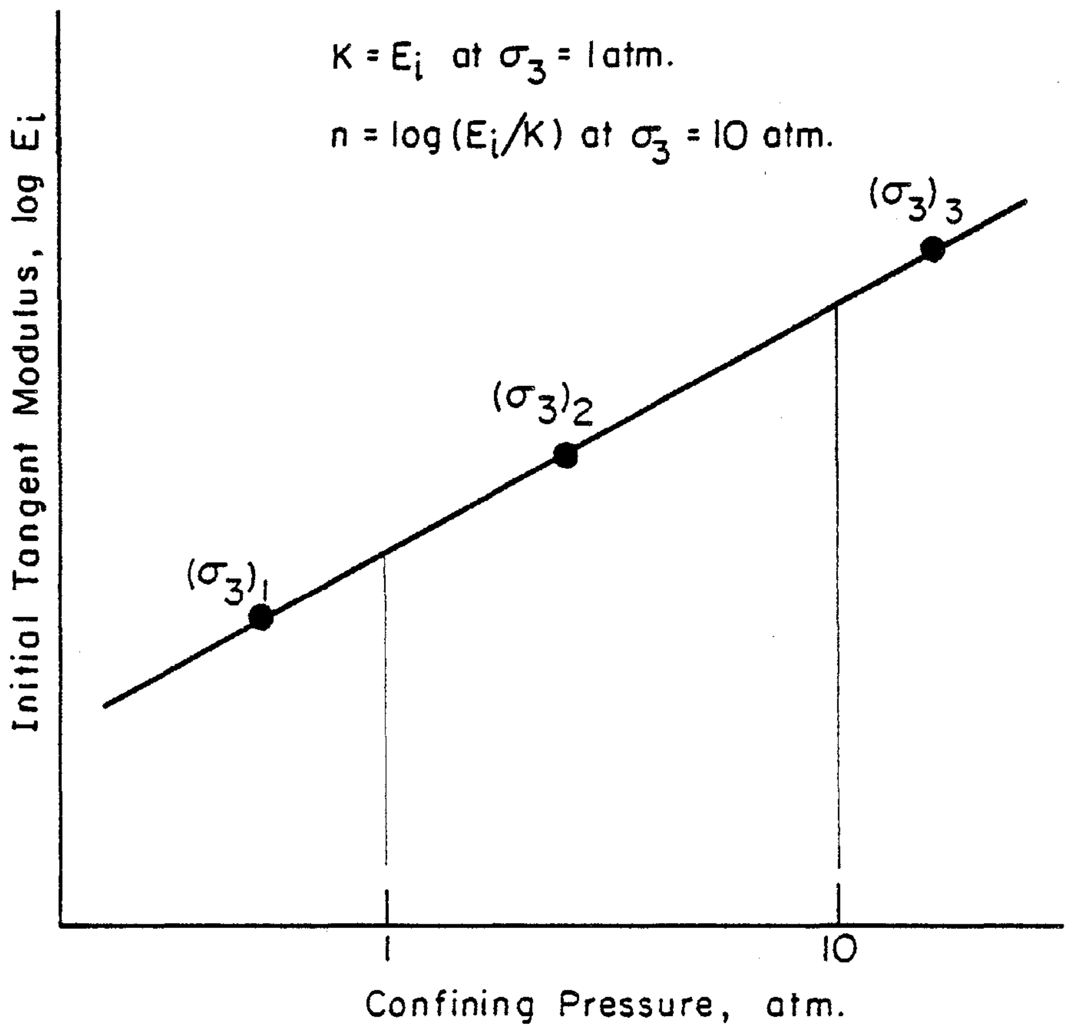

FIG. 2.2 RELATIONSHIP BETWEEN INITIAL TANGENT MODULUS AND CONFINING PRESSURE

It is possible to perform a nonlinear analysis by applying loads in increments, using the relationships derived above, using an expression to determine the tangent modulus for any point on the stress-strain curve:

$$E_t = \left[1 - \frac{R_f(1-\sin\phi)(\sigma_1-\sigma_3)}{2c\cos\phi + 2\sigma_3\sin\phi}\right]^2 KP_a\left(\frac{\sigma_3}{P_a}\right)^n \tag{2.7}$$

The above expression for E_t follows from the previous equations. Since E_t is expressed only in terms of stress, and not strain, an analysis may be performed with any arbitrary initial state of stress.

The parameters are found from appropriate laboratory triaxial tests. For the conditions existing in the dam before the earthquake, consolidated drained tests are used. If no tests results are available, typical values of the nonlinear parameters are given in tabular form by Kulhawy et al. (1969).

In a finite element analysis, it is necessary to relate stress to strain by a generalized Hooke's Law. For isotropic materials, two independent parameters, usually Young's modulus (E) and Poisson's ratio (ν) are used. Hence a nonlinear, stress dependent value of Poisson's ratio is required. The formulation used by Kulhawy is as follows:

$$\nu_t = \frac{G - F\log(\sigma_3/P_a}{\left[1 - \dfrac{d(\sigma_1-\sigma_3)}{KP_a\left(\dfrac{\sigma_3}{P_a}\right)^n\left\{1 - \dfrac{R_f(\sigma_1-\sigma_3)(1-\sin\phi)}{2c\cos\phi+2\sigma_3\sin\phi}\right\}}\right]^2} \tag{2.8}$$

where ν_t is the tangent Poisson's ratio, and

G,F,d are nonlinear Poisson's ratio parameters which are found from a series of triaxial tests.

The Hooke's law relationship used in the analysis is written in terms of the bulk modulus (K) and shear modulus (G), as proposed by Clough and Woodward (1967). This makes it possible during the analysis to more closely model the behavior of actual soils after failure by reducing the value of G to zero, but maintaining the value of K at its pre-failure value. K and G are calculated from the relationships

$$K = \frac{E_t}{2(1+\nu)(1-2\nu)} \qquad (2.9)$$

$$G = \frac{E_t}{2(1+\nu)} \qquad (2.10)$$

A program to perform this static stress analysis has been written by Kulhawy, titled LSBUILD, and later modified by Ozawa (1973) and renamed ISBILD.

Dynamic Stress Analysis

As a comprehensive analysis of a dam involves a knowledge of the stresses induced in the embankment by the earthquake, a method of calculating these stresses is required. To perform such an analysis, both the dynamic soil properties of the dam and foundation and the acceleration history of the bedrock during the earthquake must be known or estimated. Dynamic soil properties are obtained from field tests, laboratory tests, or from a knowledge of the properties of similar soils. The acceleration record for the bedrock can be an artificially generated record or an accelerogram recorded at a similar site. Analysis of the dynamic stresses in a dam have, in the past, ranged from the shear beam approach in which only shear stresses are calculated, to the finite element modal analysis approach in which the modulus of the soil varies throughout the dam but the damping is constant, to the current variable damping finite element method.

The remainder of this section is divided into two parts: a discussion of the design earthquake and a discussion of the dynamic finite element analysis.

Design Earthquake

Although the records of earthquakes exhibit many features, for engineering design purposes three of these may be considered to characterize an earthquake record:

1. Maximum peak acceleration, a_{max};
2. Predominant period, T_p; and
3. Number of significant cycles, N.

The maximum peak acceleration is related to both the Richter magnitude (M) of the earthquake and the distance from the causative fault. The predominant period, T_p, is the period of the most commonly occurring frequency in the record, and is usually taken as the period of the maximum peak of the acceleration spectrum. The predominant period is also related to magnitude and distance and increases with distance from the source of energy release. The number of significant cycles, N, is the number of uniform average cycles which is equivalent to the actual acceleration record. A study by Seed, Idriss and Kiefer (1969) describes a procedure for selecting a design earthquake. Data on the variation of a_{max} and T_p with magnitude and distance, and the variation of N with magnitude, are presented. Before a design earthquake can be selected for a particular site, a seismicity study of the area must be made to estimate the distance to nearby faults and the maximum magnitude earthquake that could occur on each fault. The next step is to select rock motion records for earthquakes of similar magnitudes (in order that the significant number of cycles is appropriately represented) and modify the peak acceleration and predominant period. These records are digitized for use with computer programs, and modification of the predominant period is simply a matter of changing the time step. After modification of a record, an appropriate base line correction such as that proposed by Berg and Housner (1961) should be made.

During an earthquake, the motion of the underlying bedrock is transferred to the dam by means of seismic waves propagating upward through the foundation and embankment. In most dynamic analyses of dams, the bedrock below the dam is considered rigid, although the earthquake motion is due to traveling seismic waves propagating outward from the hypocenter. In a study of the response of earth dams to traveling seismic waves, Dibaj and Penzien (1967) showed that if the ratio of base width of the dam, or dam and foundation system, to the shear wave velocity in the bedrock is less than 0.2 seconds, i.e.,

$$\frac{B}{Vs} \leq 0.2 \text{ seconds} \tag{2.11}$$

then the dynamic response of the dam to traveling waves will be similar to the response to rigid base motions. Assuming a shear wave velocity in the bedrock of 8000 fps, a rigid base motion analysis will be sufficiently accurate if the dam is no more than about 300 feet high.

Finite Element Analysis

The two requirements for a dynamic analysis are the base rock motion and the material dynamic properties. Selection of the design base rock motion is discussed in the previous section. The dynamic soil properties are characterized by the shear modulus and damping characteristics. By using strain-dependent values of the modulus and damping, and analyzing the dam in successive iterations until a strain compatible result is obtained, the nonlinear characteristics of the soils are incorporated into the analysis. The variation of shear modulus and damping with shear strain for sands and saturated clays is shown in Fig. 2.3. These curves are from a study of the dynamic properties of soils by Seed and Idriss (1970). For soils which are a combination of materials, some judgment is required in selecting the curve to be used. Alternatively, a series of tests may be performed on the soil to produce a curve which can then be incorporated into the analysis.

The modulus of cohesionless soils also varies with mean effective confining pressure:

$$G = 1000\ K_2(\sigma'_m)^{1/2} \tag{2.12}$$

where: G is the shear modulus in psf;

K_2 is a parameter, and is a function of the soil type, relative density and shear strain;

σ'_m is the mean effective pressure in psf.

At very low strains, in the order of 10^{-4} percent, the value of K_2 is a maximum. Once the value of $(K_2)_{max}$ is known, the curve in Fig. 2.3a may be used to calculate the value of K_2, and hence G, for any level of strain. Typical values of $(K_2)_{max}$ for various cohesionless materials have been published. Alternatively, the value can be calculated from the results of shear wave velocity tests:

$$V_s = \sqrt{\frac{G_{max}}{\rho}} \tag{2.13}$$

where: V_s is the shear wave velocity in fps;

ρ is the mass density (density/g);

G_{max} is the shear modulus at low strains.

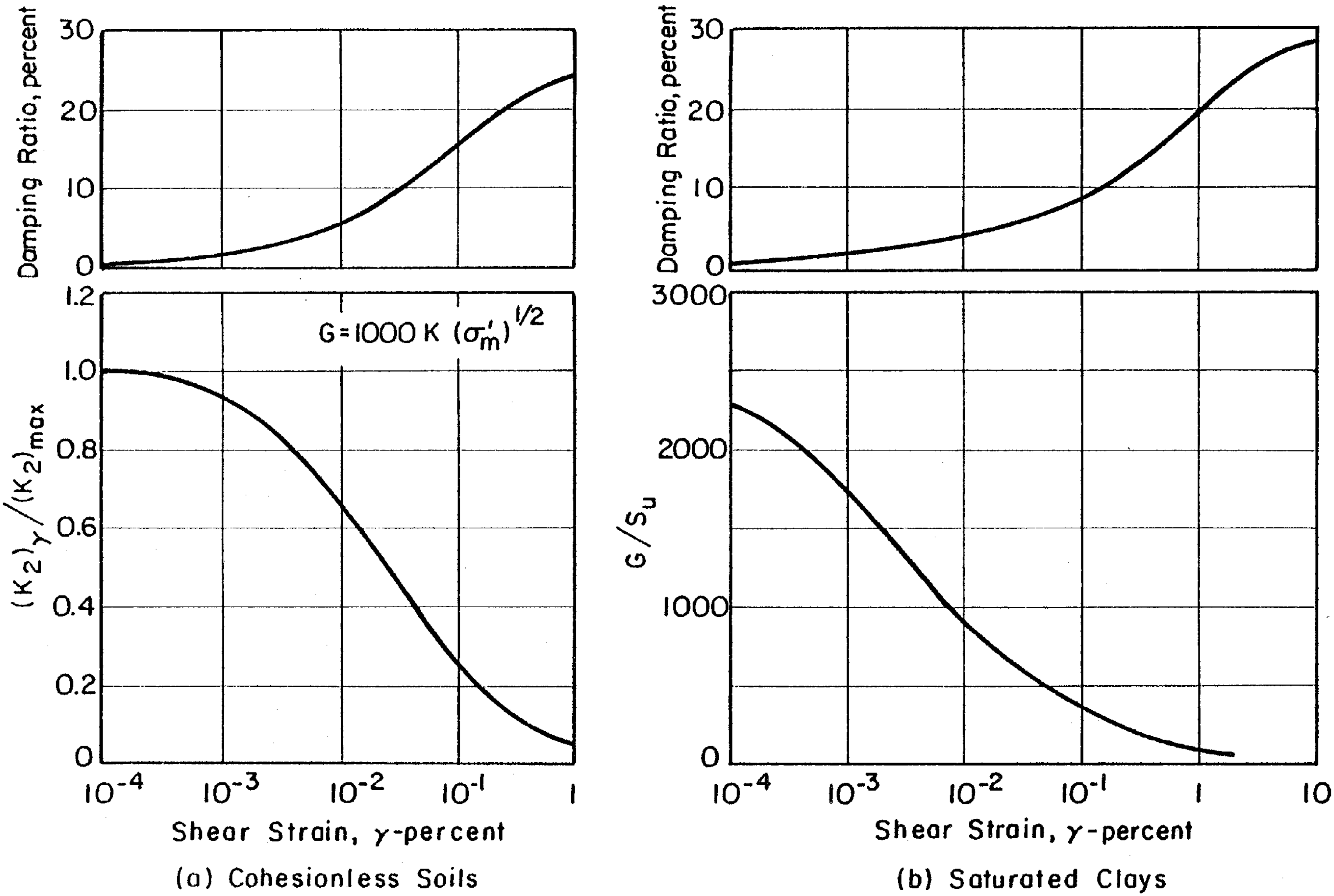

FIG. 2.3 AVERAGE SHEAR MODULI AND DAMPING CHARACTERISTICS OF SOILS (After Seed and Idriss, 1970)

Once the mean effective stress at the position of the measurement of V_s is calculated, the value of $(K_2)_{max}$ is easily found by the relationship in equation (2.12). The value of $(K_2)_{max}$ can also be found in the laboratory, e.g., by a resonant column test.

The shear modulus of a saturated cohesive soil varies with the undrained shear strength (s_u) and the shear strain, as shown in Fig. 2.3b.

The finite element analysis starts with the idealization of the cross-section. The finite element mesh should extend in the foundation sufficiently far upstream and downstream so that waves reflected from the boundaries are damped out and do not influence the solution. The size of the elements in the mesh is also important as this influences the maximum frequency which can be transmitted (Lysmer et al., 1974). If the dynamic analysis is by the step-by-step method, the element size also affects the stability of the solution, since if small elements are used a small time step is also necessary to insure stability. In general, the time step of the analysis should be less than the minimum shear wave travel time across any element of the mesh. It is convenient to use the same mesh for the static and dynamic analysis since the initial stresses acting in an element are used to determine the effect of the dynamic stresses on the behavior of the element. However, interpolation can be used to determine the static stresses in the elements of the dynamic mesh if a different mesh has been used in the static stress analysis.

It is usual in a dynamic analysis of an earth dam to apply only the horizontal component of the earthquake record. Laboratory tests have shown that volume changes, and associated pore pressure increases, caused by vertical motions are small compared to those caused by shear deformations. Also, the shear stresses induced in the dam by vertical motions are much less than those due to horizontal motions.

The maximum value of K_2 or the modulus, G, for a cohesionless soil, or the undrained shear strength for a cohesive soil, together with soil properties such as density, are supplied as input to the analysis. As the seismic response analysis is an iterative procedure which produces a strain-compatible result, a first approximation of the modulus and damping is also required.

Some areas of the dam may fail during the earthquake, thus causing the stress in surrounding areas to increase. These areas may in turn fail, redistributing the stress to neighboring zones. This type of progressive failure can be simulated in the analysis by running the analysis for a section of the earthquake, obtaining a strain-compatible result, and setting the modulus of any failed elements to a very low value. The analysis is then continued for following sections of the earthquake record until the analysis is completed. An element is said to have failed if a sample tested in the laboratory under similar consolidation stresses and cyclic stress fails, either through liquefaction or excessive strain. The method of laboratory testing is described in the following section.

The response of the dam found by the dynamic analysis consists of the acceleration history at each node of the mesh, and the stress histories for each element. To make a comparison between the behavior of laboratory samples and elements in the dam, these stress histories are expressed as an equivalent series of uniform stress cycles by an appropriate weighting of the ordinates of the stress history based on the results of laboratory cyclic test data, as proposed by Seed and described by Seed et al. (1975) and by Lee and Chan (1972). The uniform cyclic stress history is then used to determine the behavior of the dam.

Two types of programs are currently available to perform the dynamic analysis. The step-by-step direct integration procedure of Wilson and Clough (1962), incorporating Rayleigh-type damping, is employed by the program QUAD4 (Idriss et al., 1973). This form of damping damps out all but the lowest frequencies (in general there is little response above approximately 4Hz), but as most of the response of earth dams is in the lower modes this is not a serious drawback. The method also has stability problems. However, QUAD4 in general gives good results when applied to the analysis of earth dams, and has been used successfully on many analyses. The second method is an analysis in the frequency domain, and is employed by the program LUSH (Lysmer et al., 1974). This program can handle higher frequencies than QUAD4, being limited only by the time step of the digitized input acceleration and the element size in the finite element mesh. In practice, the full range of frequencies for which a solution is possible is not of interest in engineering problems, and the analysis is run only up to a selected maximum frequency.

Cyclic Load Tests

Cyclic load tests are usually performed by the triaxial method, although the cyclic simple shear test may simulate more accurately the field conditions in a dam during an earthquake. In the triaxial test, failure usually takes place along planes oriented at an angle of $45 + \phi/2$ degrees to the direction of the major principal plane, which in the finite element analysis of a dam deformation is usually considered to be along horizontal planes (Seed et al., 1973). The cyclic strength data from the triaxial test can be readily manipulated so that a direct comparison can be made between triaxial and simple shear or assumed field conditions (Peacock and Seed, 1968).

The data recorded during the cyclic triaxial test are the axial strain and the pore-water pressure vs. the number of stress cycles. Samples are consolidated under a range of consolidation ratios (K_c) and tests are run for a number of values of cyclic deviator stress (σ_{dp}) for each value of confining pressure (σ_{3c}). From the curves of axial strain (ε_a) vs. number of stress cycles (Fig. 2.4a), curves of σ_{dp} vs. N are drawn for a range of values of ε_a (Fig. 2.4b). Curves are produced from these showing the relationship between σ_{dp} and N for a range of K_c values, one set for each combination of ε_a and σ_{3c} (Fig. 2.5a). Each curve is for a specific value of K_c and σ_{3c}.

The result of the finite element dynamic analysis is to determine the stress history of each element, expressed as an equivalent number of uniform stress cycles. This number of cycles, N_{eq}, is assumed to be the same for all elements. Using a value of N equal to N_{eq}, curves are produced showing the relationship between σ_{dp} and σ_{3c} for a range of K_c values. These curves are derived from Fig. 2.5a. Sets of curves are produced for different values of ε_a (Fig. 2.5b).

To make it possible to apply the results of the laboratory testing to the analysis of the dam, it is necessary to know the value of the cyclic shear stress along the failure plane of the triaxial sample. Assuming that the failure plane is horizontal in the field, and is oriented at an angle of 45 + ϕ/2 degrees to the direction of the minor principal stress in the laboratory, the Mohr circle construction shown in Fig. 2.6 can be used to find this shear stress, termed τ_{cyclic}. In cases of isotropic consolidation (K_c = 1) it has been shown that the cyclic shear stress on the failure plane is about 60 percent of the maximum shear stress in the triaxial test (De Alba et al., 1975). For values of $K_c \geq 1.5$, τ_{cyclic} it has been found

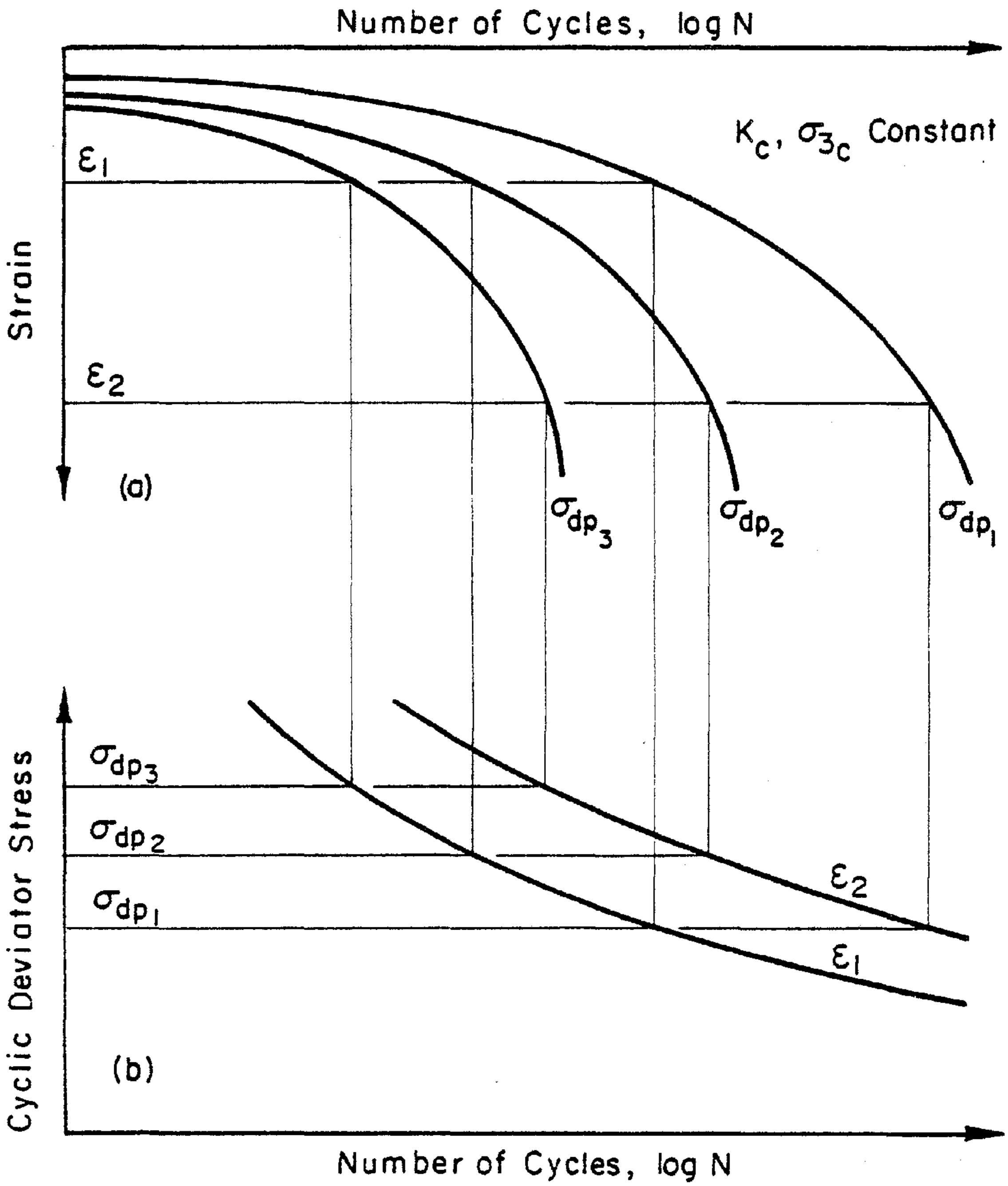

FIG. 2.4 RESULTS OF CYCLIC LOAD TESTS (1)

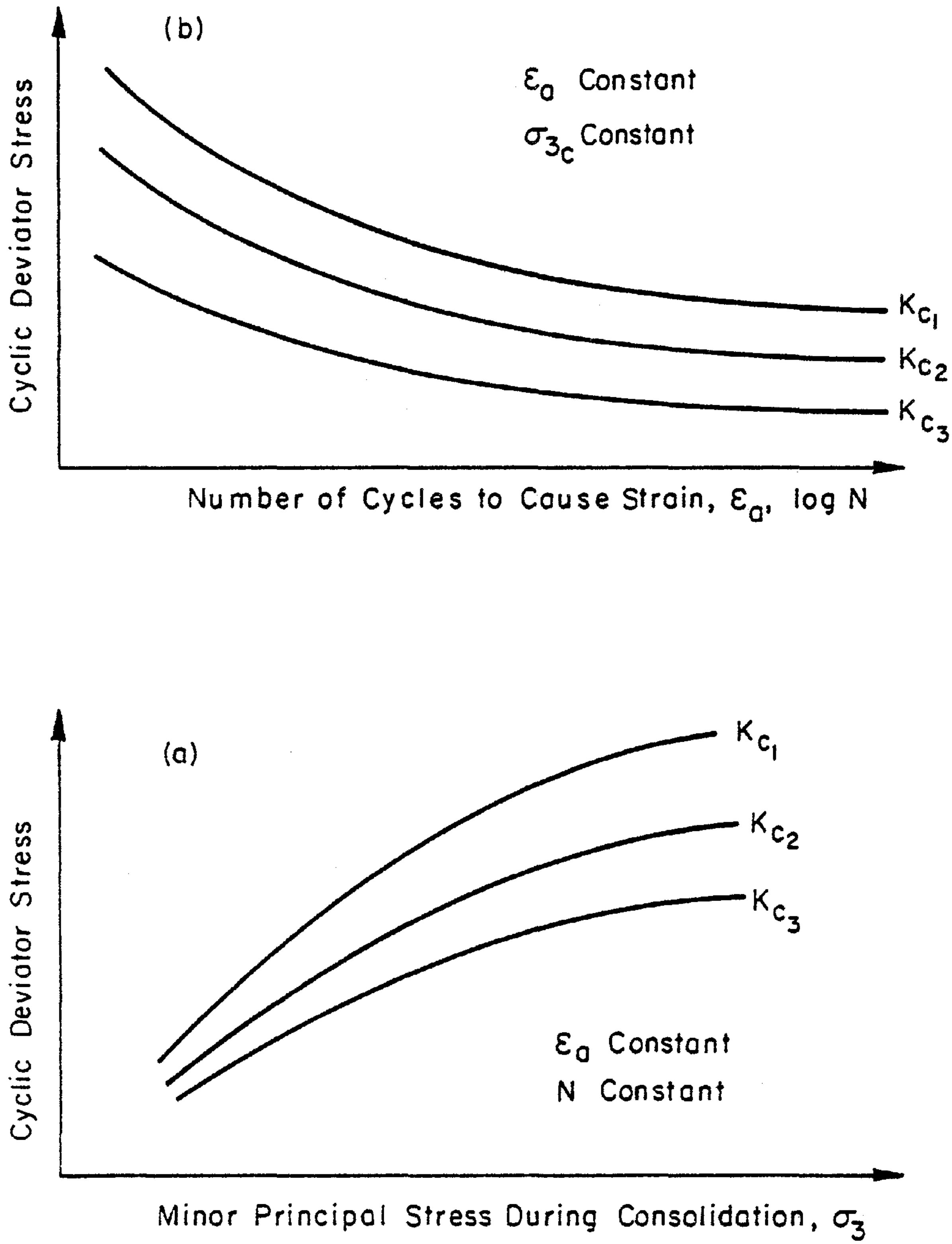

FIG. 2.5 RESULTS OF CYCLIC LOAD TESTS (2)

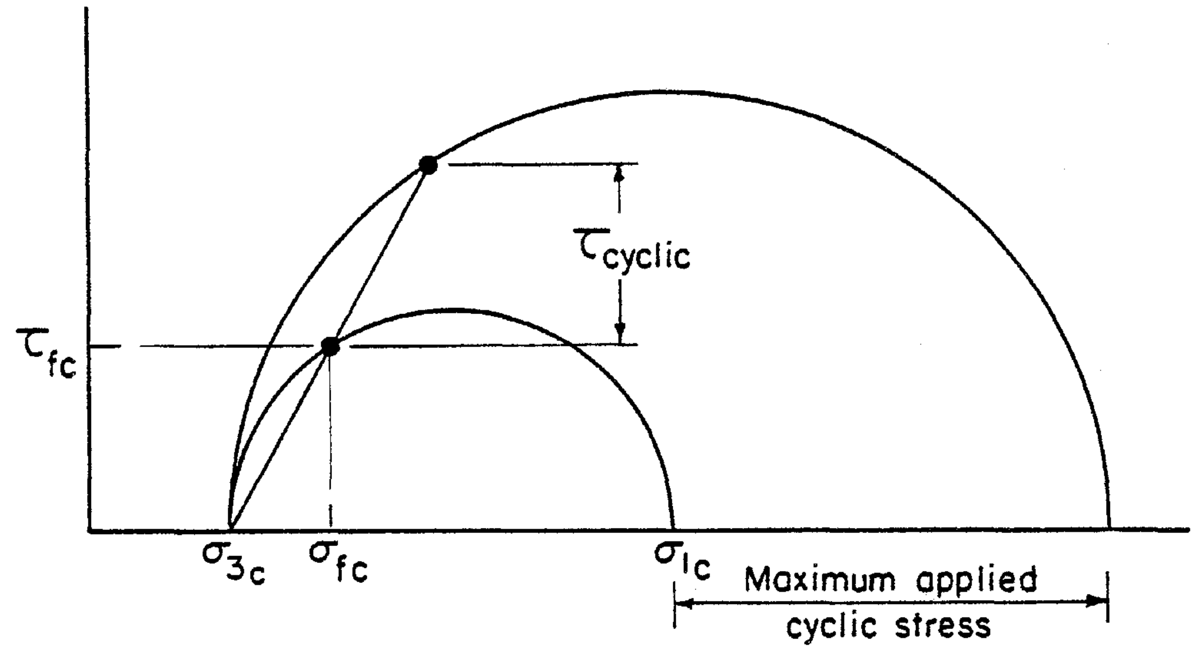

τ_{fc} = Initial shear stress on potential failure surface

σ_{fc} = Initial normal stress on potential failure surface

$\alpha = \tau_{fc}/\sigma_{fc}$

τ_{cyclic} = Cyclic shear stress developed on potential failure surface

FIG. 2.6 PROCEDURE FOR INTERPRETING CYCLIC LOAD TRIAXIAL TEST DATA TO DETERMINE CYCLIC SHEAR STRESS ON POTENTIAL FAILURE SURFACE (after Seed et al)

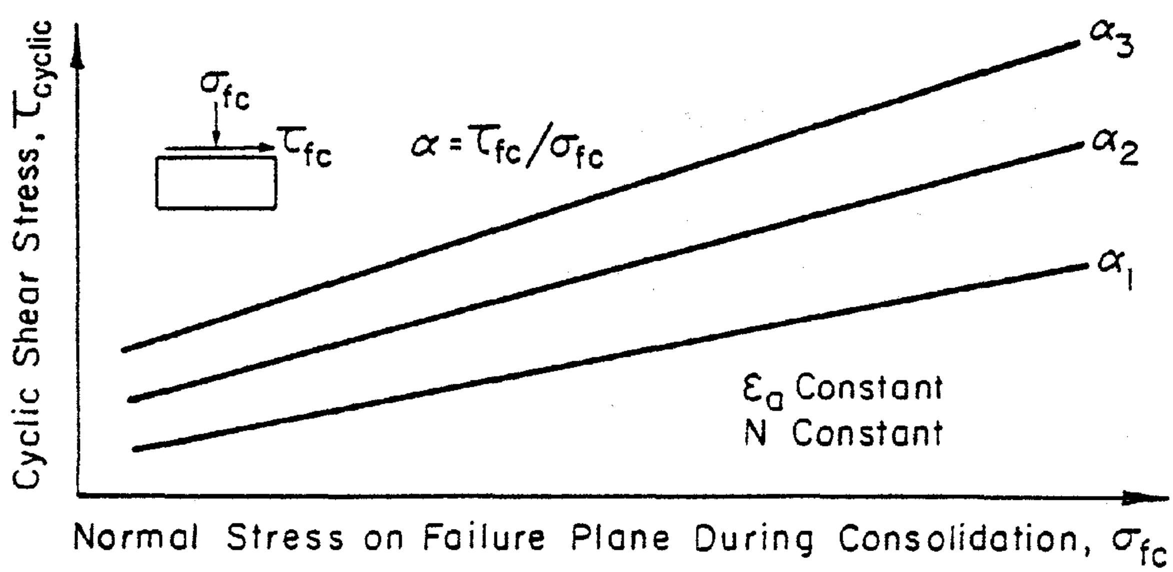

FIG. 2.7 RESULTS OF CYCLIC LOAD TESTS (3)

to be approximately equal to the maximum shear stress on the potential failure plane in the test specimen.

The final step in the reduction of the laboratory data is to produce a family of curves relating τ_{cyclic} to σ_{fc} for different levels of strain. These are derived from the curves in Fig. 2.5 and the Mohr circle construction in Fig. 2.6. The curves are shown in Fig. 2.7, and a range of curves for varying values of α are produced, where

$$\alpha = \frac{\tau_{fc}}{\sigma_{fc}} ;$$

and τ_{fc} is the shear stress on the failure plane during consolidation;

σ_{fc} is the normal stress on the failure plane during consolidation.

Sets of these curves are produced for a range of values of ε_a.

Analysis of Dam Behavior

The final step in the analysis of the dam is to use the curves obtained from the laboratory tests in conjunction with the results of the static and dynamic finite element analyses, to determine the effects of the earthquake induced stresses on the individual elements of the embankment. For each element of the dam, assuming the horizontal plane is the critical plane, σ_{fc} and τ_{fc} are known. From the dynamic analysis the superimposed cyclic shear stress in each element is known. By using the curves presented in Fig. 2.7, interpolating where necessary, the value of ε_a produced by the appropriate combination of initial and cyclic stress conditions for each element is determined. This value of strain is for an element unrestrained by surrounding elements, and is termed the "strain potential." The actual strain induced by the earthquake will depend on the effects of interaction between elements.

To make the calculations of strain potential more direct, the curves of Fig. 2.7 can be replotted as τ_{cyclic} vs. ε_a, with one curve for each value of σ_{fc}, and one set of curves for each value of α.

It is usually convenient to examine the behavior of the dam by considering horizontal layers of the dam separately, and calculating strain potentials for all the elements of a layer together. A curve of the induced shear stress in the elements of the layer is plotted (Fig. 2.8). Superimposed on this are curves of the cyclic shear stress to cause different values of strain (ε_a). The strain potential for each element on the plane is then found directly from the plot.

If a progressive analysis is run, where the response of the dam is examined after progressively longer earthquake durations, and material properties adjusted accordingly, sets of curves similar to those of Figs. 2.4, 2.5 and 2.7 are derived for values of N less than N_{eq}. These values of N correspond to the number of uniform cycles associated with the shorter duration of shaking applied at each step.

Summary

The steps involved in the earthquake analysis of a dam as proposed by Seed and his coworkers are as follows:

1. Determine the initial stress in the embankment before the earthquake by performing a static finite element analysis.
2. Select the design earthquake(s) and determine the characteristics of the motions developed in the rock underlying the embankment and its soil foundation during the earthquake.

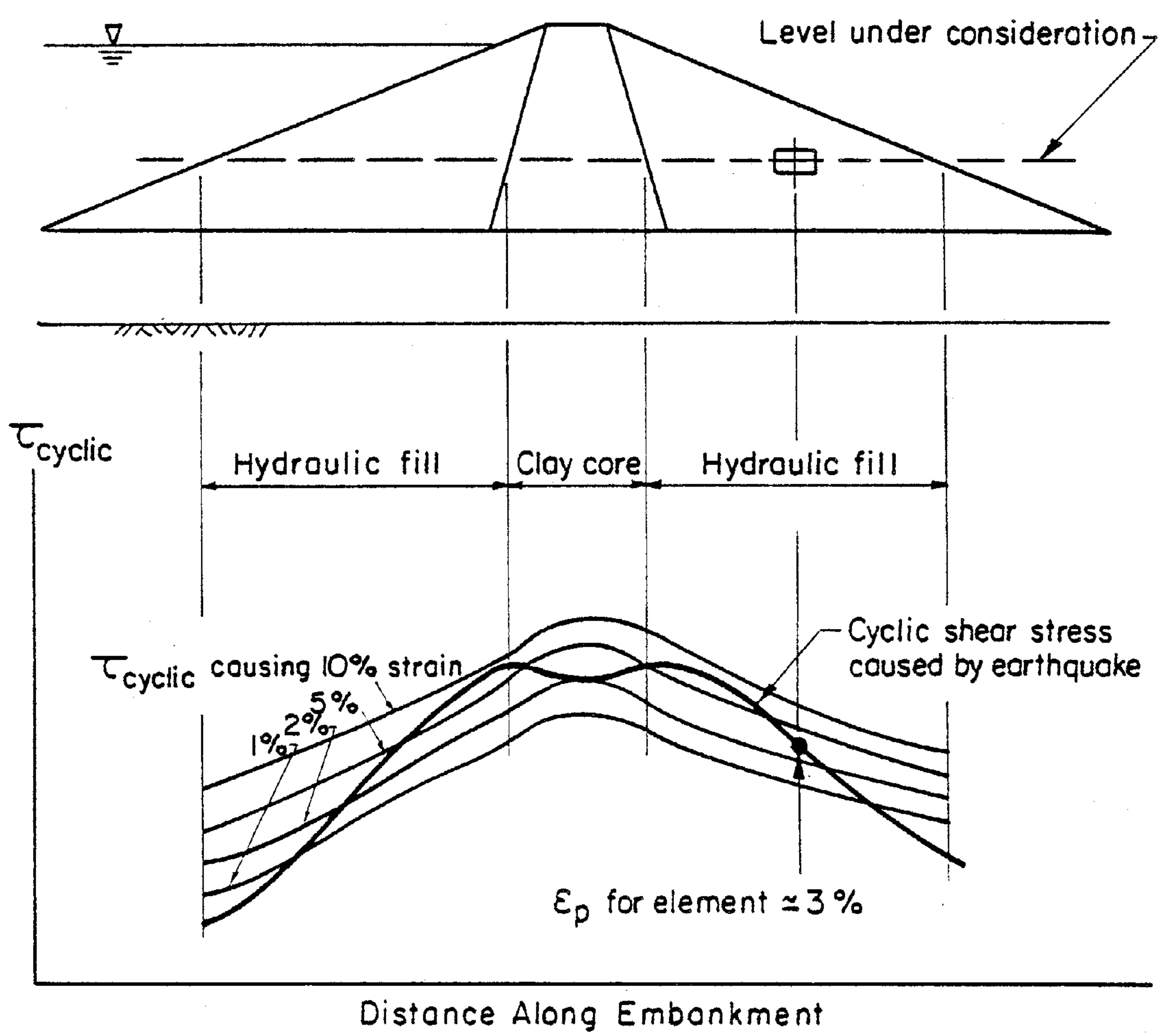

FIG. 2.8 CALCULATION OF POTENTIAL STRAINS

3. Determine the response of the embankment to the base rock motion and compute the dynamic stresses induced in representative elements of the embankment, using a dynamic finite element computer program.
4. Convert the dynamic stress histories for representative elements to a uniform stress level for a specified number of cycles, using curves developed from laboratory testing as a basis.
5. Perform laboratory tests to determine the dynamic response of the dam embankment and foundation materials (in terms of pore-water pressures and deformations produced) under cyclic loading conditions and various initial stress conditions.
6. Compare the computed dynamic stresses with the laboratory-determined response curves and estimate the potential strains in representative elements of the embankment.
7. From a knowledge of the strain potentials for representative elements in the embankment, evaluate the overall deformation and stability of the cross-section.

Using the results of this analysis, the stability of the dam after the earthquake can be checked (using the calculated values of strain potential to modify the strength of elements along a potential slip surface), and the factor of safety against sliding computed. For elements which have liquefied, for example, zero strength may be assigned in the stability analysis.

It is also possible to assess the overall stability of the dam by calculating the factor of safety against some level of strain (typcially 5%) on an element by element basis. Such a study can be very helpful to the designer if the results show a clear trend; for example, if every element shows a factor of safety greater than unity against 5% strain then the overall movements are likely to be tolerable. Alternatively, if all elements show a factor of safety less than unity against 20% strain, then the overall movements are likely to be excessive. For intermediate conditions judgement is required to interpret the significance of the results.

This method was first used by Seed (1970) in a study of Perris Dam, and has subsequently been used in numerous other studies. However, the strain potential assessment procedure developed in 1973 seems to offer greatly improved guidance in assessing embankment performance.

The last step in a comprehensive analysis of an earth dam is to estimate the permanent deformations induced by the earthquake. This problem is discussed in the following chapters, and a technique to calculate permanent deformations is developed.

Chapter 3

Analysis of Permanent Deformations

Introduction

The permanent deformations induced in an earth dam by the action of an earthquake are a function of both the static stress condition acting in the dam before the earthquake and the level and duration of the shaking due to the earthquake.

The steps taken in any analysis of the deformations must proceed from a basis of the knowledge of these criteria. Additionally, some technique to determine in the laboratory the effect of these initial stresses and applied inertia forces on the material of the dam is required.

Methods of determining the initial static stresses acting on the dam vary from an estimate based on previous experience to the most comprehensive technique currently available: a finite element approach which models the method of construction by building up the dam successively with layers of elements, while also accounting for the nonlinear behavior of the materials used.

A dynamic analysis which calculates the histories of the varying stresses throughout the dam, followed by use of these stress histories to determine the behavior in the laboratory of samples of the dam material, form the preliminary stages of a comprehensive deformation analysis. Analysis of these stress histories has developed from the original shear beam approach, which assumed the material of the dam to be uniform and that only shear forces acted, to the present comprehensive approach using the finite element method.

The static and dynamic stress analysis and the subsequent measurement in the laboratory of the behavior of specimens of the dam material subjected to these stresses, as used in the present research, are described fully in the previous chapter.

The behavior of soil samples consolidated under the initial stress conditions, due to gravity loading and seepage forces, and subjected to a cyclic stress history, is recorded in the form of the axial strain of the laboratory specimen. This strain, the major principal strain, is referred to as the strain "potential," since a corresponding element in the dam, unlike the laboratory sample, is restrained by surrounding material from undergoing the same degree of deformation. The final result of the dynamic stability analysis of the dam is the determination of the strain potential for each element in the dam, and use of these values both to modify the strength of elements along potential failure surfaces and to assess the overall deformations of the embankment. A stability analysis, using zero strength for the regions where the slip surface passes through "failure zones," i.e., areas where the strain potential exceeds the failure strain, and appropriately reduced strength where the strain potential is less than the failure strain, can be used to estimate the overall stability of the embankment after the earthquake. However, as with all limit analyses, the result indicates only whether or not total failure of the dam will occur. In the cases where failure does not occur, this approach gives no assessment of the deformations that may result as the soil undergoes strain in order to develop the strength necessary to resist failure.

A method of expressing the strain potential in terms of the overall earthquake-induced deformation of the dam is required in order to perform a complete analysis. A knowledge of these deformations, together with calculated post-earthquake stress and strain distribution which is derived from such an analysis, would help the designer of the dam to recognize areas of potential weakness in the event of an earthquake.

Deformation Analyses

Analyses of the seismically induced deformations of an earth dam by four different approaches are presented in this chapter. The first approach is a rough approximation and follows directly from a knowledge of the strain potentials of the elements. It was used by Seed et al. (1973) in the analysis of the Upper San Fernando Dam. The second and third methods are based on the concept that the effect of the strain potential of an element is a reduction in the modulus of the material, followed by settlement of the dam to a new position of equilibrium under gravity loads. The second method is a linear gravity turn-on analysis, as proposed by Lee (1974), while the third method is a nonlinear version of the second, with the loads applied in increments, thus making it possible to approximate the stress-strain curve of the soil by a series of straight line segments.

The fourth method, which seems to offer the most rational approach, and for which a computer program has been developed (listed in the Appendix), is a true pseudo-static approach. The effect of the earthquake is represented by a set of nodal point forces which are derived from the element strain potentials. The method incorporates the nonlinear characteristics of the soils and loading is incremental.

The results of these analyses, when applied to the Upper San Fernando Dam to calculate the deformations due to the earthquake of February 9, 1971, are presented in the following chapter. The four methods are briefly described in the following paragraphs.

First Approximation

An approach for assessing embankment deformations, applied by Seed et al. (1973), is to average the strain potentials, expressed as shear strains, along a vertical section through the dam, and to calculate the movement at the top of the section from the product of the average shear strain and the height of the section. This method determines only horizontal displacements, and it assumes that the maximum shear stresses act along horizontal planes.

Modified Modulus Approach--Linear

An alternative approach involves the use of linear, static finite element analyses, in which the effect of the earthquake on the soil properties is simulated by a reduction in the modulus, as proposed independently by Lee (1974). The analysis is run in three stages.

In the first stage, a linear gravity turn-on analysis, which includes gravity loads and seepage forces, is run. Initial values of the modulus, E_i, are determined from static triaxial tests, or estimated from published data for similar soils. The calculated deformation of each node in the dam is recorded and stored for later use. The deformations are merely reference deformations and are not representative of any actual pre-earthquake deformation.

The effect of cyclic loading on a soil is represented as a softening of the soil, resulting in a reduced modulus. The dam will then deform under both its own weight and the hydrostatic forces acting on the upstream slope. Thus, the second stage of the analysis is to perform another linear gravity turn-on analysis, using reduced values of the modulus in the elements.

The third and final step calculates the difference between the deformations obtained from the second and first steps of the analysis to give the displacement of each node in the dam due to the softening caused by the earthquake.

The initial values of the modulus, E_i, used in the first stage of the analysis, are determined from triaxial tests or published data for similar soils. To determine the final value of the modulus, E_f, it is assumed that the stresses developed during the earthquake return to the initial value and that the net change in stress is zero (Fig. 3.1). During the earthquake, the strain changes from the initial value ε_i to the final value ε_f, an increase equal to the strain potential ε_p. The final value of the modulus is then:

$$E_f = \frac{\sigma_i}{\varepsilon_i + \varepsilon_p} = \frac{\sigma_i}{\varepsilon_f} \tag{3.1}$$

Because the critical zones of the dam are saturated, and most of the rest of the dam is nearly saturated, the bulk modulus of the soil in the dam cannot change significantly. Hence, all of the softening is assumed to be due to a reduction of the shear modulus. To incorporate this in a finite element analysis, the stress-strain relationship is formulated in terms of the bulk modulus and shear modulus, rather than in the usual manner in terms of Young's modulus and Poisson's ratio. This formulation is that originally proposed by Clough and Woodward (1967):

$$\underline{C} = \begin{bmatrix} K+G & K-G & 0 \\ K-G & K+G & 0 \\ 0 & 0 & G \end{bmatrix} \tag{3.2}$$

where C is the elastic stress-strain relationship (Hooke's Law) for plane

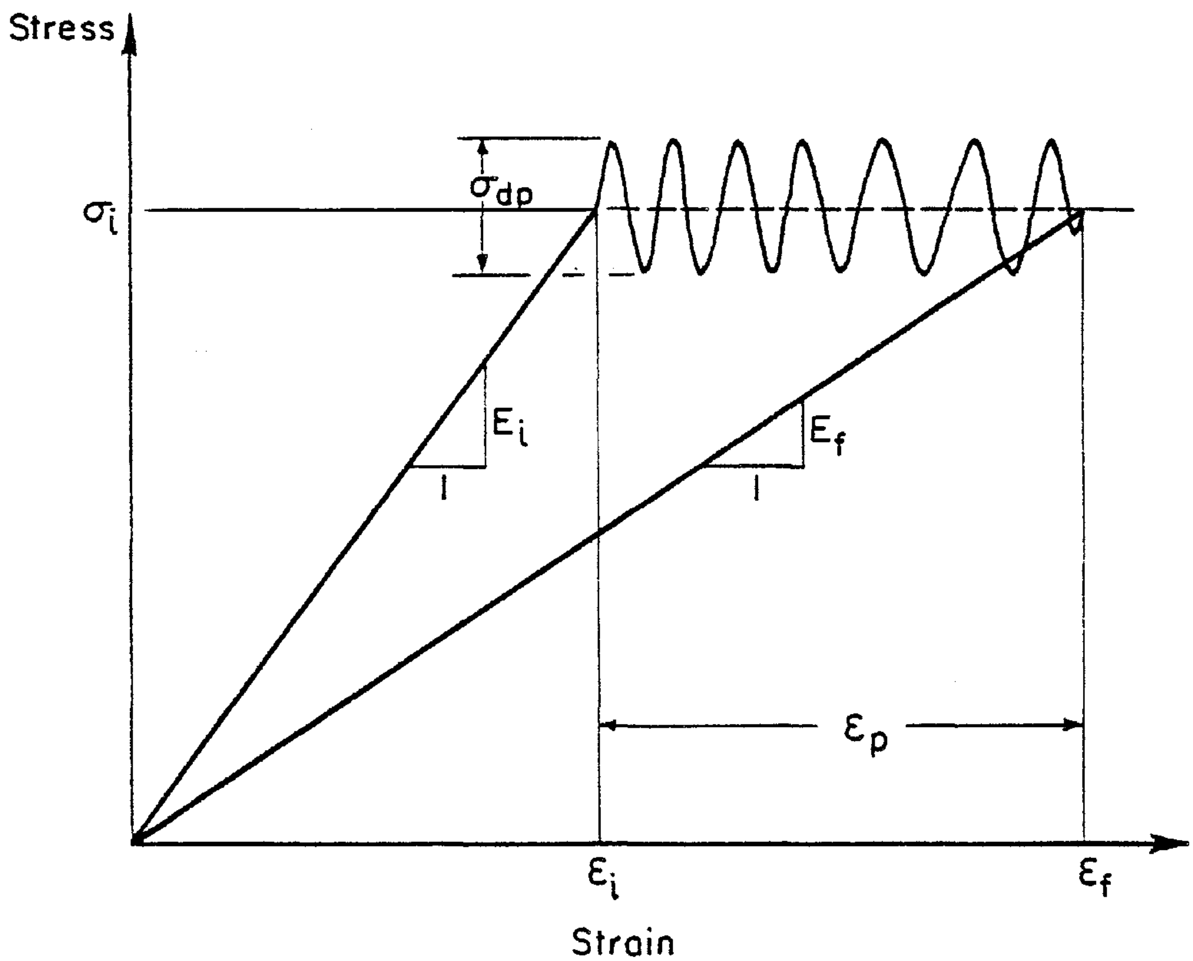

$E_i = \sigma_i / \varepsilon_i$ Modulus before earthquake

$E_f = \sigma_i / (\varepsilon_i + \varepsilon_p)$ Modulus after earthquake

FIG. 3.1 MODIFIED MODULUS METHOD - LINEAR strain conditions, defined by

$$\underset{\sim}{\sigma} = \underline{C}\,\underset{\sim}{\varepsilon}$$

and expressed in terms of the bulk modulus (K) and the shear modulus (G) of the soil:

$$K = \frac{E}{2(1+\nu)(1-2\nu)} \tag{3.3}$$

$$G = \frac{E}{2(1+\nu)} \tag{3.4}$$

where E is the appropriate value of Young's modulus (E_i or E_f) and ν is Poisson's ratio, which is usually estimated. For elements below the phreatic line, ν is assumed to be 0.49; for other elements the value will vary with the material type and can be estimated from published values. The bulk modulus is calculated using $E = E_i$ for both first and second stages of the analysis; the shear modulus is calculated using $E = E_i$ in the first stage, and $E = E_f$ in the second stage.

During the earthquake, drainage of excess pore water pressure does not have time to occur since the dam is effectively impermeable for the relatively short duration of shaking. Thus, in the second stage of the analysis, water forces may more appropriately be applied to the upstream slope of the dam, rather than as seepage forces throughout the dam.

A similar analysis has been published independently by Lee (1974). In this approach, a pseudo-secant modulus for each element is first calculated from the results of the finite element dynamic analysis. The modulus is defined as:

$$E_p = \frac{\sigma_i}{\varepsilon_p} \tag{3.5}$$

where σ_i is the initial stress in the element (i.e., before the earthquake) and ε_p is the element strain potential resulting from the earthquake shaking.

A final secant modulus is then defined by:

$$\frac{1}{E_{ip}} = \frac{1}{E_i} + \frac{1}{E_p} \tag{3.6}$$

where E_i is the initial (pre-earthquake) secant modulus.

Using the initial and final values of the secant moduli, two linear analyses are run, the difference in displacements giving the earthquake-induced deformations. Only the shear modulus is changed in the second stage of the analysis, as described previously, and hydrostatic forces are assumed to act on the upstream slope during the earthquake. The deformations calculated by Lee are compared with those determined in the present study in the following chapter.

Modified Modulus Approach--Nonlinear

This approach is an improvement on the preceding analysis and takes into account the nonlinear stress-strain behavior of soils. The analysis is run in three stages as before. The first stage consists of a finite element analysis to determine the conditions in the dam before the earthquake. The stress-strain relationship for the pre-earthquake condition is determined from the nonlinear parameters for the soil which are calculated by the method of Kulhawy et al. (1969) as explained in the previous chapter, or some similar approach. Fig. 3.2 shows representative curves for the stress-strain relationship in an element for the conditions before and after the earthquake. Deviator stress is plotted against principal strain.

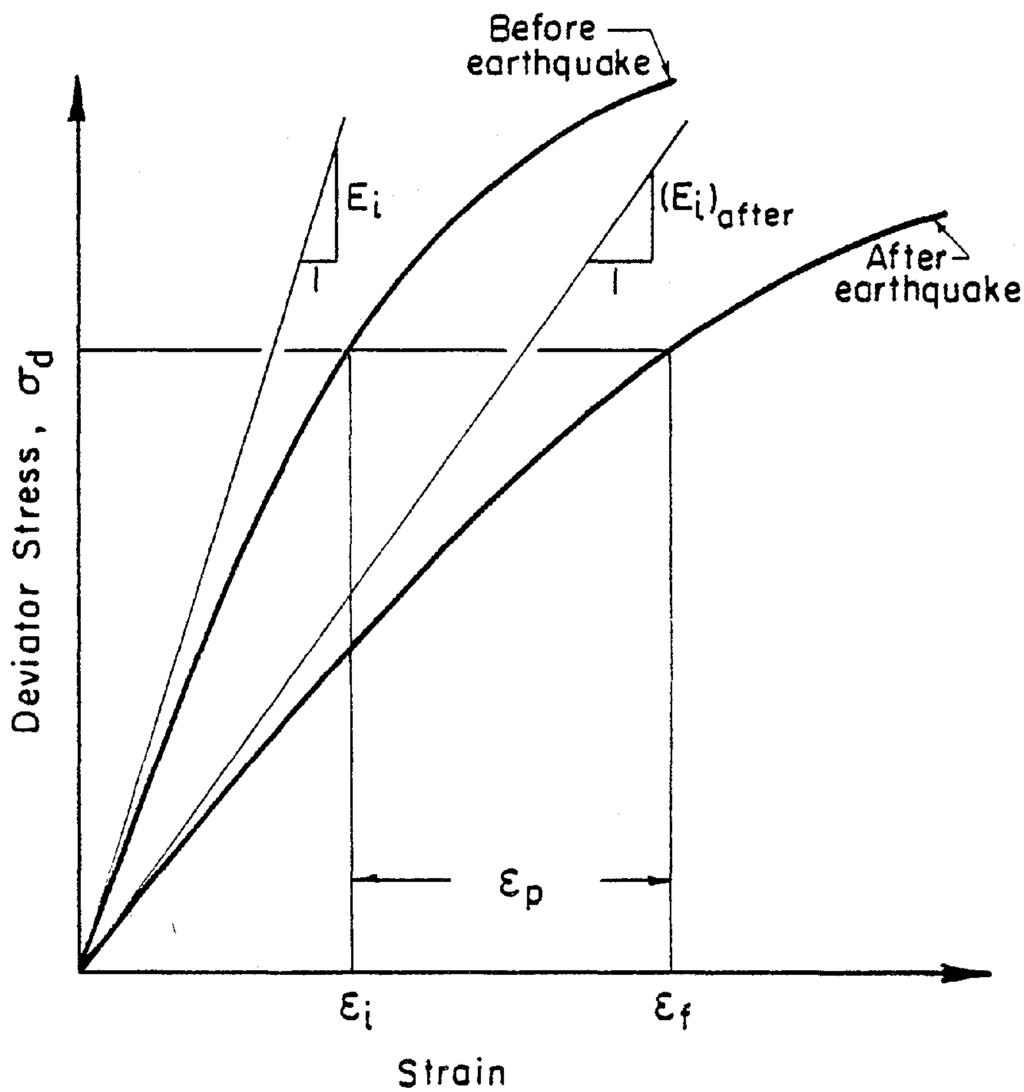

$$(E_i)_{after} = E_i\left[\varepsilon_i/(\varepsilon_i + \varepsilon_p)\right]$$

FIG. 3.2 MODIFIED MODULUS METHOD - NONLINEAR

In performing a nonlinear static analysis for the post-earthquake conditions, some additional assumptions must be made about the stress-strain relationships for the soil. Accordingly, it is assumed that the static shear stress in an element of the dam, represented by the static deviator stress, applied to a representative sample in the laboratory, will be unchanged due to the earthquake. During the earthquake, or simulated earthquake loading in the laboratory, the cyclic shear or deviator stress will pulsate about the pre-earthquake static shear stress condition. In the laboratory test, this effect will cause an accumulative strain, ε_p, in the sample at the end of the simulated loading. Thus, the final total strain, ε_f, after the earthquake will be $\varepsilon_i + \varepsilon_p$, as shown in Fig. 3.2.

It is further assumed that the shape of the post-earthquake stress-strain curve between the origin and the final post-earthquake condition can be represented by a hyperbola similar to that of the pre-earthquake curve. Finally, it is assumed that the factors n and R_f, as defined in Chapter 2, used to define this hyperbolic curve are the same as those used for the pre-earthquake curve and that the initial moduli before and after the earthquake are in direct proportion to the strain in the laboratory sample simulating the element in the dam:

$$(E_i)_{after} = (E_i) \frac{\varepsilon_i}{\varepsilon_i + \varepsilon_p} \qquad (3.7)$$

In this way, a nonlinear stress-strain curve for an element for the post-earthquake condition can be fully defined.

The first step of the method consists of an incremental loading analysis using the initial stress-strain curve for each element. The stress-strain matrix used in the computer program is defined in terms of G and K. The load vector for the finite element analysis is formed of the gravity loads and the seepage forces and is applied in a number of steps. The stiffness properties are recalculated at each load step and the stiffness matrix reformed, thus following the stress-strain curve by a number of straight segments. In the second step, the analysis is repeated using the post-earthquake soil properties. The deformations calculated in the first two steps are subtracted in the third step to give the deformations of the dam due to the earthquake.

In the second step of the analysis, only the shear modulus is changed, the reasoning for this being as presented in the previous section on the linear approach.

The results of the preceding methods of analysis applied to the Upper San Fernando Dam are presented in the next chapter. However, since neither of the above methods includes consideration of the deformations produced by the inertia stresses induced by the earthquake shaking, another approach giving consideration to this aspect of the problem was developed, as described below.

Equivalent Nodal Point Force Approach

The ultimate effect of the earthquake, assuming the dam does not fail, is to cause each element of the dam to undergo some degree of strain; this may be expressed by the strain potential for each element, although the actual strain will necessarily be different from the strain potential values in order to ensure compatibility of deformations.

It is possible to postulate an array of static forces at the nodes of the finite element mesh which would result in the same deformations of the elements as those produced by the computed strain potentials. Thus, the effects of the earthquake can be represented by a series of equivalent static forces producing a truly pseudo-static analysis.

To estimate the equivalent static nodal point forces for an element in the embankment, it is necessary to determine the change in stress for that element corresponding to the computed strain potential induced by the earthquake loading. This can be achieved once a stress-strain relationship for the material during the earthquake has been defined. In the present analysis two assumptions have been made: (1) the stress-strain behavior of the material during the earthquake may be represented by a nonlinear hyperbolic relationship determined from consolidated-undrained laboratory tests; and (2) the nonlinear stress-strain relationship for a particular soil during the earthquake is dependent only on the initial effective confining pressure existing in the embankment before the earthquake. The first assumption is a reasonable one in most cases, especially for low permeability soils, given the short duration of the earthquake loading during which the material can be assumed for all practical purposes to exhibit undrained behavior. The second assumption can reasonably be made since the approach followed in the analysis is a total stress approach where the properties of the material depend on the initial stress conditions before loading.

Accordingly, the increment in stress, $\Delta\sigma_d$, corresponding to a specified strain potential, ε_p, for an element of soil can be determined as shown in Fig. 3.3. The initial pre-earthquake stress condition (σ_{di}, ε_{i-D}) may be conveniently determined by an incremental finite element procedure (as described in Chapter 2) using nonlinear parameters obtained from drained triaxial test results. For the same initial stress conditions (σ_{3i}, σ_{di}), the undrained stress-strain relationship used during the earthquake is also shown in Fig. 3.3, and the corresponding strain on this curve for the same stress, σ_{di}, is ε_{i-UD}. It is assumed that deformations during the earthquake

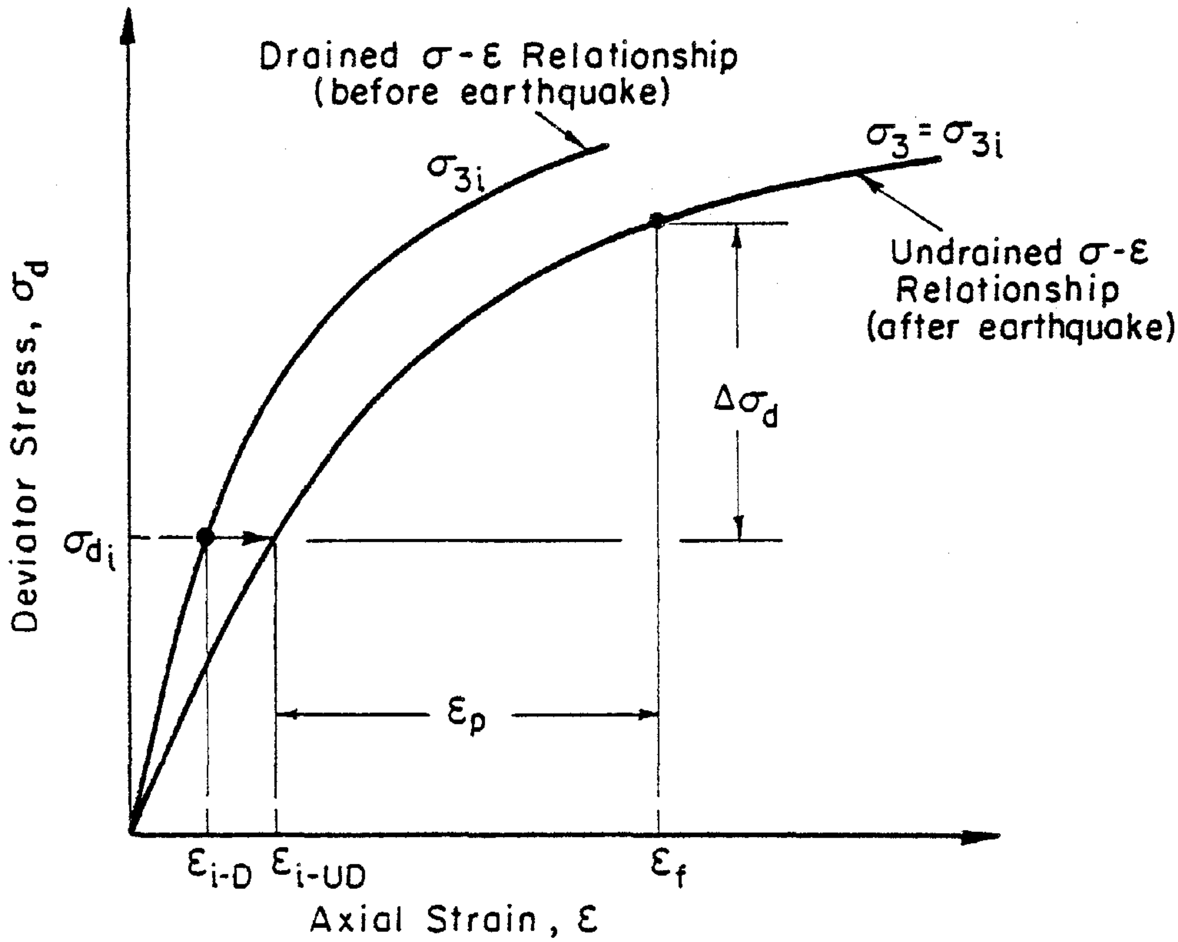

FIG. 3.3 EQUIVALENT FORCE METHOD - DETERMINATION OF EQUIVALENT STRESS

start from this point on the undrained curve. The differences between ε_{i-UD} and ε_{i-D} are very small compared to the strain potential, ε_p, and since the interest of the analysis is in the earthquake-induced deformations rather than the pre-earthquake displacements, such differences may be neglected for practical purposes without affecting the results of the analysis. The change in stress, $\Delta\sigma_d$, corresponding to the strain potential, ε_p, can then readily be determined using the undrained stress-strain relationship, as shown in Fig. 3.3.

Dynamic analyses have indicated that the response of earth dams to horizontal base motions is, in general, predominantly a shear deformation and that the maximum induced shear stresses occur along directions within about ±10° of the horizontal. It may, therefore, be assumed conservatively that the maximum induced dynamic shear stress, $\Delta\tau_{max}$, acts along the horizontal plane and is equal to $\Delta\tau_{xy}$. The maximum dynamic shear stress, $\Delta\tau_{max}$, can readily be determined since it is equal to half the deviator stress increment, $\Delta\sigma_d$, determined above.

To estimate the equivalent nodal point forces, it is further assumed that the distribution of shear stress over the area of an element is uniform and constant. Thus, the nodal point forces for an element in plane strain can be estimated from $\Delta\tau_{xy}$ (which is equal to $\Delta\tau_{max}$) by multiplying it by the width and the height of the element to determine the horizontal and vertical node forces, respectively, as shown in Fig. 3.4. These nodal forces are applied in the direction of the initial horizontal shear stress acting on the element, since a soil element under simple shear cyclic loading conditions will show a residual deformation in the direction of the initial shear stress.

A nonlinear finite element analysis is then run in which only these

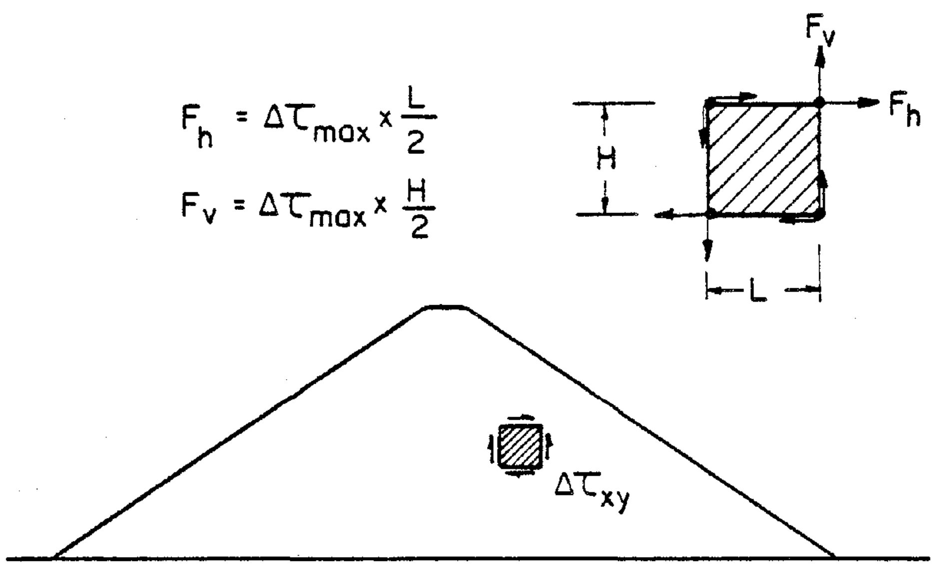

FIG. 3.4 EQUIVALENT FORCE METHOD - DETERMINATION OF NODAL POINT FORCES

forces are applied, and the resulting deformations in the dam are those due to the earthquake. The loads due to gravity and seepage forces are not included in the analysis since the effects of these forces have already been included in the evaluation of the strain potential. Since the soil was consolidated before dynamic testing under the stress conditions existing in the embankment prior to the earthquake, these initial stresses are due to the gravity loads and seepage forces.

A nonlinear finite element program (DEFORM) was written incorporating the method presented above. A description and full listing of the program is given in the Appendix. The nonlinear analysis procedure of Kulhawy et al. (1969) is used. As a first stage, a nonlinear step-by-step loading analysis, including seepage forces, is run to determine the initial stresses in the dam. The pseudo-static nodal point forces representing the earthquake are then calculated for each node based on the undrained stress-strain relationship of the material during the earthquake and the strain potentials for the elements.

With the initial stresses as a starting point, a second analysis is run in which only the pseudo-static nodal point forces calculated in the first stage are applied. The resulting displacements are the deformations induced in the dam by the earthquake.

In the first stage of the analysis, soil properties for the drained condition are used; in the second stage, undrained soil properties are used, as these are more representative of the conditions existing in the dam during the earthquake. The Hooke's Law relationship used throughout the analysis is that previously described under Modified Modular Approach--Linear. During the second stage of the analysis, only the shear modulus of the soil is changed, the bulk modulus remaining constant, to model as accurately as possible the behavior of saturated soil during the earthquake.

The analysis cannot incorporate the effect of time, although the deformations are not necessarily immediate and may continue after the earthquake has stopped. However, if it were possible to incorporate this time effect and allow the changing stresses to affect the soil properties, the effect would be for the soil modulus to decrease, causing a smaller stress change to be required to produce the potential strain. This would result in lower equivalent nodal point forces acting on a softer material. While it cannot be claimed that the end result would be the same, the indication is that the effect would tend to give similar displacements.

Due to the nature of the nonlinear stress-strain formulation, tensile stresses cannot be handled. Soils generally used in earth dams cannot support tension, resulting in the opening of cracks near the surface of the dam. If, during the analysis, large tensile stresses develop in any element, the modulus should be reduced to a very small positive value.

An alternative approach to the above, which is described below, may be more applicable in cases where the specified strain potential values for a considerable number of elements are of such large magnitude as to exceed the failure strain of the material, since the use of the hyperbolic stress-strain relationship shown in Fig. 3.3 may cause some mathematical difficulties in the computational procedure for the permanent deformations. For such conditions, an equivalent linear modulus approach may be used where the equivalent modulus E_f is estimated from the nonlinear relationship on the basis of the strain potential, as shown in Fig. 3.5. The deviator stress increment, $\Delta\sigma_d$, used to establish the value of E_f will be the same as that determined in Fig. 3.3.

The equivalent nodal point forces in this approach are determined in

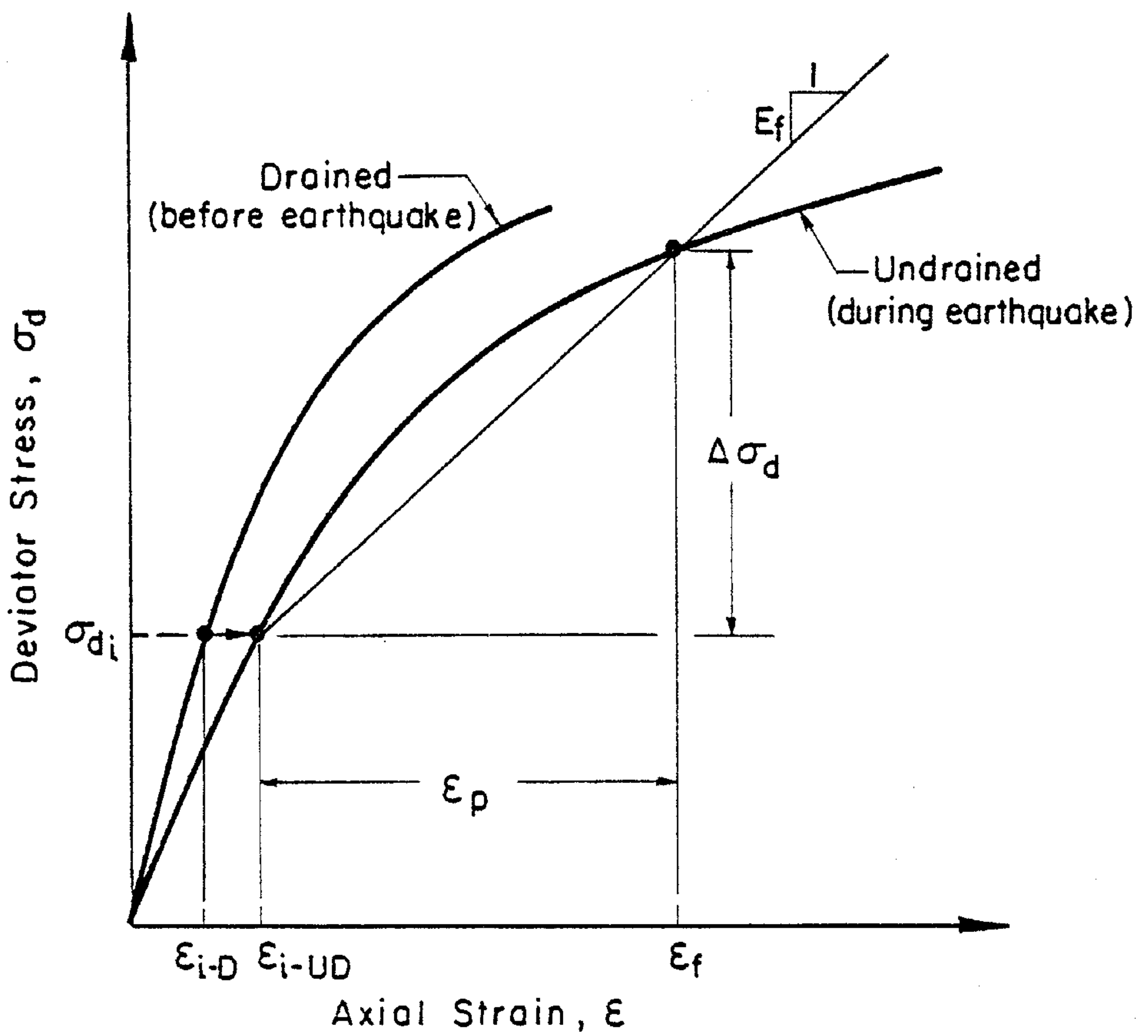

FIG. 3.5 EQUIVALENT FORCE METHOD - ALTERNATIVE METHOD OF DETERMINING EQUIVALENT MODULUS

the same manner as that described in the nonlinear approach (see Fig. 3.4); however, in this case, the second stage displacement computations are carried out using a one-step linear analysis instead of the incremental nonlinear approach described above.

As with any similar analysis, the results produced are limited in usefulness by the accuracy with which the soil properties are known.

In the next chapter, the method is applied to evaluate the deformations of the Upper San Fernando Dam during the earthquake of February 1971.

Chapter 4

Analysis of Permanent Deformations of the Upper San Fernando Dam

The Upper San Fernando Dam

Introduction

The Upper San Fernando Dam is a part of the Van Norman Lake Complex, a system of dams, reservoirs, dikes, and storm and diversion structures, which forms the terminal storage area for two aqueducts and was the main water distribution center for the surrounding area before the earthquake of February 9, 1971.

Construction of the Dam

Construction of the Upper San Fernando Dam was begun in 1921. Half a million cubic yards of material were placed that year, bringing the crest elevation to 1200 feet. It was originally planned to raise the embankment to a final crest elevation of 1238 feet in 1922. However, the dam was completed by the addition of a rolled fill section at the upstream side of the dam, bringing the final crest elevation to 1218 feet. The completed dam has a crest width of 20 feet and a 100-foot berm on the downstream side at elevation 1200 feet. The slopes are 2.5:1, and the upstream face is protected by concrete paving. The maximum cross-section height is approximately 82 feet (Fig. 4.1).

Construction details for the dam do not exist, but the general technique employed was the "semihydraulic" fill method, a variation on the hydraulic fill construction method. In the hydraulic fill method of

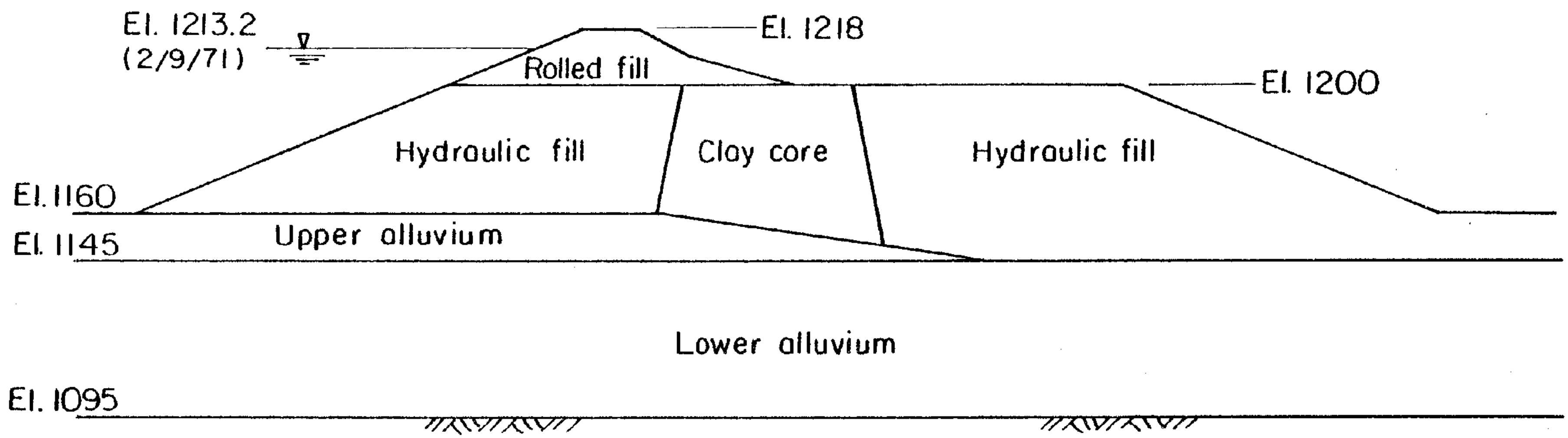

FIG. 4.1 IDEALIZED CROSS-SECTION THROUGH UPPER SAN FERNANDO DAM

construction, material for the dam is sluiced at the borrow area and conveyed to the site, through pipes by pumping or gravity. It is then discharged on beaches at the upstream and downstream edges of the dam and flows toward the center, coarser material being deposited quickly to form the shell of the dam and finer material settling out more slowly from the pool which forms at the center to form the "impermeable" core. Ideally, the end result is an overall gradation from coarse material at the face, forming a strong shell, to the finest material at the center, forming an impermeable core. In practice, this is rarely realized, and lenses of sand and silt sometimes penetrate the core partially negating the effect of the impermeable barrier and making the dam more prone to failure from piping. However, it was felt at the time by the designers that if adequate care was taken during construction, and if the rate of progress was controlled so that local failures did not occur on the slopes during construction, a sound embankment could be built.

Possibly due to lack of an adequate water supply, the hydraulic fill method was not used to build the Upper San Fernando Dam, though the Lower San Fernando Dam was built by this technique in 1912. In the semihydraulic fill method used, borrow material was loaded by Fresno scrapers or steam shovels at the borrow area and transported by horse-drawn carts to the dam site. Here the material was dumped on the beaches at the upstream and downstream toes and was spread by sluicing it with a jet of water pumped from a barge floating on the pool between the beaches. As with the hydraulic fill method, the finer material was transported down into the pool to form the core, while the coarser material stayed near the beaches to form the shell.

The volume of material placed by this method in 1921 was 500,000 cubic yards. The following year the rolled fill section was added at the upstream face. This added a further 50,000 cubic yards to the dam. The material for the rolled fill section was brought to the dam by horse-drawn cart, spread in thin lifts by Fresno scrapers, sprinkled and then compacted by routing the hauling equipment over the filled area. Total cost of the dam was approximately $280,000.

Despite the difference in construction methods for the Upper and Lower San Fernando Dams, investigation by bore holes and trenches, made after the earthquake of February 1971, showed no appreciable difference in the material of the dams.

Foundation of Dam

The Upper San Fernando Dam is founded on alluvium, consisting of alternating layers of stiff clays and clayey gravels, varying from 50 feet to 60 feet deep. The alluvium is underlain by a poorly cemented conglomeritic sandstone and coarse-grained sandstone of the Saugus formation (Lower Pleistocene), which also forms the abutments.

The dam is constructed directly on the alluvium with a cut-off trench approximately 4 feet deep and 30 feet wide, under the axis of the dam, as the only site preparation (see Fig. 4.2).

Reservoir and Auxiliary Structures

The dam contains a reservoir of 1,850 acre-feet capacity. Originally, the reservoir capacity was 1,977 acre-feet, but this was reduced by alluvium washed down by the flood of 1938 and by later construction of dikes along the western side of the reservoir. The spillway, at elevation 1,212.5 feet, is located near the left abutment of the dam.

An outlet tower is located near the upstream toe of the midpoint of the dam. The tower is founded at elevation 1,149 feet and rises to

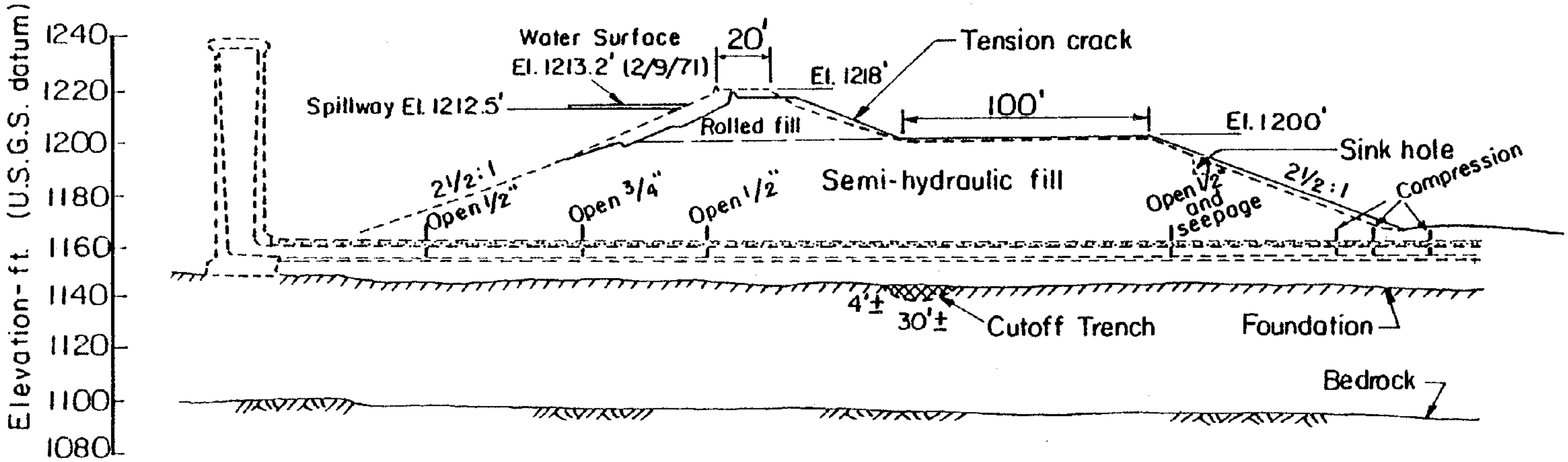

FIG. 4.2 CROSS-SECTION THROUGH UPPER SAN FERNANDO DAM
(after L.A. Dept. of Water and Power)

elevation 1,239 feet, approximately 90 feet high. The tower has an outside diameter of 20 feet, with stepped internal diameters. It connects to an 8-foot diameter cast-in-place concrete outlet conduit lined with a 62-inch inside diameter, concrete-lined steel pipe, which passes through the embankment. A second outlet pipe, 99 inches in diameter, and passing through the right abutment at an inlet elevation of 1,185 feet, was constructed in 1968.

Instrumentation

Observation wells on the berm and the downstream slope were used to locate the phreatic line. Monuments embedded in the embankment were used to measure deformations. Seepage losses were measured at drains at the abutments and at the downstream toe of the dam.

Earthquake of February 9, 1971

An earthquake, measuring M = 6.6 on the Richter Scale, occurred at 6:00 a.m. on February 9, 1971 in the San Gabriel Mountains north of the City of Los Angeles. The epicenter was approximately 6 miles NE of the San Fernando Dam complex. Fault movement was of the thrust type, the north block moving up and over the south block at an angle of about 45 degrees. The focal depth of the onset of rupture was approximately 8 miles. The fault break apparently propagated upward to the south, intersecting the ground surface in the San Fernando area. The fault scarp formed by the earthquake reached a maximum height of about 4 feet at its eastern end, diminishing in height toward the west. However, features resembling a fault break were traced nearly to the eastern edge of the Lower Van Norman reservoir.

Seismoscope records obtained on the crest and the abutment of the lower dam were obtained during the earthquake, and the record for the abutment has been interpreted by R. F. Scott to provide a record of the time history of accelerations at the bedrock underlying the dam. Based on a study of this record, and of the maximum accelerations recorded at sites with varying epicentral distances, Seed et al. (1973) concluded that the maximum rock acceleration at the site of the dams was in the range of 0.55 to 0.69.

Effects of the Earthquake on the Dam

When the water level in the reservoir of the Upper San Fernando Dam was drawn down after the earthquake, several longitudinal cracks were observed running nearly the full length of the dam. The cracks appeared to be multiple shear scarps resulting from the downstream movement of the main body of the dam, the crest showing a settlement of nearly 3 feet and a downstream movement of nearly 5 feet at the center-line of the dam (Fig. 4.2). The downstream movement was evident from the bowing of the parapet wall and the scarps on the upstream face.

A vertical longitudinal crack opened on the downstream slope of the rolled fill section (indicated in Fig. 4.2) and a 2-foot high pressure ridge formed at the downstream toe. Sand boils also formed below the downstream toe.

Damage to the outlet conduit was revealed on inspection after the earthquake. Several cracks, up to 3/4-inch, opened in the section of the conduit in the upstream and central areas of the dam. Compression failure occurred near the downstream toe (Fig. 4.2). However, the magnitude of the movements at the conduit was relatively small, indicating that most of the movement occurred in the embankment above the conduit. A sinkhole, extending to the surface of the dam downstream from the berm, appears to have been formed by seepage and erosion through a crack in the conduit.

Although the transverse movement of the dam was the major movement, relative longitudinal movement of the abutments, probably less than 2 feet, caused cracks in the spillway and in the roadway across the crest of the dam.

Variations in the water level in three piezometers during and after the earthquake are shown in Fig. 4.3. The shear strains induced in the embankment during the earthquake caused increases in the pore water pressure, which slowly dissipated after the earthquake. These increases are evidenced by the changes in water level in the piezometers. During the earthquake, the water overflowed from piezometers #1 and #2, so the true increase is not known.

Judging from the field observations, movements appear to have been general throughout the dam, and not confined to a unique slip surface. The movements were probably due to a weakening of the soil due to the rise in pore water pressure. The sand boils indicate that liquefaction did take place in some areas, and part of the movements may have been due to strength loss due to liquefaction.

Measured Displacements

A survey of the monuments embedded in the dam was made shortly after the earthquake. Vertical and horizontal displacements were measured at several points on the maximum section of the dam (Fig. 4.4) including: the upstream parapet wall, the midpoint of the downstream slope of the rolled fill section, the upstream and downstream ends of the berm, the midpoint of the downstream slope and the downstream toe. The displacement

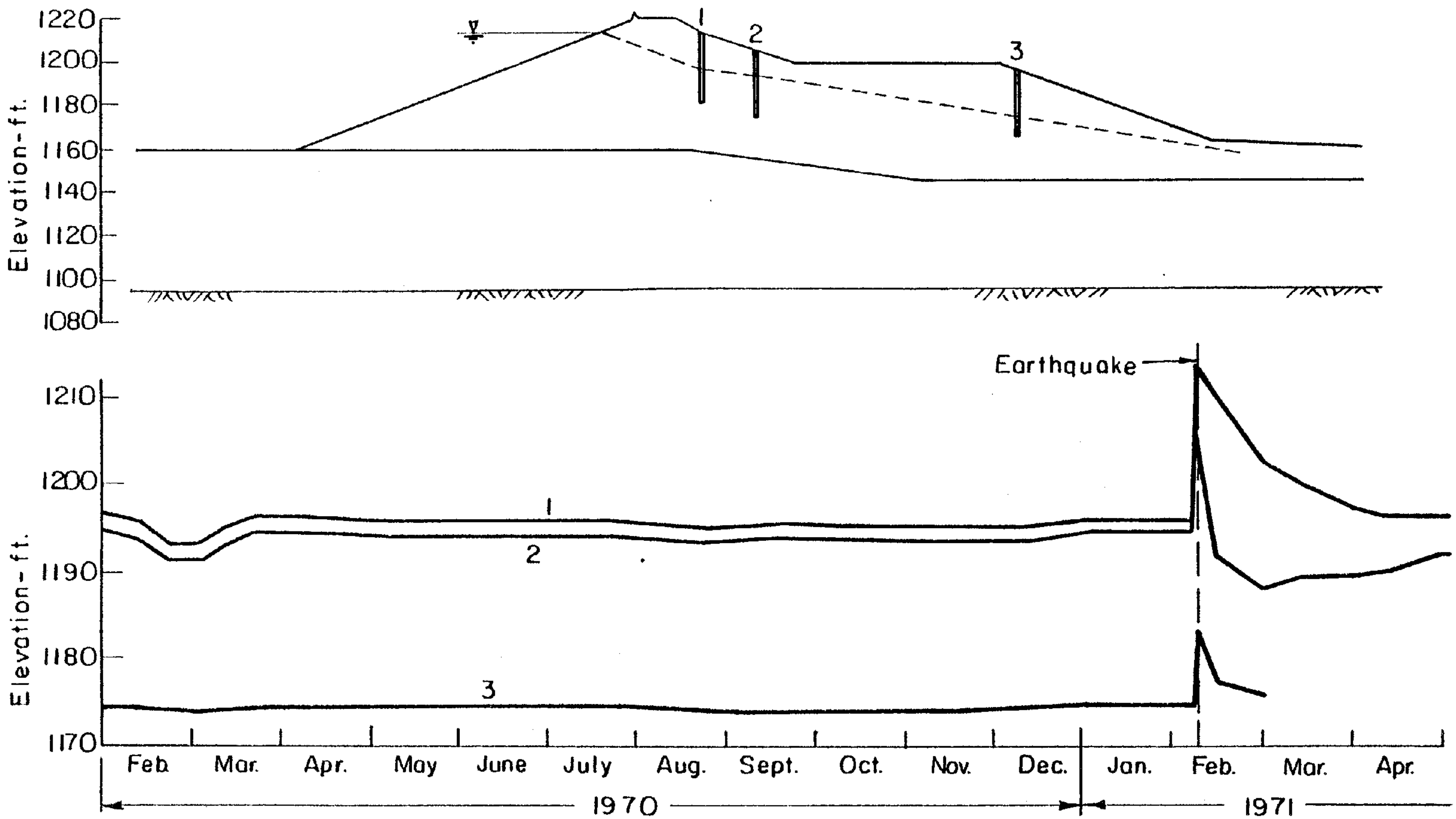

FIG. 4.3 CHANGES IN WATER LEVEL IN PIEZOMETERS FOLLOWING THE EARTHQUAKE - UPPER SAN FERNANDO DAM (after Seed et al)

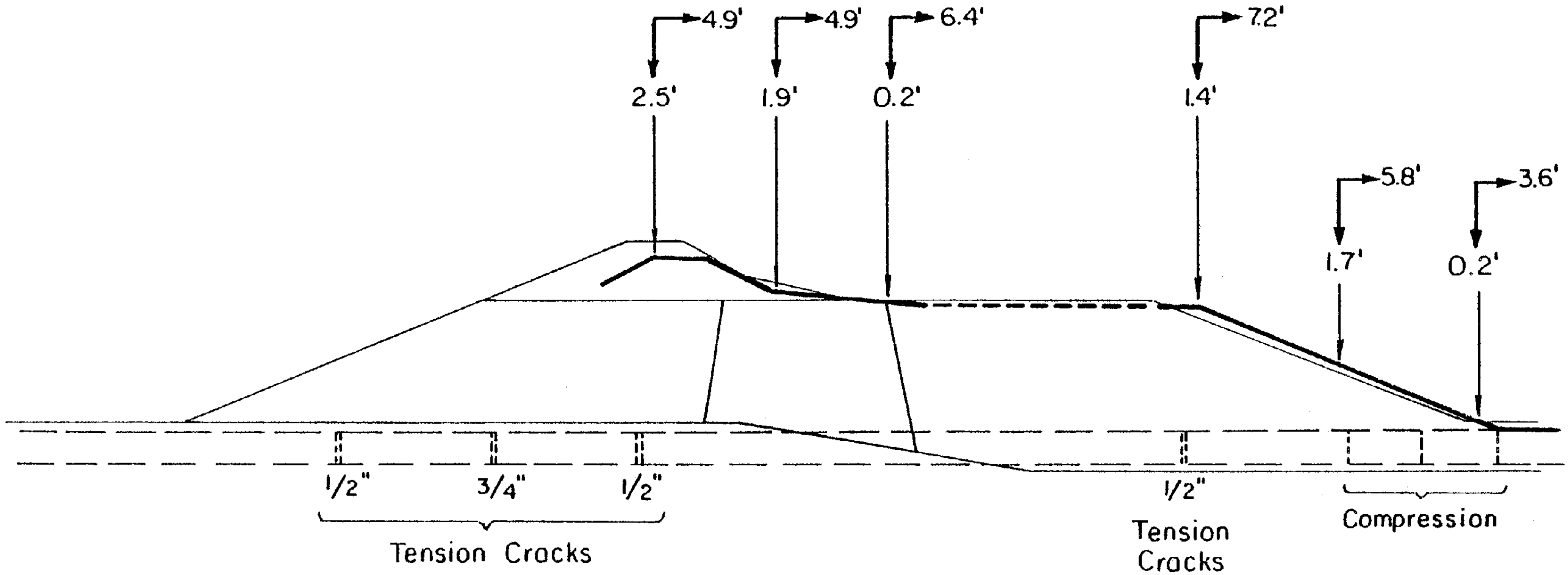

[displacements in feet]

FIG. 4.4 DISPLACEMENTS MEASURED AFTER EARTHQUAKE of the crest was 4.9 feet downstream and 2.5 feet vertically downward. The horizontal movements were progressively larger toward the downstream end of the berm where the displacement was 7.2 feet. Settlement was 2.5 feet at the crest and 1.4 feet at the downstream edge of the berm, but only 0.2 feet at the toe of the rolled fill section. Unfortunately, this is the only measured movement of the central core section of the dam and so the maximum amount of heaving is not known. The measured displacement at the middle of the slope was 5.8 feet downstream with 1.7 feet vertical settlement, and the measured displacements at the downstream toe were 3.6 feet horizontal downstream movement and 0.2 feet vertical heaving. A 2-foot high pressure ridge was reported to have developed at the downstream toe of the dam -- though this ridge may have occurred in the hydraulic fill blanket somewhere below the toe of the dam. No measurements were made on the upstream slope.

Static and Dynamic Analysis of the Dam

Soil Properties

The field investigation carried out as a preliminary to the stability analysis of the Upper San Fernando Dam consisted of borings, trenches, and seismic surveys (Seed et al., 1973). Trenching showed the hydraulic fill to be made up of alternating layers of fairly clean sand and silty to clayey sands, with occasional layers of clay. Layering was most pronounced at the outer edge of the embankment where the material was generally coarser, while at the center of the embankment layering was not evident and the material was a fine sandy silt with some clay. Gradation curves of the material taken from the bottom of a transverse trench cut into the downstream berm are shown in Fig. 4.5. A cross-section through the middle of the embankment

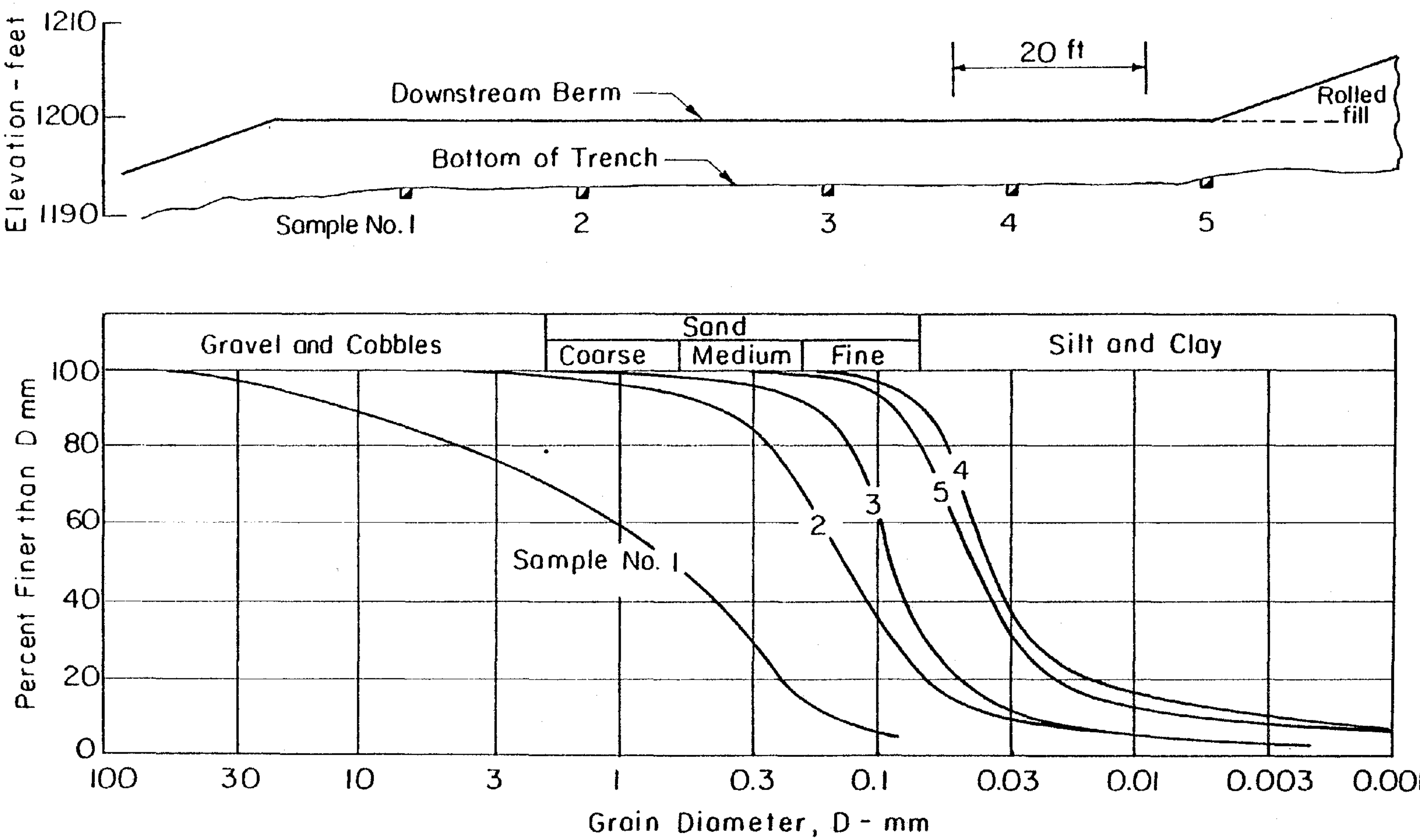

FIG. 4.5 DISTRIBUTION OF GRAIN SIZES IN HYDRAULIC FILL FROM OUTER SHELL TOWARDS CENTER OF EMBANKMENT - UPPER SAN FERNANDO DAM (after Seed et al)

showing the locations of some of the borings and the materials encountered is shown in Fig. 4.5.

Static Analysis

A static finite element analysis was performed by Seed et al. (1973) as a preliminary step in the stability analysis of the Upper San Fernando Dam. The analysis, using nonlinear soil properties and in which construction conditions are simulated by progressively adding layers of elements to the model, is described fully in Chapter 2 and by Kulhawy, Duncan, and Seed (1969). This analysis, which includes seepage forces, gives the stress conditions acting in the dam prior to the earthquake. The initial stresses determined for each element are later used in conjunction with the dynamic analysis and laboratory testing program to calculate the strain potential for the element. The finite element mesh used is shown in Fig. 4.6. The nonlinear soil properties used are shown in Table 4.1. The contours of horizontal stress and strain (σ_x & ε_x) and shear stress and shear strain (τ_{xy} & γ_{xy}) are shown in Fig. 4.7 and 4.8.

Dynamic Analysis

The dynamic finite element analysis performed on the Upper San Fernando Dam is described by Seed et al. (1973). The earthquake acceleration history used as input to the dynamic analysis was a modification of the record obtained at Pacoima Dam, with a peak acceleration of 0.6 g (Fig. 4.13). Only the horizontal component of the Pacoima record was used in the analysis since shear stresses caused by vertical motions are insignificant compared to those caused by the horizontal motions. Also, the change in pore water pressure caused by vertical motions is small compared to that caused by horizontal motions. Since it is the weakening of the soil due to pore-water pressure

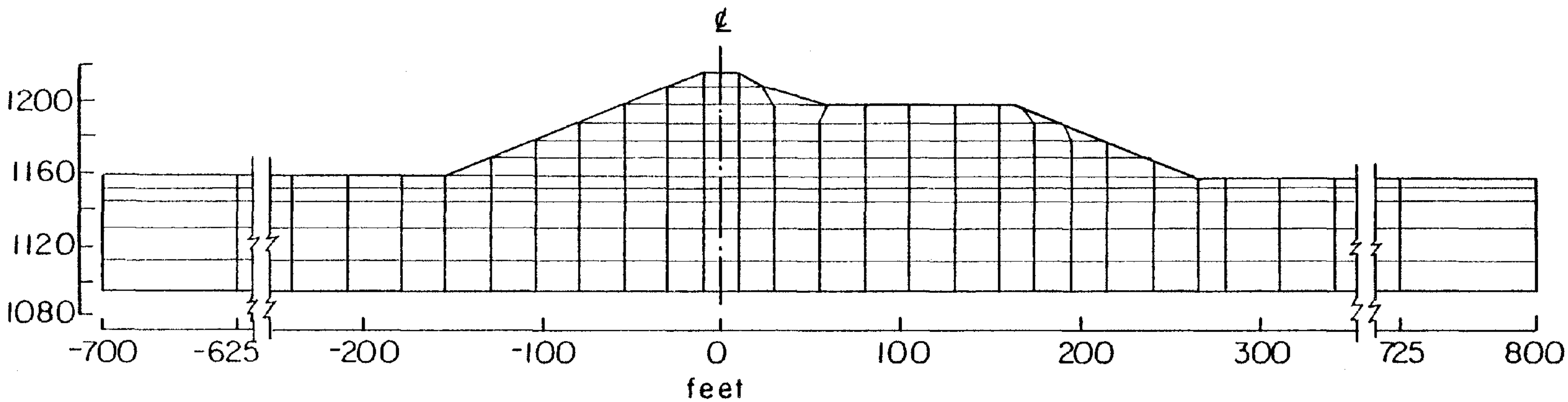

FIG. 4.6 FINITE ELEMENT MESH USED IN DEFORMATION ANALYSIS

Table 4-1

Soil Parameters Used in Nonlinear Static Analysis

Upper San Fernando Dam

Soil Parameter	Symbol	Values used in Analysis			
		Rolled Fill	Hydraulic Fill	Clay Core	Foundation Layer
Dry Unit Weight	γ_d (pcf)	125	100	100	107
Buoyant Unit Weight	γ_b (pcf)	78	60	60	67
Cohesion	c (psf)	2600	0	0	0
Friction Angle	ϕ	25°	37	37	37
Modulus Number	K	300	420	420	280
Modulus Exponent	n	0.76	0.52	0.52	0.80
Failure Ratio	R_f	0.90	0.78	0.78	0.66
Poisson's Ratio Parameters	G	0.30	0.33	0.33	0.32
	F	0.10	0.12	0.12	0.10
	d	3.8	10	10	9

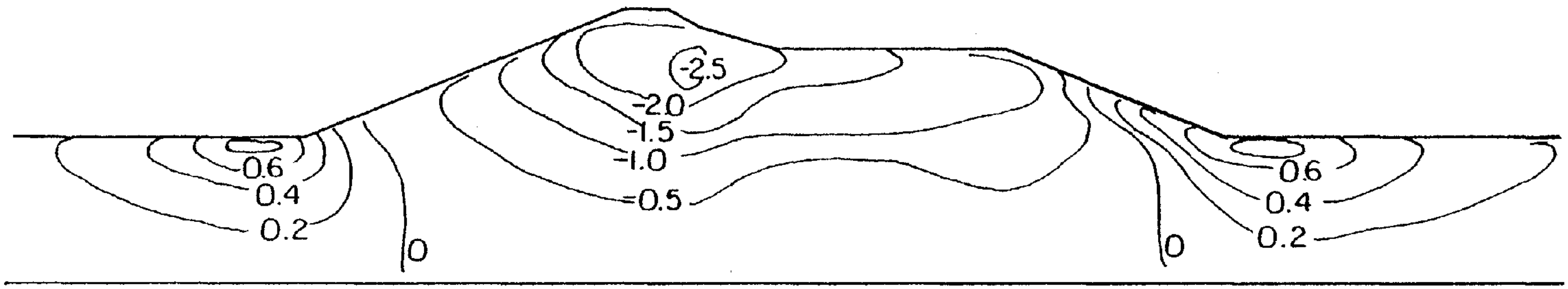

Horizontal Strain (ε_x) - percent

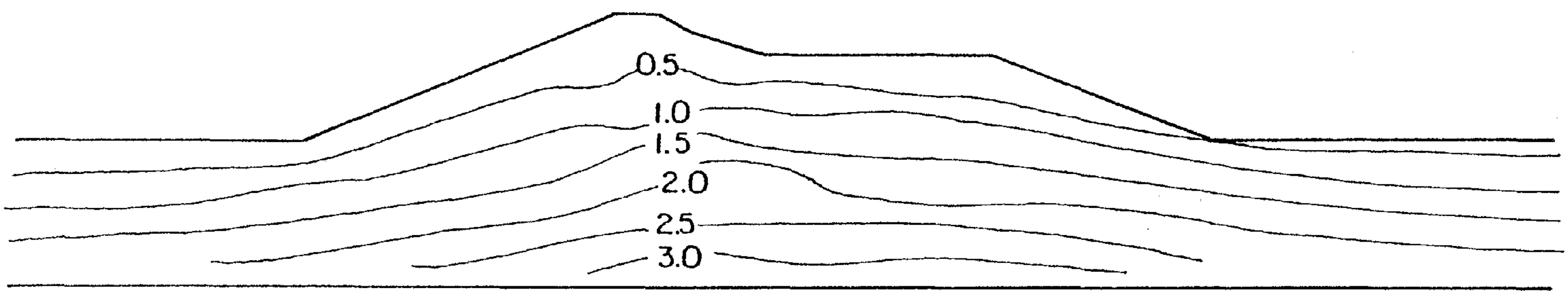

Normal Stress on Verticle Plane (σ_x) - tons / sq.ft.

FIG. 4.7 STRESS AND STRAIN IN EMBANKMENT BEFORE EARTHQUAKE

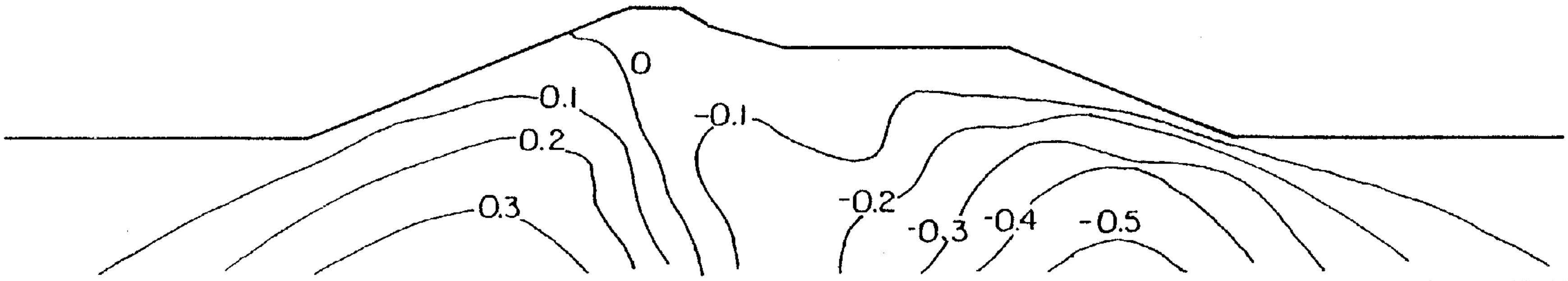

Shear Stress on XY-plane, τ_{xy} – tons/sq.ft.

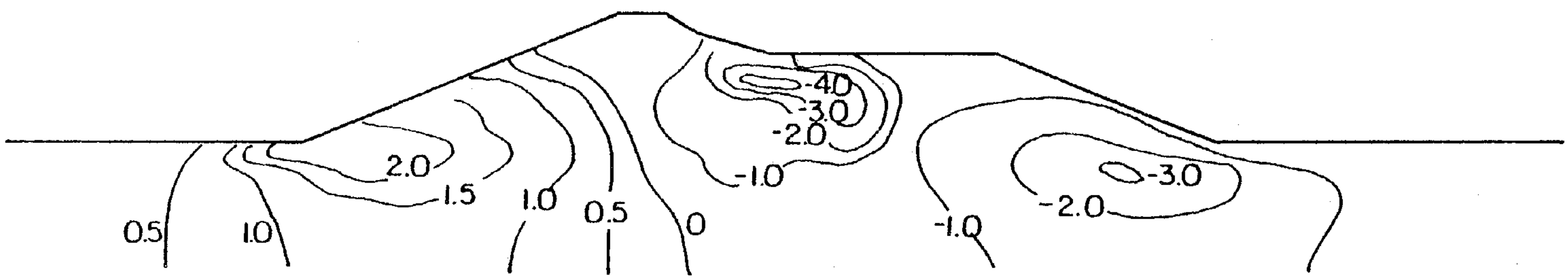

Shear Strain on XY- plane, γ_{xy} – percent

FIG. 4.8 STRESS AND STRAIN IN EMBANKMENT BEFORE EARTHQUAKE increases which permits significant deformations to occur during the earthquake, the neglect of the vertical component of ground motion is felt to have little effect on the results.

The method used is described fully in Chapter 2 of this report. The mesh was the same as that used for the static analysis. In conjunction with this analysis, cyclic triaxial tests were performed on all materials of the dam, under a range of consolidation conditions and cyclic loads. By comparing an element of the dam with a sample in the laboratory under the same initial stress conditions and cyclic stress history, interpolating as necessary, it is possible to determine a strain potential for each element of the dam. The results of the dynamic analysis, expressed as strain potential values, are shown in Figs. 4.10 and 4.11.

Analysis of Permanent Deformations

Approximate Method

The first attempt to approximate the deformations of the Upper San Fernando Dam was made by Seed et al. (1973). The average shear strain potential for a vertical section at the center of the dam was multiplied by the section height to obtain a first estimate of the downstream movement of the crest, as shown in Fig. 4.12. The value calculated for the horizontal downstream movement was approximately 6 feet. This method of analysis does not permit computation of vertical movements.

Linear Modified Modulus Analysis

Permanent deformations of the Upper San Fernando Dam may also be computed by the linear gravity turn-on analysis procedure. In this procedure it is assumed that the effect of the earthquake on the dam is a

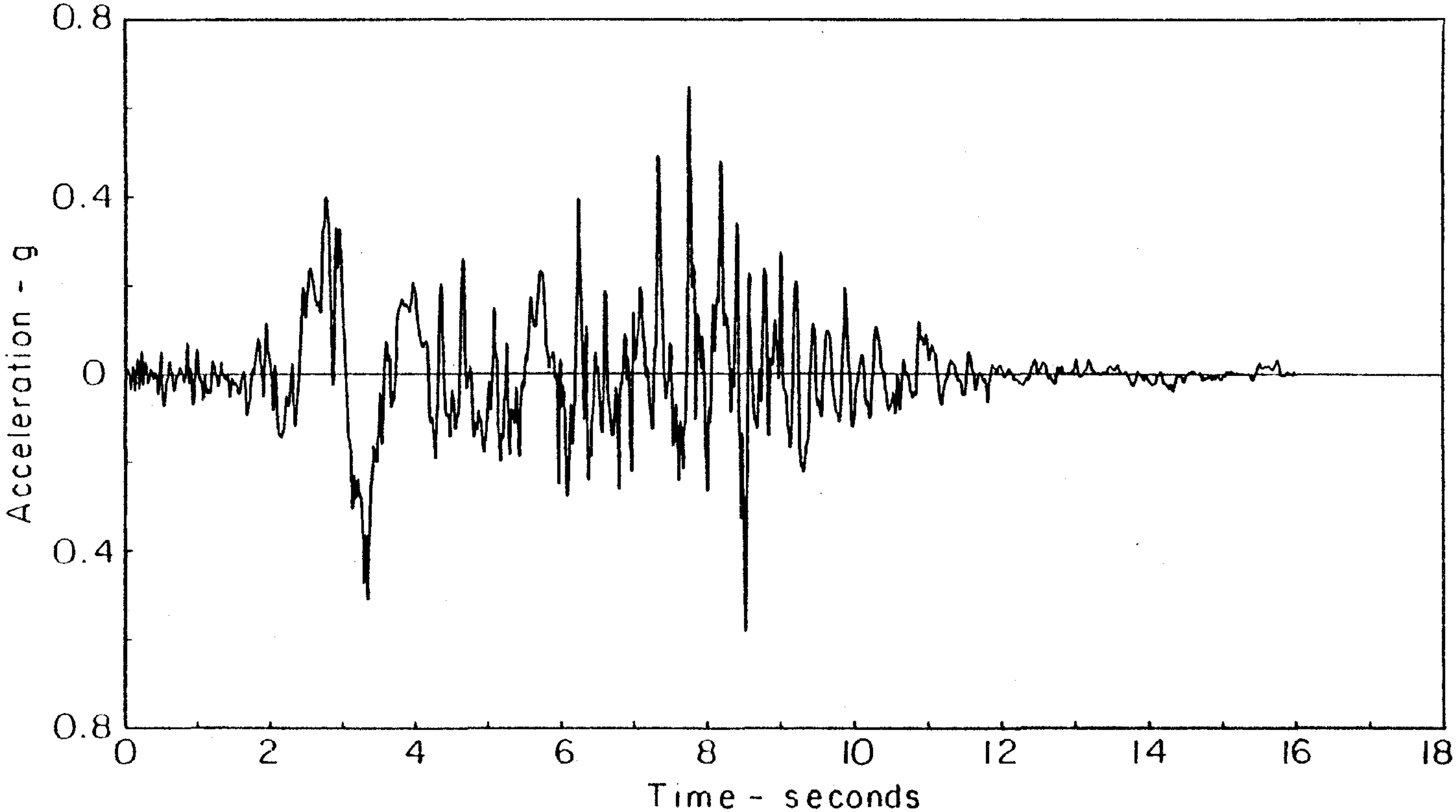

MODIFIED PACOIMA RECORD

FIG. 4.9 TIME HISTORY OF ACCELERATION IN BASE ROCK

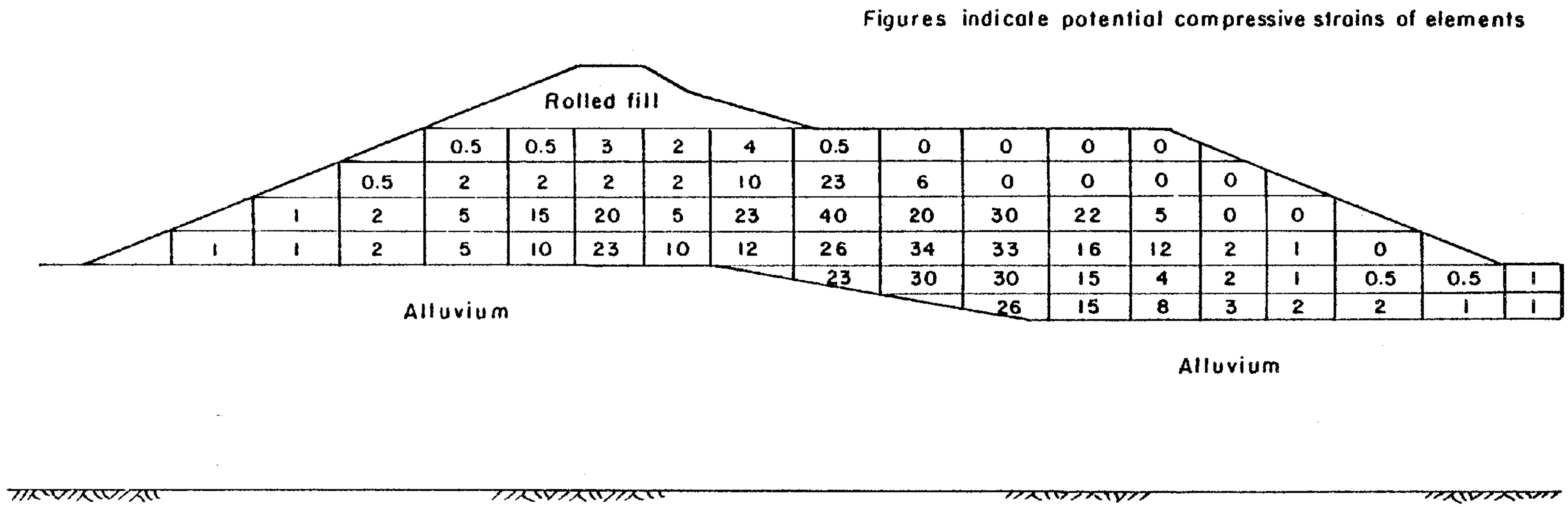

FIG. 4.10 STRAIN POTENTIAL IN HYDRAULIC FILL - UPPER SAN FERNANDO DAM
(after Seed et al)

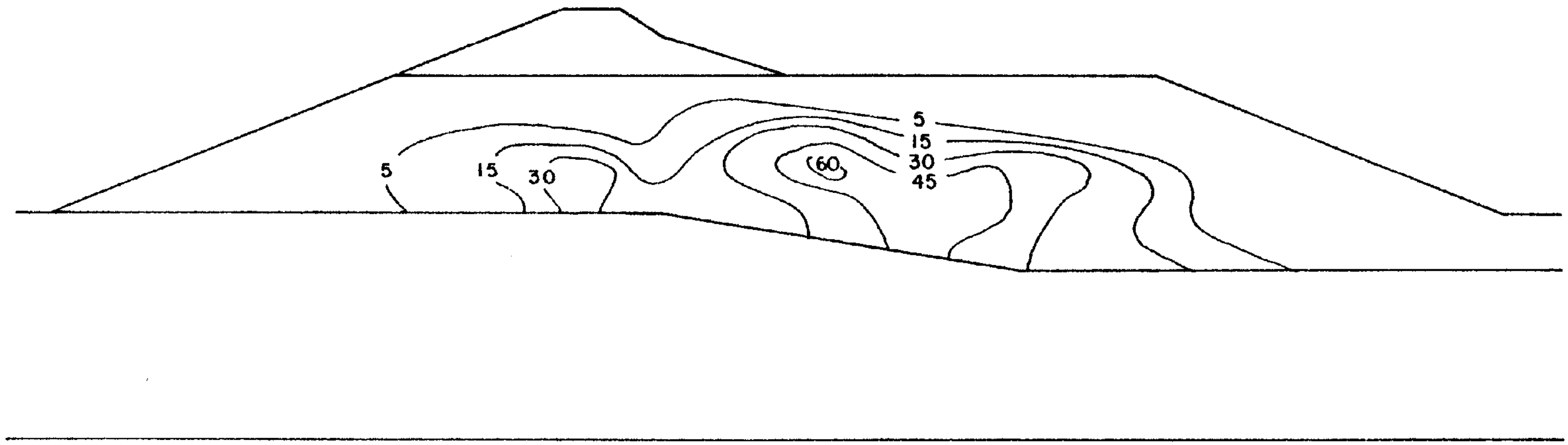

FIG. 4.11 CONTOURS OF SHEAR STRAIN POTENTIAL (PERCENT) IN HYDRAULIC FILL

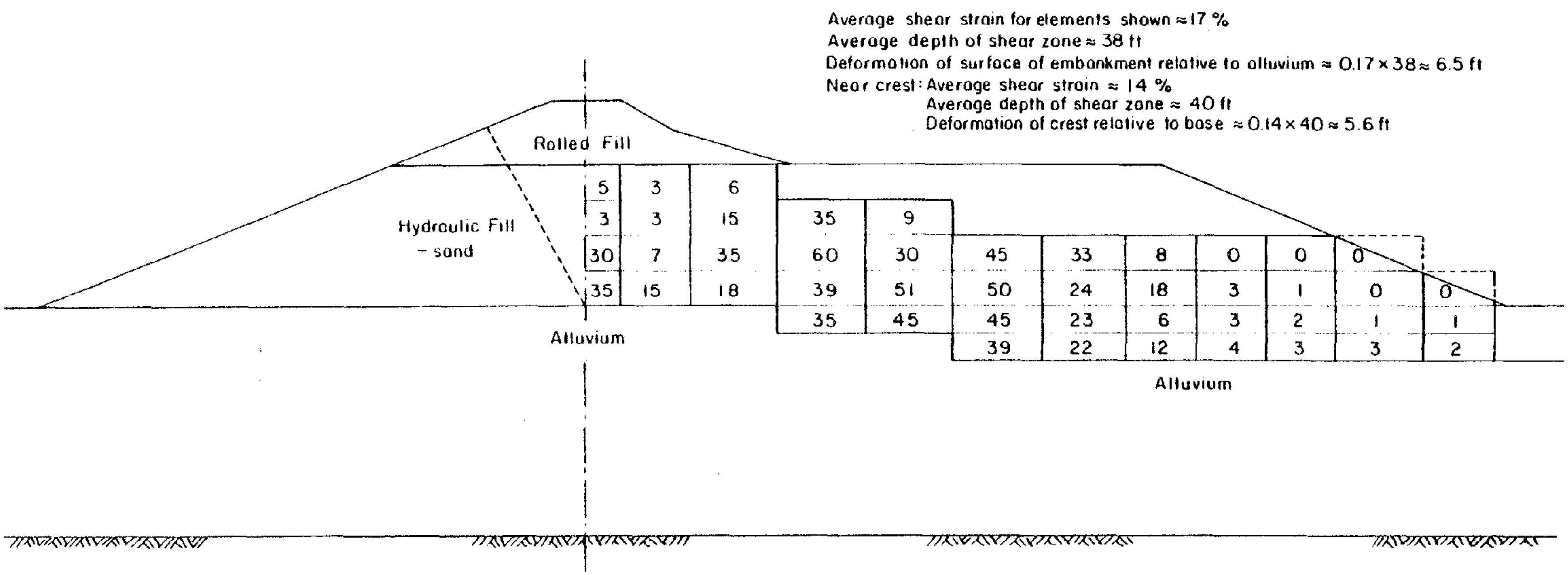

FIG. 4.12 DISTRIBUTION OF SHEAR STRAIN POTENTIAL VALUES FOR UPPER SAN FERNANDO DAM

weakening of the material due to the cyclic shear strains caused by the earthquake motions. The calculated deformations are the difference in displacements between an analysis made with the initial modulus and one made with modified modulus values. The initial modulus is easily found from the initial stress conditions ($E_i = \sigma_i/\varepsilon_i$). The modified modulus is calculated for each element using the initial stresses and strains and the value of the strain potential for the element. For the present study, the reservoir forces were considered to act on the upstream slope, which was assumed to be impermeable for the duration of the earthquake. The method is more fully described in the previous chapter. The results of the analysis applied to the Upper San Fernando Dam are shown in Fig. 4.13(a). With the exception of points near the crest, the horizontal movement at any point is greater than the vertical movement. However, values are considerably less than the measured displacements, by a factor of approximately 6 for the horizontal displacements and a factor of about 3 for the vertical. Vertical settlement over the core area is less than that in the areas upstream and downstream, indicating that a slight amount of heaving is taking place in the core.

The results of a similar analysis performed independently by K. L. Lee are presented in Fig. 4.13(b). Agreement with the method described above is good, with the exception of the central zone of the dam. This is due to a different technique used by Lee to calculate the strain potentials, which gave considerably higher values in the central core zone.

Nonlinear Modified Modulus Analysis

This analysis is similar to that discussed above, with the exception that nonlinear stress-strain properties are assumed for the soil. Water

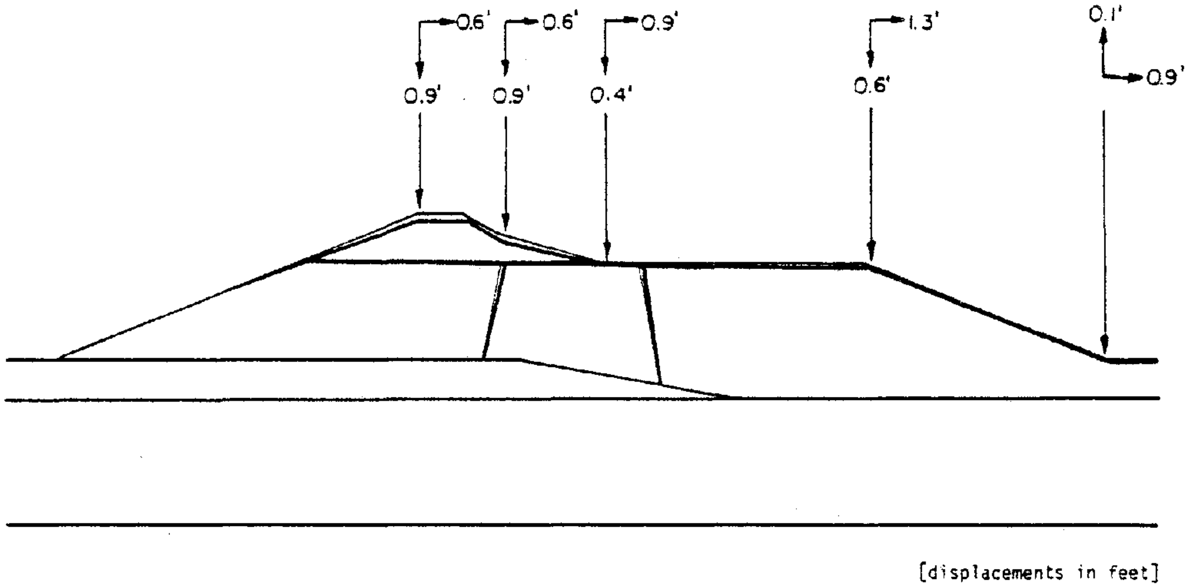

FIG. 4.13(a) CALCULATED DISPLACEMENTS - LINEAR MODIFIED MODULUS METHOD

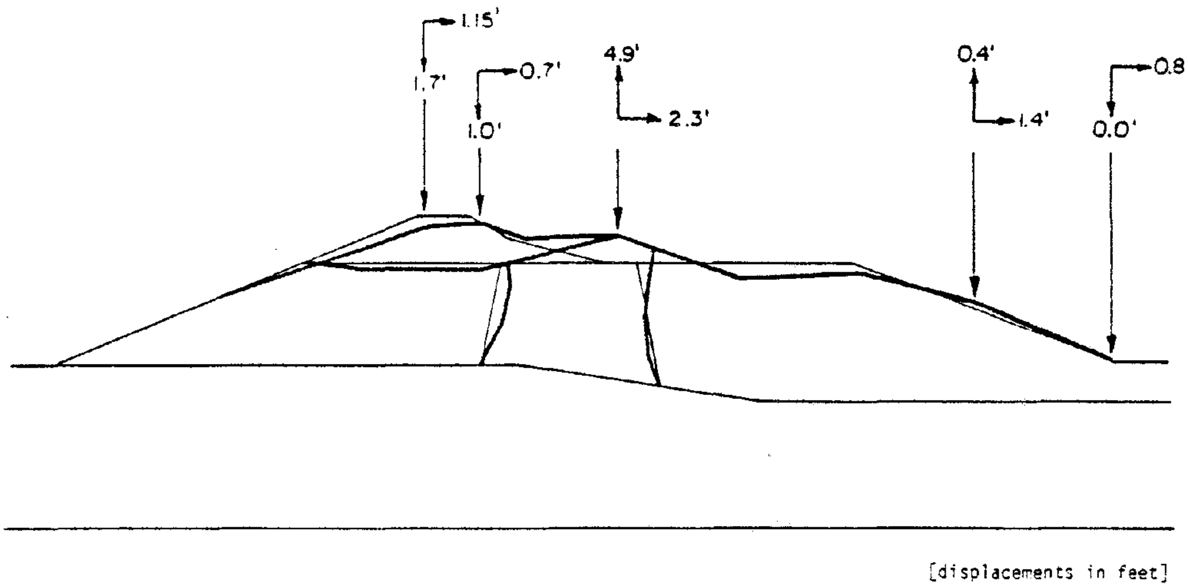

FIG. 4.13(b) CALCULATED DISPLACEMENTS - LINEAR ANALYSIS (after K. L. Lee)

forces were applied to the upstream slope as before, and only the shear modulus of the soil was considered to be affected by the cyclic shear strains. The method is described in detail in the previous chapter. The deformations calculated by this method are shown in Fig. 4.14. Although horizontal deformations are in general about twice as large as those calculated with the linear analysis approach, the overall deformed shape of the embankment is similar. However, computed displacements are still significantly below those measured after the earthquake.

Nonlinear Analysis Using Equivalent Nodal Point Forces

In this method, a set of nodal point forces was applied to the nodes of the finite element mesh to simulate the deforming effect of the earthquake. [In all the finite element analyses, the same mesh was used (Fig. 4.6).] Only one deformation analysis is required in this approach, but it is necessary to know the stress distribution throughout the dam before the earthquake. In the nonlinear analysis used, the strength properties of the soil are a function of the stress, and hence the first step of the deformations analysis is a determination of the initial stress conditions in the dam. A nonlinear incremental load analysis was used for this purpose; however, a study by Lee and Idriss (1975) has shown that a linear analysis can give good results for the initial stress conditions in a dam. The pre-earthquake stress analysis requires a knowledge of the seepage forces acting in the dam before the earthquake; these forces are easily calculated from a flow net, and finite element programs exist for this purpose (Finn, 1967). However, these analyses require the horizontal and vertical components of permeability as input, and no permeability tests were run on the samples obtained from the field investigation at the Upper San Fernando

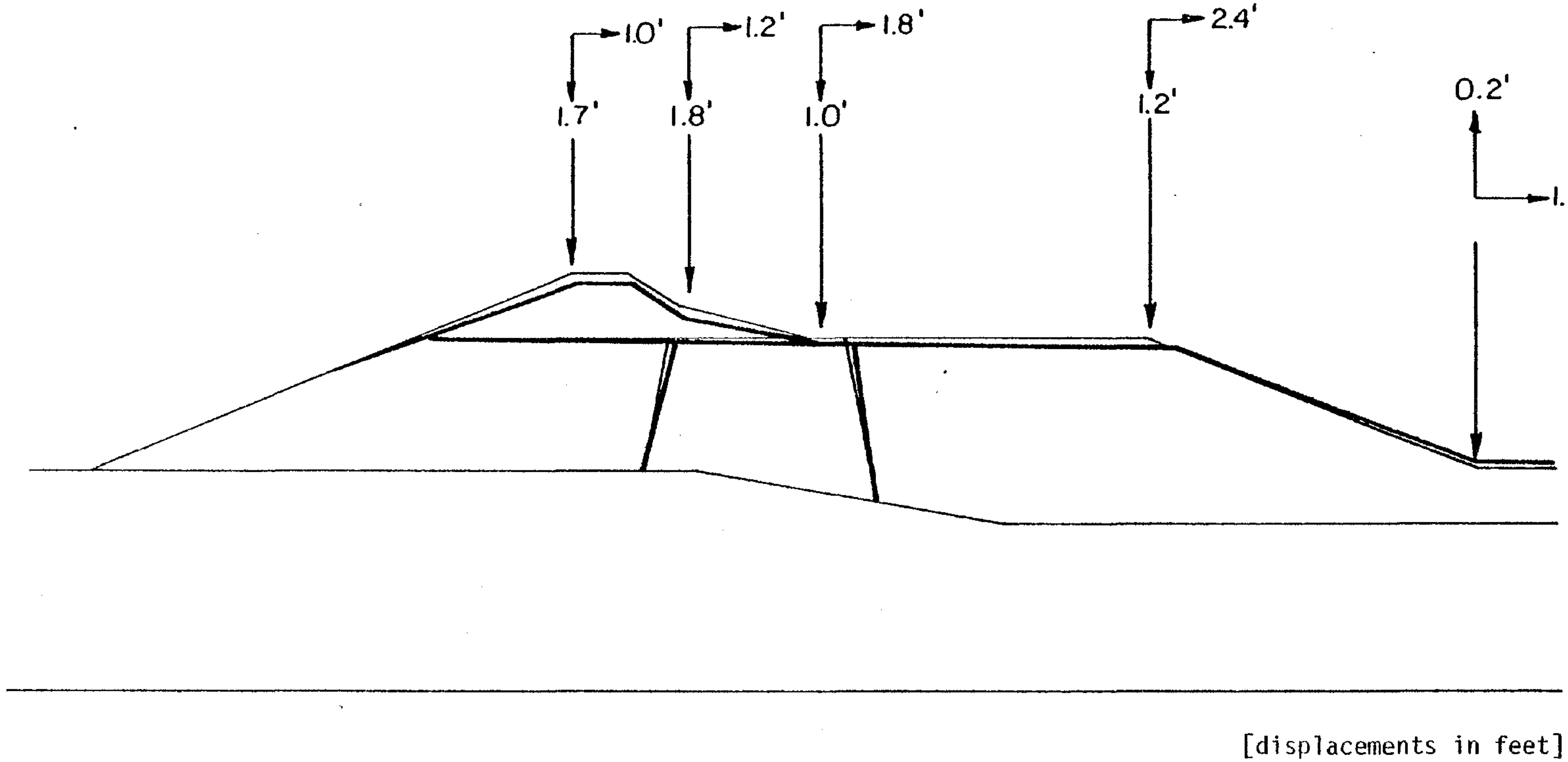

FIG. 4.14 CALCULATED DISPLACEMENTS - NONLINEAR MODIFIED MODULUS METHOD

Dam. Fortunately, water level readings before the earthquake in three piezometers along the middle of the dam are known (Fig. 4.6) and from these an approximation to the phreatic line could be made. Equipotential lines were drawn by dividing the head loss through the dam into equal increments, and from these the magnitude and direction of the seepage forces at each element node below the phreatic line were evaluated. One-quarter the volume of the four surrounding elements is associated with each node. The average gradient was found across this area and the seepage force calculated. The seepage force can be assigned to act at the node in the direction of flow, which was estimated, and then resolved into its horizontal and vertical components to give an estimate of the seepage forces acting in the dam. It can be seen from Fig. 4.6 that the slope of the phreatic line is less in the central part of the embankment, the reverse of what would be expected if the material of the core has a lower permeability than the shell. This may be due to lenses or layers of silt or coarser material traversing the core, a possibility with hydraulic fill type of construction.

As the deformation analysis performed is nonlinear, a knowledge of the nonlinear soil parameters is required. These parameters for the drained condition have already been derived for the static analysis performed on the Upper San Fernando Dam by Seed et al. (1973). These parameters are appropriate to the conditions in the dam before the earthquake. For the saturated soils during the earthquake, excess pore pressure built up by the cyclic shear strains will not have time to dissipate, and hence, undrained conditions exist. Nonlinear soil parameters for these soils were therefore calculated from the results of consolidated-undrained tests. Very few such tests were run on the core material and thus considerable uncertainty exists for the parameters for the clayey core material. The parameters used in this analysis are shown in Table 4.2. In the analysis, undrained parameters were used for material below the phreatic line and also for core material above the phreatic line, as capillary action in the fine core material makes use of these parameters more meaningful. Drained parameters were used elsewhere in the embankment.

A full description of the deformation analysis procedure is given in the previous chapter. Using the nonlinear, undrained stress-strain parameters shown in Table 4.2 and nodal point forces representative of the computed earthquake-induced strain potentials presented in Fig. 4.10, the embankment deformations were computed by the incremental non-linear approach using the program DEFORM-2 and the deformed shape together with the original section are presented in Fig. 4.15. In this computation a zone which is located downstream of the toe of the embankment (see Fig. 4.15) and which was found to have liquefied during the earthquake (as evidenced by sand boils at the ground surface) was assigned very low modulus values to simulate the loss of shearing resistance due to liquefaction. As can be seen from Fig. 4.15, the computed deformations are again much lower than those observed during the earthquake (Fig. 4.15), although they are qualitatively in reasonable agreement in terms of the direction of horizontal movement and vertical settlement at most locations in the embankment. The computed deformations were of the order of 1/4 to 1/5 of those measured after the earthquake. The results of a similar analysis using the procedure illustrated schematically in Fig. 3.5 and embodied in the program DEFORM-1 are shown in Fig. 4.16. Again the computed movements are considerably less than those observed.

However, it was noted in these analyses that significant tension zones

Table 4-2

Soil Parameters Used in Nonlinear Deformation Analysis (Equivalent Force Method)

Soil Parameter	Symbol	Values Used in Deformation Analysis						
		Rolled fill		Hydraulic fill		Clay core		Foundation Layer
		above WT	below WT	above WT	below WT	above WT	below WT	
Unit Weight (pcf)	γ	125	72	120	62	104	48	67
Cohesion (psf)	c	2600	1300	0	550	1000	1000	710
Friction Angle	°	25	20	37	24	0	0	32
Modulus Number	K	300	100	420	100	102	70	80
Modulus Exponent	n	0.76	0.76	0.52	0.66	1.76	1.16	116
Failure Ratio	R_f	0.90	0.90	0.78	0.76	0.87	0.88	0.7
Poisson's Ratio Parameters	G	0.30	0.49	0.33	0.49	0.40	0.49	0.49
	F	0.10	0	0.12	0	0	0	0
	d	3.80	0	10.0	0	0	0	0

Notes: (1) buoyant weight used for soils below the water table

(2) data from consolidated-undrained tests (CU) used to determine parameters for soils below the water table (soil assumed impermeable during the earthquake)

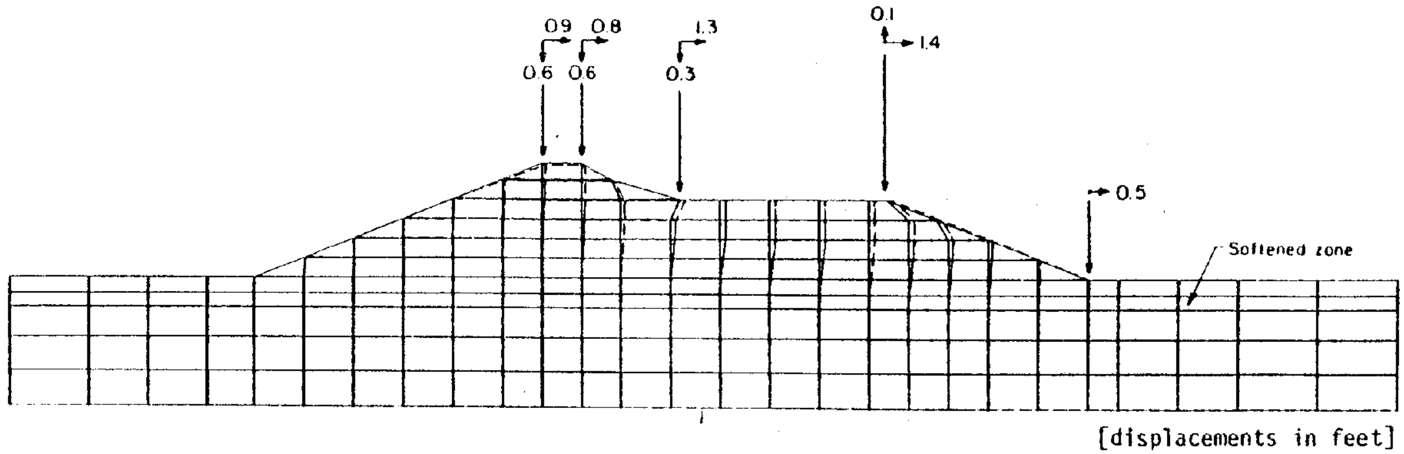

FIG. 4.15 COMPUTED DISPLACEMENTS USING NODAL POINT FORCE ANALYSIS (DEFORM-2)

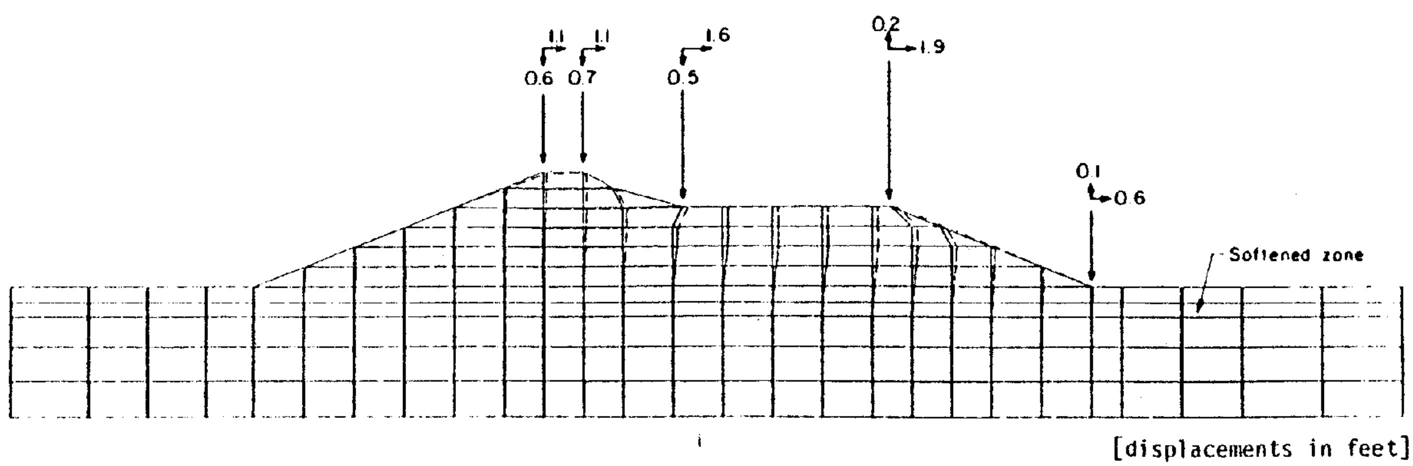

FIG. 4.16 COMPUTED DISPLACEMENTS USING NODAL POINT FORCE ANALYSIS (DEFORM-1)

developed in the dam, requiring the use of some computational modifications to simulate the cracking which would develop under these conditions. In fact, in making such analyses a special problem arises with elements near the center-line of the embankment where the initial shear stresses are zero. On either side of this zone, nodal point forces are applied, acting in the direction of the initial horizontal static shear stresses. Thus, elements upstream of the center-line are subjected to nodal point forces acting upstream, while elements downstream of the center-line are subjected to nodal point forces acting downstream. As a result, the central section of the core tends to hold the two sides together and is placed in a condition of tension. This is a fictitious condition since the soil would tend to fail in tension rather than hold the two sides of the embankment together. It may be noted that there was physical evidence of tension cracks in this zone following the earthquake.

As it is difficult in the present finite element analyses to correctly simulate the formation of tension cracks without the use of special joint elements, it was assumed that the above mechanism could be simulated approximately by a softening of the column of elements located in the central portion of the embankment where the tension cracks are expected to form. Accordingly, the computations were repeated with very low modulus values assigned to a column of elements located near the center-line of the embankment as shown in Fig. 4.17. The results for both the nonlinear and the equivalent linear modulus procedures are presented in Figs. 4.17 and 4.18. Again the displacements computed using the equivalent linear modulus procedure were about 30 to 40 percent higher than those using the non-linear procedure. However, the computed deformations in both procedures were found to be about twice to three times the values estimated earlier for the case where no simulation of the formation of tension cracks was attempted. A

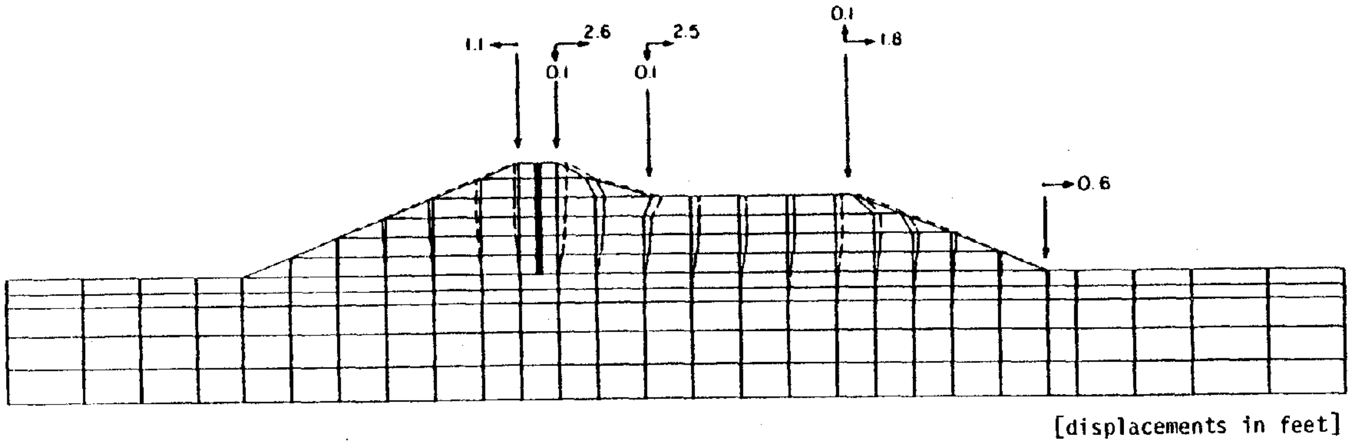

FIG. 4.17 COMPUTED DISPLACEMENTS USING NODAL POINT FORCE ANALYSIS (DEFORM-2) WITH SOFT CENTRAL ZONE

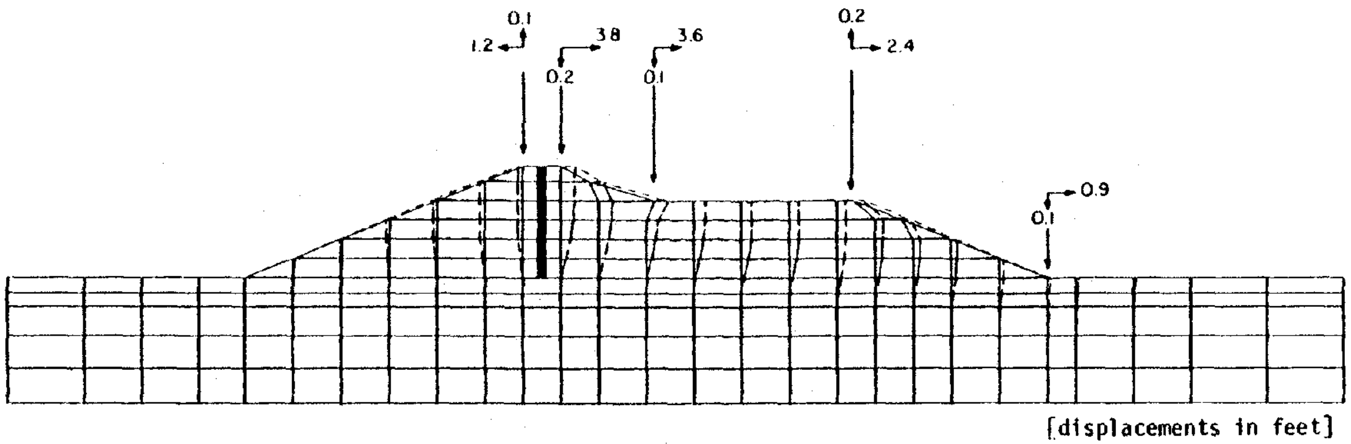

FIG. 4.18 COMPUTED DISPLACEMENTS USING NODAL POINT FORCE ANALYSIS (DEFORM-1) WITH SOFT CENTRAL ZONE

comparison with the observed deformations in Fig. 4.4 shows that the computed results for the equivalent linear modulus procedure (Fig. 4.18) ranged from about 60 to 70 percent of the observed values near the crest and central portions of the embankment to about 30 percent at the downstream edge of the berm and the toe of the embankment. Considering the relative horizontal movement between the two points at the crest located on either side of the centerline of the embankment, Fig. 4.18 shows a total relative displacement of about 5 feet. This is analogous to the formation of an open longitudinal tension crack along the crest of the dam. Any tendency for a crack of such dimension to form would undoubtedly allow wedges on the upstream portion to slip into a configuration similar to that shown schematically in Fig. 4.19 providing a distorted section very similar to that observed during the earthquake.

In fact, from an examination of the multiple shear scarps on the upstream slope of the embankment after the earthquake (Fig. 4.2), it seems reasonable to believe that such a deformation pattern may have resulted from a failure mechanism similar to that proposed above. Thus, due to the inertia forces induced by the earthquake, longitudinal tension cracks might be expected to tend to open up along the crest of the embankment due to the tendency of the main body of the dam to move downstream; these cracks may extend to various depths depending on the magnitude of the inertia forces. As a result of this condition several wedges of the upstream portion of the embankment would then tend to slip in the downstream direction to fill up the resulting gaps. Such a mechanism, shown schematically in Fig. 4.19 would explain the formation of the observed shear scarps on the upstream face of the embankment after the earthquake.

Although the analytical approach described above is based on a number

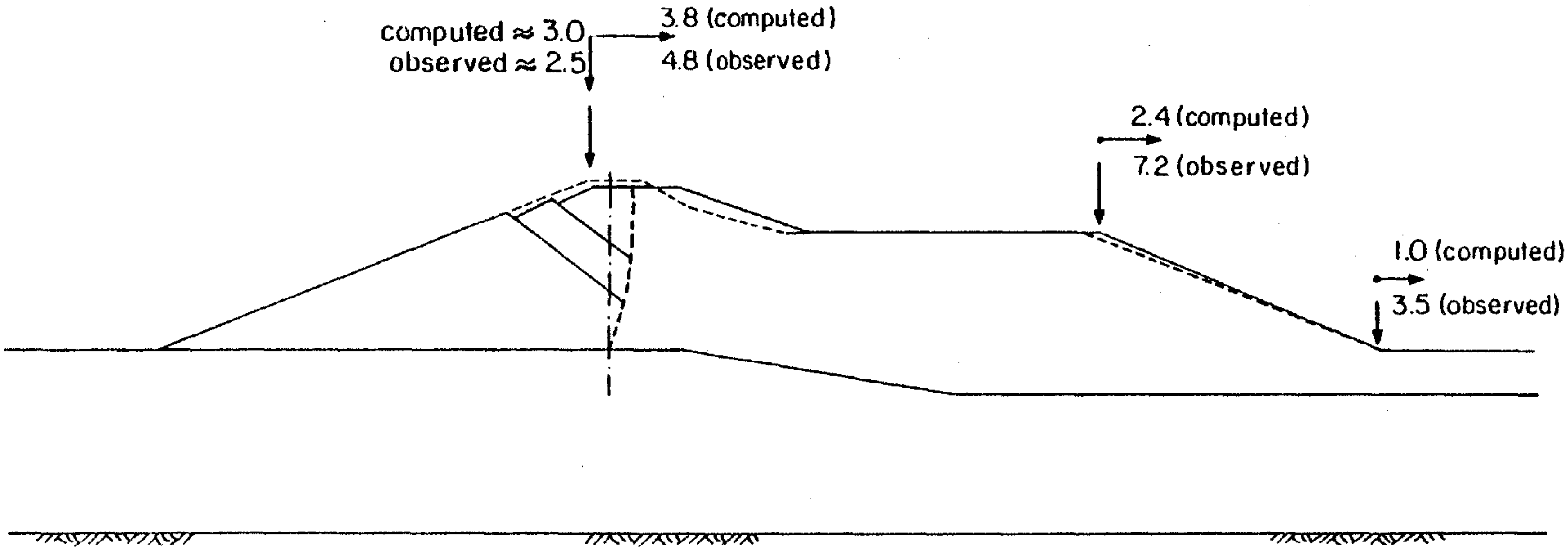

[displacements in feet]

FIG. 4.19 SCHEMATIC CONCEPT OF DEFORMATIONS OF UPPER SAN FERNANDO DAM of simplifying assumptions and approximations and the exercise of some degree of judgment, considering the uncertainties in the material properties used in the analysis, it appears to provide a reasonable assessments of the deformations of the Upper San Fernando Dam during the earthquake and a basis for evaluating deformations in other dams where major movements are likely to occur. When movements are relatively small, the use of the program DEFORM, in either of the two formulations presented, would seem to provide a reasonable basis for assessing the overall deformed shape of an earth dam due to earthquake shaking.

Chapter 5

Summary and Conclusions

Summary

The deformations induced in the Upper San Fernando Dam by the earthquake of February 9, 1971, were studied by four different methods and the results compared with the deformations measured shortly after the earthquake.

The first method was a direct use of the strain potentials to obtain an approximation of the downstream movement of the crest, and was first used by Seed et al. (1973). Horizontal movements only can be calculated.

The second and third methods were linear and nonlinear analyses respectively, and used a reduced value of the modulus for the soil in conjunction with gravity loading to simulate the earthquake effects. Deformations calculated by the linear method (Lee, 1974) were too low; those calculated by the nonlinear method were higher, but still well below the measured values.

The fourth method, a pseudo-static approach using nonlinear soil properties, gave results in reasonable agreement with the measured deformations, where the upstream and downstream parts of the embankment were allowed to move relative to each other through the introduction of a softened core. This method is basically a pseudo-static technique in which the potential shear strains induced in elements of the dam are used with the nonlinear stress-strain properties to determine the corresponding shear stress changes. Forces are calculated which, if acting at the element nodes, would produce the same changes in shear stress. These forces are then applied to the nodes of the mesh and the resulting deformations are calculated.

A number of assumptions were made in formulating the method. To calculate the stress change due to the induced strain it was necessary to assume that the confining pressure remains constant during the earthquake and that equivalent nodal point forces act in the direction of the pre-earthquake horizontal shear stresses. The horizontal plane is considered the most critical in the dam, and the shear stresses acting on this plane are considered to have the major effect on the behavior of the dam during the earthquake. These shear stresses are assumed to be the maximum shear stresses.

The applied nodal point forces represent all the forces acting on the dam during the earthquake, as the strain potential calculated in the dynamic analysis is a function of all the forces. Gravity and seepage forces are included in the stresses under which laboratory samples are consolidated. The inertia forces during the earthquake are represented by the cyclic stress applied to the sample.

In the nonlinear stress-strain formulation used in the analysis, the modulus of the soil is a function of the confining pressure. If tensile stresses occur, the modulus of the soil is reduced to a very low value in the analysis, and the surrounding elements are forced to assumed the extra load. Soils in general cannot take tension, requiring the use of special elements or a softened zone near the axis of the embankment to allow for this effect.

It should be noted that during the analysis of the Upper San Fernando Dam using the softened soil concept and gravity load procedure, large vertical settlements were calculated in the soft clay core under the downstream toe of the rolled fill section. The resulting deformation created tension in the rolled fill causing instability in the analysis. It appears to be a limitation of such analyses that adjacent zones of very different strength cannot be handled. In the analysis of the Upper San Fernando Dam the modulus number of the rolled fill had to be reduced to overcome this problem. As the major deformation occurred in the hydraulic fill, the softening of the rolled fill would not appreciably affect the calculated displacements of the dam.

In embankments of the type studied the potential strains may be very large. The theory of the finite element method used is based on small strains, and hence some error is introduced into the analysis due to this cause. Nevertheless the method appears to provide a reasonable basis for assessing the deformed shape of an embankment dam due to earthquake shaking with a sufficient degree of accuracy for most practical purposes.

References

Ambraseys, N. N. (1960) "On the Shear Response of a Two-Dimensional Truncated Wedge Subjected to an Arbitrary Disturbance," Bulletin of the Seismological Society of American, Vol. 50, No. 1, January, pp. 45-52.

Ambraseys, N. N. and Sarma, S. (1967) "The Response of Earth Dams to Strong Earthquakes," Geotechnique, Vol. XVII, No. 3, September.

Berg, G. V. and Housner, G. W. (1961) "Integrated Velocity and Displacement of Strong Earthquake Ground Motion," Bulletin of the Seismological Society of America, Vol. 51, No. 2, April, pp. 175-189.

Clough, R. W. and Chopra, A. K. (1966) "Earthquake Stress Analysis in Earth Dams," Journal of the Engineering Mechanics Division, ASCE, Vol. 2, No. EM2, Proc. Paper 4793, April.

Clough, R. W. and Woodward, R. J. (1967) "Analysis of Embankment Stresses and Deformations," Journal of the Soil Mechanics and Foundation Division, ASCE, Vol. 93, No. SM4, July, pp. 529-549.

DeAlba, P., Chan, C. K., and Seed, H. B. (1975) "Determination of Soil Liquefaction Characteristics by Large Scale Laboratory Test," Report No. EERC 75-14, Earthquake Engineering Research Center, University of California, Berkeley.

Desai, C. S. and Abel, J. F. (1972) "Introduction to the Finite Element Method," Van Nostrand Reinhold Co., New York.

Dibaj, J. and Penzien, J. (1967) "Dynamic Response of Earth Dams to Travelling Seismic Waves," Report No. TE 67-3, to the State of California, Department of Water Resources, Institute of Traffic and Transportation Engineering, University of California, Berkeley.

Finn, W.D.L. (1967) "Finite Element Analysis of Seepage Through Dams," Journal of the Soil Mechanics and Foundation Division, ASCE, Vol. 93, No. SM 6, November, pp. 41-48.

Goodman, R. E. and Seed, H. B. (1966) "Earthquake Induced Displacements in Sand Embankments," Journal of the Soil Mechanics and Foundation Division, ASCE, Vol. 92, SM 2, March, pp. 125-146.

Idriss, I. M. and Seed, H. B. (1967) "Response of Earth Banks During Earthquakes," Journal of the Soil Mechanics and Foundation Division, ASCE, Vol. 93, No. SM 3, May, pp. 61-82.

Idriss, I. M., Lysmer, J., Hwang, R. N., and Seed, H. B. (1973) "QUAD4: A Computer Program for Evaluating the Seismic Response of Soil Structures by Variable Damping Finite Element Procedures," Report No. EERC 73-16, Earthquake Engineering Research Center, University of California, Berkeley (July).

Janbu, N. (1963) "Soil Compressibility as Determined by Oedometer and Triaxial Tests," Proceedings, European Conference on Soil Mechanics and Foundation Engineering, Vol. 1, Weisbaden, pp. 19-25.

Kondner, R. L. (1963) "Hyperbolic Stress-Strain Response: Cohesive Soils," Journal of the Soil Mechanics and Foundation Division, ASCE, Vol. 89, No. SM 1, February, pp. 115-143.

Kulhawy, F. H., Duncan, J. M., and Seed, H. B. (1969) "Finite Element Analysis of the Stresses and Movements in Embankments During Construction," Geotechnical Engineering Report No. TE 69-4, Department of Civil Engineering, University of California, Berkeley.

Lee, K. L. (1974) "Seismic Permanent Deformations in Earth Dams," Report to the National Science Foundation, School of Engineering and Applied Science, University of California, Los Angeles, December.

Lee, K. L. and Chan, K. (1972) "Numbers of Equivalent Significant Cycles in Strong Motion Earthquakes," Proceedings of the Microzonation Conference, Seattle, Vol. II, pp. 609-627.

Lee, K. L. and Idriss, I. M. (1975) "Static Stresses by Non-Linear Methods," Journal of the Geotechnical Engineering Division, ASCE, Vol. 101, No. GT 9, September, pp. 871-887.

Lee, K. L. and Walters, H. G. (1973) "Earthquake Induced Cracking of Dry Canyon Dam," Proceedings of the Fifth World Conference on Earthquake Engineering, Rome, Italy.

Lowe, J. and Karafiath, L. (1959) "Stability of Earth Dams Upon Drawdown," Proceedings of the First Panamerican Conference on Soil Mechanics and Foundation Engineering, Mexico, September 1959, pp. 537-552.

Lysmer, J., Udaka, T., Seed, H. B., and Hwang, R. N. (1974) "LUSH: A Computer Program for Complex Response Analysis of Soil-Structure Systems," Report No. EERC 74-4, Earthquake Engineering Research Center, University of California, April.

Martin, G. R., Finn, W.D.L., and Seed, H. B. (1974) "Fundamentals of Liquefaction Under Cyclic Loading," University of British Columbia, Department of Civil Engineering, Soil Mechanics Series No. 23.

Mononobe, N., Takata, A., and Matamura, M. (1936) "Seismic Stability of the Earth Dam," Transactions, Vol. 4, Second Congress on Large Dams, Washington, D.C.

Newmark, N. M. (1965) "Effects of Earthquakes on Dams and Embankments," Geotechnique, Vol. 15, No. 2, June, pp. 139-173.

Ozawa, Y. and Duncan, J. M. (1973) "ISBILD: A Computer Program for Analysis of Static Stresses and Movements in Embankments," Geotechnical Engineering Report No. TE 73-4, University of California, Berkeley, December.

Peacock, W. H. and Seed, H. B. (1968) "Sand Liquefaction Under Cyclic Loading Simple Shear Conditions," Journal of the Soil Mechanics and Foundation Division, ASCE, Vol. 94, No. SM 3, May, Proc. Paper 5957.

Seed, H. B. (1966) "Method of Earthquake Resistant Design of Earth Dams," Journal of the Soil Mechanics and Foundation Division, ASCE, Vol. 92, SM 1, January, pp. 13-41.

Seed, H. B. and Goodman, R. E. (1964) "Earthquake Stability of Slopes of Cohesionless Soils," Journal of the Soil Mechanics and Foundation Division, ASCE, Vol. 90, No. SM 6, November, pp. 43-73.

Seed, H. B. and Idriss, I. M. (1970) "Soil Moduli and Damping Factors for Dynamic Response Analyses," Report No. EERC 70-10, Earthquake Engineering Research Center, University of California, Berkeley, December.

Seed, H. B., Idriss, I. M., and Kiefer, F. W. (1969) "Characteristics of Rock Motions During Earthquakes," Journal of the Soil Mechanics and Foundation Division, ASCE, Vol. 95, No. SM 5, September, pp. 1199-1218.

Seed, H. B., Idriss, I. M., Makdisi, F., and Banerjee, N. (1975) "Representation of Irregular Stress Time Histories by Equivalent Uniform Stress Series in Liquefaction Analysis," Report No. EERC 75-29, Earthquake Engineering Research Center, University of California, Berkeley.

Seed, H. B., Lee, K. L., and Idriss, I. M. (1969) "An Analysis of the Sheffield Dam Failure," Journal of the Soil Mechanics and Foundation Engineering Division, ASCE, Vol. 94, No. SM 6, November.

Seed, H. B., Lee, K. L., Idriss, I. M., and Makdisi, F. (1973) "Analysis of Slides in the San Fernando Dams During the Earthquake of February 9, 1971," Report No. EERC 73-2, Earthquake Engineering Research Center, University of California, Berkeley.

Seed, H. B. and Martin, G. R. (1966) "The Seismic Coefficient in Earth Dam Design," Journal of the Soil Mechanics and Foundation Division, ASCE, Vol. 92, No. SM 3, May, pp. 25-58.

Turner, M. J., Clough, R. W., Martin, H. C., and Topp, L. J. (1956) "Stiffness and Deflection Analysis of Complex Structures," Journal of Aeronautical Science, Vol. 23, pp. 805-823.

Wilson, E. L. and Clough, R. W. (1962) "Dynamic Response by Step-by-Step Matrix Analysis," Symposium on the Use of Computers in Civil Engineering, Lisbon, October.

Wong, K. S. and Duncan, J. M. (1974) "Hyperbolic Stress-Strain Parameters for Nonlinear Finite Element Analyses of Stresses and Movements in Soil Masses," Report No. TE 73-3 to the National Science Foundation, Office of Research Services, University of California, Berkeley, July.

Zienkiewicz, O. C. (1971) "The Finite Element Method in Engineering Science," McGraw-Hill, London.

APPENDIX

Computer Program "DEFORM"

DEFORM is a finite element program used to calculate the permanent deformations induced in an earth dam by an earthquake. The method of analysis is presented in Chapter 3 of this report; the organization of the program, subroutine by subroutine, is described in this Appendix. Instructions for preparing input for the program are also presented, followed by a listing of the program.

The analysis is run in two stages: in the first, the stresses in the dam before the earthquake are calculated, using a nonlinear step-by-step loading technique. The forces acting on the dam, including gravity and seepage forces, are applied gradually in a preselected number of steps, enabling the nonlinear stress-strain curve of the soil to be approximated by a number of straight segments. The stresses calculated in such an analysis are essentially the same as those determined by the more sophisticated technique where the dam is built up in layers to simulate the actual construction conditions (Kulhawy et al., 1969). The displacements calculated by the first stage of the analysis are not used.

The stress-strain curve for each element is a function of the confining pressure and, therefore, changes with each load step. When the stresses at the end of a load increment are determined, the tangent modulus can be calculated and, consequently, the new stiffness matrix can be formed. The stresses at the end of the next load increment are then calculated, but a process of iteration is required to ensure that the curved stress-strain relationship is followed. Two iterations per loadstep were found to give sufficient accuracy and are used in this analysis. Thus, the tangent modulus calculated from the previous load step is used in the first iteration to obtain an intermediate value of the stress increase. A mean value of stress is calculated, a new tangent modulus formed, and the second iteration gives the final stress conditions at the end of the load step.

After the second iteration of the final load step, the final values of modulus and Poisson's ratio are calculated. The stresses will be the stresses acting throughout the dam before the earthquake. By assuming that the confining pressure acting on each element does not change due to the earthquake, and thus the strength curve is constant, the strain potential for an element can be used with the stress-strain curve to find the corresponding change in stress. From the change in element shear stress, a set of equivalent horizontal and vertical nodal point forces are calculated.

The second stage of the analysis is to apply the equivalent forces to the dam. The stresses and strains calculated in the first stage are the starting point for the second stage, but the displacement vector is first initialized to zero. Thus, the displacements calculated are those due to the earthquake, and the stresses and strains at the end of the stage are the conditions in the dam after the earthquake.

Two options are available to compute the displacements due to the application of the equivalent nodal point forces. The first option (referred to as DEFORM-1 in Chapter 4) is to use an equivalent linear modulus estimated from the specified strain potential. The second (referred to as DEFORM-2 in Chapter 4) is to use an incremental nonlinear approach where the load is applied in steps similar to that described for the first stage calculations. Both approaches have been described in detail earlier (Chapter 3).

Material properties used in the first stage will generally be determined from consolidated drained tests. Saturated zones of the embankment may be considered impermeable during the earthquake, and hence material properties derived from consolidated-undrained tests are more appropriate for the second stage of the analysis.

The program DEFORM prints the input data, the stresses, strains, moduli, etc. at the end of each load step, and the equivalent nodal point forces at the end of the first stage. At the end of each load step of the second stage, the displacements, both incremental and cumulative, are also printed.

DEFORM uses a dynamic storage technique where all variable arrays are stored in blank common. This technique uses core storage space most economically. After reading the input data, calculating the band width and allocating storage in blank common, the program transfers control to the subroutine EXEC. From EXEC, subroutines are called which form the load vector for the current load step and also the structure stiffness matrix, taking into account the nonlinear behavior of the soil. Boundary conditions are applied and an equation solver, USOL, is used to calculate the displacements. From these, the strains and stresses are calculated by STRESS and the process is repeated for the second iteration. This procedure is repeated for each load step. After the last load step of the first stage, the equivalent nodal point forces are calculated and substituted for the gravity and seepage forces in the load vector, and the analysis is repeated, resulting in the calculation of the deformations due to the earthquake.

Because in a nonlinear analysis as described in this report the modulus of the soil is a function of the stresses, it is necessary to make an estimate of the stresses corresponding to the initial load step in order to start the analysis. The process of iteration that takes place ensures that the stresses estimated have been corrected by the end of the first load step. The initial estimate of the first load step stresses is made by the subroutine APPROX.

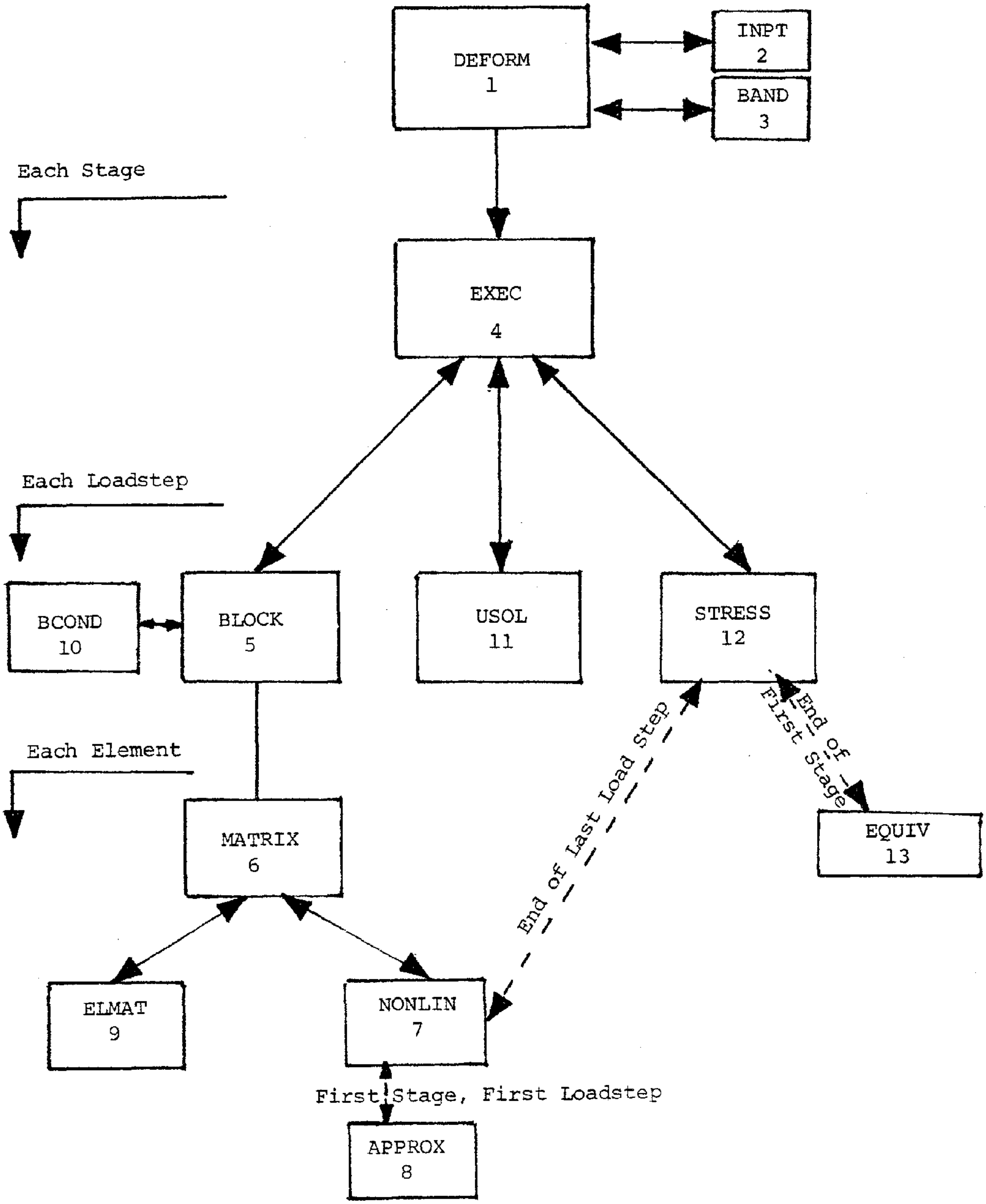

ORGANIZATION OF PROGRAM DEFORM

Organization of Program DEFORM

(1) DEFORM (main program)

(a) Reads initial data required to set dynamic storage

(b) Dynamically assigns core storage to arrays

(c) Calls INPT - input data reader

(d) Calls BAND - band width calculator

(e) Calculates block size and number of blocks

(f) Calls EXEC - the control subroutine

(2) INPT (subroutine)

Reads:

(a) Material properties

(b) Nodal point data

(c) Element data

(d) Coordinates of boundary nodes (used by APPROX)

(e) Strain potentials of elements

(3) BAND (subroutine)

Calculates band width of stiffness matrix

(4) EXEC (subroutine)

Control subroutine

(a) Initializes stress, strain, displacement, and load vectors

(b) Calls BLOCK

(c) Calls USOL to solve simultaneous equations formed by BLOCK

(d) Reads displacements (calculated by USOL) from tape; prints displacement at each iteration punches displacements at end of analysis

(e) Calls STRESS

(f) Repeats steps "b" through "e" for each load step

(5)	BLOCK	Forms the structure stiffness matrix in blocks and stores the blocks sequentially on tape. Forms the load vector in blocks and stores it on tape with the stiffness matrix: (a) Calls MATRIX for each element (b) Adds element stiffness matrices to form structure stiffness matrix (c) Forms structure load vector from gravity loads and seepage forces (first stage) and from equivalent nodal point forces (second stage) (d) Calls BCOND to apply boundary conditions
(6)	MATRIX (subroutine)	(a) Calls NONLIN (b) Forms Hooke's law relationship for elements (c) Calls ELMAT (d) Calculates gravity load vector for elements (first stage only)
(7)	NONLIN (subroutine)	Uses the nonlinear material parameters and the stress in each element (estimated initially by the subroutine APPROX; determined by the subroutine STRESS for subsequent load steps) to determine the current value of the tangent and Poisson's ratio; from these the bulk modulus and shear modulus are calculated for use by subroutine MATRIX
(8)	APPROX (subroutine)	Estimates the initial stress in each element for the first iteration of the first load step (first stage only). The vertical stress is assumed equal to the weight of soil above the center of the element; the horizontal stress is calculated from the stress and the Poisson's ratio
(9)	ELMAT (subroutine)	Forms the isoparametric stiffness matrix for each element using 3x3 Gaussian quadrature; writes the strain-displacement relationship for elements on tape.
(10)	BCOND (subroutine)	Called by BLOCK when the structure stiffness matrix has been formed to apply boundary conditions. If a nodal point is fixed in either direction, the equation corresponding to this degree-of-freedom is

zeroed out and the diagonal term is set to unity. The corresponding value in the solution vector is set to zero, or the fixed displacement if the boundary condition is a specified displacement.

(11) USOL (subroutine)

Solves the simultaneous equations block by block and stores the calculated displacements on tape. The technique used is an efficient Gaussian elimination algorithm, with no operations on zero terms in the stiffness matrix. The subroutine was coded by E. Wilson, U.C., Berkeley. Called by EXEC.

(12) STRESS (subroutine)

(a) Reads strain-displacement relationship for each element from tape (written by ELMAT) and calculates the strain.

(b) Calculates the stresses; on the first iteration, the stresses calculated are used to determine the mean stress increase in the element; this is used to determine an intermediate value of the modulus. This modulus is used in the second iteration to arrive at a final value of stress increase for the load step. The stress increase is then added to the cumulative stress.

(c) Calls NONLIN at the second iteration of the last load step to calculate the final values of modulus and Poisson's ratio.

(d) Calls EQUIV on the second iteration for the last load step (first stage only).

(e) Transfers equivalent nodal point forces to the load vector at the end of the first stage.

(13) EQUIV (subroutine)

Calculates the equivalent nodal point forces due to the change in element shear stress corresponding to the shear strain for the element.

List of Variables and Arrays Used in DEFORM

A — array containing the current two blocks of the stiffness matrix. [The stiffness matrix is formed in square blocks - the number of equations equals the band width - and stored with the load vector on TAPE2.] Only two adjacent blocks are held in core storage at any given time for processing by the equation solver, USOL.

A_1, A_2, A_3 — working arrays used by equation solver, USOL.

B — array containing current blocks of load vector (see under A above).

BINT — working array containing intermediate values of load vector

BMOD — array containing the bulk moduli of elements

C — matrix contains Hooke's law relationship

CM — array containing value of soil cohesion for each material

CODE — array containing fixity code for nodes -

1 fixed in X-direction

2 fixed in Y-direction

3 fixed in X & Y-direction

COEF — array - nonlinear modulus parameter K

DISP — matrix containing nodal displacements

DM — array - nonlinear Poisson's ratio parameter d

DPHI — array - change in ϕ over 1 log cycle of pressure ($\Delta\phi$)

ENF — matrix - equivalent nodal point forces

EP — array - strain potentials of elements

ETAN — array - tangential Young's modulus of elements

EXP — array - nonlinear modulus exponent n

FM — array - nonlinear Poisson's ratio parameter F

GAM — array - density of soil for each material

GAMW — variable - density of water in units of analysis

GM — array - nonlinear Poisson's ratio parameter G

ITER	current iteration number - 2 iterations are made at each load step to determine the value of the tangent modulus
IX	matrix - contains the 4 nodal points associated with each element and the material type of the element
MAT	variable - number of different materials
MTYPE	material number of element under consideration
NANA	variable - defines one of the two options in Stage 2 analysis
NDP	variable - number of nodal points in mesh
NEL	variable - number of elements in mesh
NLC	variable - number of nodes along upper boundary of mesh required to define the geometry of the dam and foundation
NLD	variable - number of load steps to be taken in analysis
NSTEP	variable - current value of load step
NUMBLK	variable - number of blocks into which the stiffness matrix and load vector are divided (computed by program)
P	array - element gravity loads
PATM	variable - standard atmospheric pressure in units of analysis
PHI	array - friction angle of each material (ϕ)
Q	array in blank common which holds all the variably dimensioned arrays used in the program
RF	array - nonlinear parameter - failure ratio R_f
S	matrix - element stiffness matrix
SIGMA	matrix - element stresses (σ_x,σ_y,τ_{xy})
SIGIT	matrix - intermediate element stresses used in iterating
SIGI3	array - minor principal stress for each element before earthquake. These values are used to compute modulus and Poisson's ratio for each element in Stage 2 analysis.
SL	array - stress level (ratio of element deviator stress to deviator stress at failure - SL = 1 at failure)
SMOD	array - shear moduli of elements
ST	matrix - element strain-displacement relationship

STAGE variable - contains current stage of analysis

(STAGE=1, analysis to compute initial stresses before earthquake; STAGE=2, analysis to compute permanent deformations due to strain potential)

STRN matrix - element strains ($\varepsilon_x, \varepsilon_y, \gamma_{xy}$)

TNU array - tangent Poisson's ratio for elements

VOL variable - volume (area) of element

X array - horizontal nodal coordinates

XL array - horizontal nodal coordinates of boundary nodes

XLD array - horizontal nodal forces (seepage forces in Stage 1, equivalent nodal point forces in Stage 2)

Y array - vertical nodal coordinates

YL array - vertical nodal coordinates of boundary nodes

YLD array - vertical nodal forces (as in XLD above)

Files Used By DEFORM

TAPE1	scratch tape (file) used by USOL
TAPE2	stores equations in block form (stiffness matrix and load vector). Written by BLOCK, read by USOL.
TAPE3	displacements written on TAPE3 by USOL, read by EXEC.
TAPE4	stores strain-displacement relationship (array ST) for each element. Stored by ELMAT, read by STRESS.
TAPE5	standard card input file
TAPE6	standard printer file
TAPE7	standard card punch file
TAPE8	scratch tape (file) used by USOL
TAPE9	scratch tape (file) used by USOL
TAPE10	physical tape (file) to store element stresses before earthquake used by STRESS, and read by INPT.

Input Data for DEFORM

(1) Control Cards

(a) Title Card (8A10)

Columns 1-80		Job Identification (any characters)

(b) Finite Element Mesh and Analysis Control Parameters (8I5)

Columns 1-5	NDP -	No. of nodes in mesh
Columns 6-10	NEL -	No. of elements
Columns 11-15	MAT -	No. of different materials in dam
Columns 16-20	NLD -	No. of steps in which loads are applied (can be 1 through 5) for both Stages 1 and 2 analyses
Columns 21-25	NLC -	No. of nodes which are necessary to define the geometry of the upper boundary of the mesh (used to calculate the weight of soil above each element in order to estimate stresses for the first load step)
Columns 26-30	KPNCH -	Key for punching element stresses at end of Stage 1 analysis and nodal displacements at end of Stage 2 analysis onto cards if KPNCH = 1
Columns 31-35	KSTART -	Key for restarting Stage 2 analysis after initial stresses before earthquake has been computed (KSTART ≠ 0) and no Stage 1 analysis is made in current computer run. If KSTART = 0, initial stresses are to be computed from Stage 1 analysis; If KSTART = 1, initial stresses are to be read from cards; If KSTART = 2, initial stresses are to be read from TAPE10.
Columns 36-40	NANA -	Option to conduct Stage 2 analysis as a one-step linear analysis (NANA = 1) or an incremental nonlinear analysis (NANA = 2).

For example:

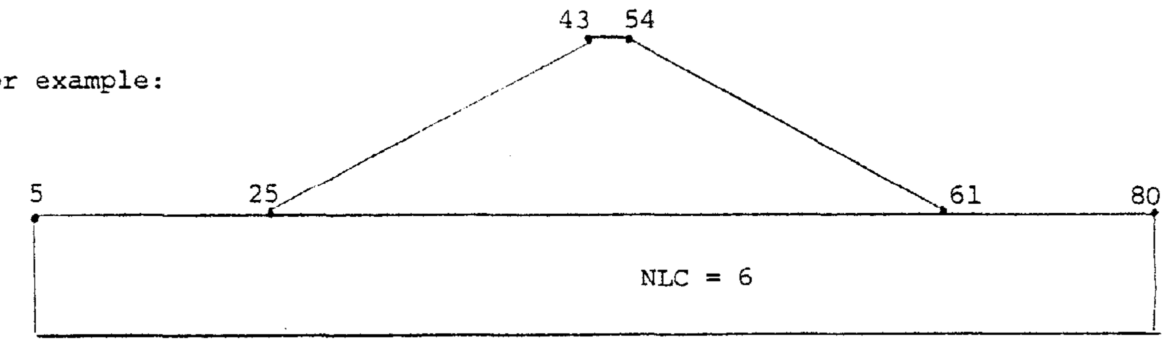

(c) Constants (2F10.0)

Columns 1-10	PATM -	Standard atmospheric pressure (in units of analysis).
Columns 11-20	GAMW -	Density of water (in units of analysis).

(2) Material Property Cards

Card 1 (I10,6F10.0)

Columns 1-10	N	-	material number
Columns 11-20	GAM(N)	-	density of material γ
Columns 21-30	COEF(N)	-	modulus coefficient K
Columns 31-40	EXP(N)	-	modulus exponent n
Columns 41-50	DM(N)	-	Poisson's ratio parameter d
Columns 51-60	GM(N)	-	Poisson's ratio parameter G
Columns 61-70	FM(N)	-	Poisson's ratio parameter F

Card 2 (4F10.0)

Columns 1-10	CM(N)	-	cohesion c
Columns 11-20	PHI(N)	-	friction angle ϕ
Columns 21-30	DPHI(N)	-	change in ϕ per log cycle of pressure
Columns 31-40	RF(N)	-	failure ratio R_f

Note: Above sequence of two cards per material in the dam repeated for each different material, specifying pre-earthquake properties. Sequence is then repeated specifying the properties during the earthquake.

(3) Nodal Point Cards (2I5,4F10.0)

Columns 1-5	N	-	nodal point number
Columns 6-10	CODE(N)	-	fixity code for node (see below)
Columns 11-20	X(N)	-	x coordinate of node
Columns 21-30	H(N)	-	y coordinate of node
Columns 31-40	XLD(N)	-	horizontal component of nodal force
Columns 41-50	YLD(N)	-	vertical component of nodal force

Note 1:

CODE(N) = 0 Node free in x-direction, Node free in y-direction.

CODE(N) = 1 Node fixed in x-direction, Node free in y-direction.

CODE(N) = 2 Node free in x-direction, Node fixed in y-direction.

CODE(N) = 3 Node fixed in x-direction, Node fixed in y-direction.

Note 2: If nodal point cards are missing, coordinates of missing nodes will be calculated by linear interpolation; CODE will be set to 0.

Note 3: Coordinates are positive to the right and upward.

Note 4: Applied forces are seepage forces or any other forces applied to the dam.

(4) Element Cards (6I5)

Columns 1-5	M	-	element number
Columns 6-10	IX(M,1)	-	lower left node number
Columns 11-15	IX(M,2)	-	lower right node number
Columns 16-20	IX(M,3)	-	upper right node number
Columns 21-25	IX(M,4)	-	upper left node number
Columns 26-30	IX(M,5)	-	element material number

Note 1: For triangular elements, third node number is repeated.

Note 2: If elements are missing, nodal numbers will be generated for the missing elements by incrementing the nodal point numbers of the previous element by unity (NB - this interpolation can be used only if nodes are numbered in the same direction as the elements in a system which may be inconsistent with numbering for minimum band width) and the material number is set equal to that of the previous element.

Note 3: The sequence of numbering element nodes MUST be as listed above, otherwise the nodal forces calculated to simulate the earthquake will be applied incorrectly.

(5) Upper Boundary Nodal Point Cards (2F10.0)

Columns 1-10 x - coordinate of node

Columns 11-20 y - coordinate of node

One card per boundary node (i.e., NLC cards). Nodes in sequence from left to right (i.e., nodes 5, 25, 43, 54, 61, and 80) as shown in the example under the control cards input.

(6) Element Strain Potential Cards (I5,F10.0)

Columns 1-5 N - element number

Columns 6-15 EP(N) - element strain potential

One card per element; only elements with a non-zero strain potential need be supplied. However, a card MUST be supplied for the last element even if the strain potential is zero. Strain will be assumed zero for missing elements.

(7) Initial Stress Cards (I5,1X,2F7.1,6E10.3) Skip if KSTART = 0 on Card (1b)

Columns 1-5 N - element number

Columns 7-13 XC

Columns 14-20 YC

Columns 21-30 SIGMA(1,N) - element normal stress (σ_x)

Columns 31-40 SIGMA(2,N) - element normal stress (σ_y)

Columns 41-50 SIGMA(3,N) - element shear stress (τ_{xy})

Columns 51-60 STRN(1,N) - element strain (ε_x)

Columns 61-70 STRN(2,N) - element strain (ε_y)

Columns 71-80 STRN(3,N) - element shear strain (γ_{xy})

END OF INPUT DATA

FORTRAN LISTING OF PROGRAM "DEFORM"

```
      PROGRAM DEFORM (INPUT,OUTPUT,TAPE5=INPUT,TAPE6=OUTPUT,TAPE1,TAPE2,
     1          TAPE3,TAPE4,TAPE8,TAPE9,TAPE10,PUNCH,TAPE7=PUNCH)
C
      COMMON/CONST1/ NLD,VOL,MTYPE,NSTEP,PATM,GAMW,NNN,TIME(3)
      COMMON/CONST2/ ITER,MBAND,NUMBLK,TITLE(8),STAGE,XL(50),YL(50),NLC
      COMMON/CONST3/KPNCH,KSTART,NANA
C
      INTEGER CODE, STAGE
C
C
C     THE DIMENSION OF ARRAY Q AND THE CONSTANT NCOM SET FOR EACH PROBLE
C     ACCORDING TO THE FORMULA BELOW
C
C
C         MINIMUM VALUE OF NCOM AND DIMENSION OF Q
C
C
C                =   2
C                + 21 TIMES NUMBER OF ELEMENTS (NEL)
C                + 13 TIMES NUMBER OF NODAL POINTS (NDP)
C                + 20 TIMES NUMBER OF DIFFERENT MATERIALS (MAT)
C                +  2 TIMES BANDWIDTH SQUARED (MBAND**2)
C                +  3 TIMES BANDWIDTH (MBAND)
C
C
      COMMON Q(12000)
      NCOM=12000
C
C
C
      READ(5,1000)  TITLE
      WRITE(6,2000) TITLE
      READ(5,1001) NDP,NEL,MAT,NLD,NLC,KPNCH,KSTART,NANA
      WRITE(6,2001) NDP,NEL,MAT,NLD,KPNCH,KSTART,NANA
      READ(5,1002)  PATM, GAMW
      WRITE(6,2002) PATM, GAMW
C
C     ASSIGN STORAGE IN BLANK COMMON
C
      L01   =   2
      L02   =   L01 + NEL*6
      L03   =   L02 + NEL
      L04   =   L03 + NEL*3
      L05   =   L04 + NEL*3
      L06   =   L05 + NDP
      L07   =   L06 + NDP
      L08   =   L07 + NDP
      L09   =   L08 + NDP
      L10   =   L09 + NDP
      L11   =   L10 + NDP*2
      L12   =   L11 + MAT*2
      L13   =   L12 + MAT*2
      L14   =   L13 + MAT*2
      L15   =   L14 + MAT*2
      L16   =   L15 + MAT*2
      L17   =   L16 + MAT*2
      L18   =   L17 + MAT*2
      L19   =   L18 + MAT*2
```

```
      L20  =  L19 + MAT*2
      L21  =  L20 + MAT*2
      L22  =  L21 + NEL
C
      CALL INPT(Q(L01),Q(L05),Q(L06),Q(L07),Q(L08),Q(L09),Q(L11),Q(L12),
     1          Q(L13),Q(L14),Q(L15),Q(L16),Q(L17),Q(L18),Q(L19),Q(L20),
     2          Q(L21),Q(L03),Q(L22),NEL,NDP,MAT)
C
      CALL BAND(Q(L01),NEL)
C
      M2 = MBAND*2
      M3 = MBAND
      N2 = NDP*2
      NB = MBAND/2
      NBB = MOD(NDP,NB)
      IF(NBB.EQ.0) GO TO 10
      NBLK = (NDP/NB) + 1
      GO TO 20
   10 NBLK = NDP/NB
   20 CONTINUE
      WRITE(6,2005) NBLK
C
      NSB = (MBAND+1)*MBAND
C
      L23  =  L22 + NEL*3
      L24  =  L23
      L25  =  L24 + NSB
      L26  =  L25 + NSB
      L27  =  L26 + MBAND
      L28  =  L27 + NDP*2
      L29  =  L28 + NDP*2
      L30  =  L29 + NDP*2
      L31  =  L30 + NEL
      L32  =  L31 + NEL
      L33  =  L32 + NEL
      L34  =  L33 + NEL
      LEND =  L34 + NEL
C
C     END OF STORAGE ALLOCATION
C
C     CHECK IF DIMENSION OF ARRAY IS SUFFICIENT
C
      NDIF = NCOM - LEND
      WRITE(6,2003) LEND
      IF(NDIF.GE.0) GO TO 30
      NDIF = IABS(NDIF)
      WRITE(6,2004) NDIF
      STOP
   30 CONTINUE
C
      STAGE = 1
C
   40 CONTINUE
C
      IF(STAGE.EQ.1) WRITE(6,2006)
      IF(STAGE.EQ.2) WRITE(6,2007)
C
```

```
      CALL EXEC(Q(L01),Q(L02),Q(L03),Q(L04),Q(L05),Q(L06),Q(L07),Q(L08),
     1          Q(L09),Q(L10),Q(L11),Q(L12),Q(L13),Q(L14),Q(L15),Q(L16),
     2          Q(L17),Q(L18),Q(L19),Q(L20),Q(L21),Q(L22),Q(L23),Q(L24),
     3          Q(L25),Q(L26),Q(L27),Q(L28),Q(L29),Q(L30),Q(L31),Q(L32),
     4          Q(L33),Q(L34),
     5          NEL,NDP,MAT,M2,M3,NSB,N2)
C
      STAGE = STAGE + 1
C
      IF(NANA.EQ.1) NLD=1
      IF(STAGE.EQ.2) GO TO 40
C
 1000 FORMAT(8A10)
 1001 FORMAT(8I5)
 1002 FORMAT(2F10.0)
 2000 FORMAT(1H1,8A10/)
 2001 FORMAT(30H0 NUMBER OF NODAL POINTS------ I10 /
     1       30H0 NUMBER OF ELEMENTS---------- I10 /
     2       30H0 NUMBER OF DIFF. MATERIALS--- I10 /
     3       30H0 NUMBER OF LOAD STEPS-------- I10 /
     4       30H0 KEY FOR PUNCH OUTPUT-------- I10/
     5       30H0 KEY FOR RESTARTING RUN------ I10,29H(IF.NE.0,START WIT
     6H STAGE 2)/30H0 OPTION FOR TYPE OF ANALYSIS- ,I10,
     750H(1 FOR 1-STEP LINEAR, 2 FOR INCREMENTAL NONLINEAR))
 2002 FORMAT(/1X,29H ATMOSPHERIC PRESSURE-------- F10.3//
     1         1X,29H UNIT WEIGHT OF WATER--------F10.3)
 2003 FORMAT(////10X,34HSTORAGE REQUIRED BY BLANK COMMON =,I8,2X,
     1                5HWORDS///)
 2004 FORMAT (10X,63HSPECIFIED DIMENSION FOR ARRAY Q IN BLANK COMMON IS
     *TOO SMALL BY,I8,2X,5HWORDS)
 2005 FORMAT(///10X,18HNUMBER OF BLOCKS =, I5)
 2006 FORMAT(1H1,5X,73HFIRST STAGE - CALCULATION OF INITIAL STRESSES AND
     * EQUIVALENT NODAL FORCES)
 2007 FORMAT(1H1,5X,71HSECOND STAGE - CALCULATION OF PERMANENT DEFORMATI
     *ONS AND FINAL STRESSES)
C
      END




      SUBROUTINE INPT(IX,CODE,X,Y,XLD,YLD,GAM,COEF,EXP,DM,GM,FM,CM,PHI,
     1                DPHI,RF,EP,SIGMA,STRN,NEL,NDP,MAT)
C
      COMMON/CONST1/ NLD,VOL,MTYPE,NSTEP,PATM,GAMW,NNN,TIME(3)
      COMMON/CONST2/ ITER,MBAND,NUMBLK,TITLE(8),STAGE,XL(50),YL(50),NLC
      COMMON/CONST3/KPNCH,KSTART,NANA
C
      DIMENSION GAM(MAT),COEF(MAT),EXP(MAT),DM(MAT),GM(MAT),FM(MAT),
     1          CM(MAT),PHI(MAT),DPHI(MAT),RF(MAT)
      DIMENSION X(NDP),Y(NDP),XLD(NDP),YLD(NDP),CODE(NDP)
      DIMENSION IX(NEL,5),EP(NEL),SIGMA(3,NEL),STRN(3,NEL)
C
      INTEGER CODE, STAGE
C
      WRITE(6,2014)
```

```
      WRITE(6,2003)
C
C     READ MATERIAL PROPERTIES
C
      DO 40 J = 1,2
      IF(J.EQ.1) GO TO 10
      WRITE(6,2015)
      WRITE(6,2003)
   10 DO 30 I = 1,MAT
      K = (J-1)*MAT
      READ(5,1003) N,GAM(N+K),COEF(N+K),EXP(N+K),DM(N+K),GM(N+K),FM(N+K)
     1               ,CM(N+K),PHI(N+K),DPHI(N+K),RF(N+K)
      WRITE(6,2004)N,GAM(N+K),COEF(N+K),EXP(N+K),DM(N+K),GM(N+K),FM(N+K)
     1               ,CM(N+K),PHI(N+K),DPHI(N+K),RF(N+K)
   30 CONTINUE
   40 CONTINUE
C
C
C
C     READ NODAL POINT COORDINATES AND FORCES (INTERPOLATE FOR MISSING V
C
      WRITE(6,2006)
      L=0
   60 READ(5,1005) N,CODE(N),X(N),Y(N),XLD(N),YLD(N)
      NL=L+1
      ZX=N-L
      IF(L .EQ. 0) GO TO 70
      DX = (X(N)-X(L))/ZX
      DY = (Y(N)-Y(L))/ZX
   70 L=L+1
      IF(N-L) 100,90,80
   80 CODE(L)=0
      X(L) = X(L-1) + DX
      Y(L) = Y(L-1) + DY
      XLD(L) = 0.0
      YLD(L) = 0.0
      GO TO 70
   90 WRITE(6,2005) (K,CODE(K),X(K),Y(K),XLD(K),YLD(K), K = NL,N)
      IF(NDP-N) 100,110,60
  100 WRITE(6,2009) N
      STOP
  110 CONTINUE
C
C     READ ELEMENT NODAL NUMBERS AND MATERIAL NUMBERS
C
      WRITE(6,2013)
      N=0
  130 READ(5,1001) M,(IX(M,I),I=1,5)
  140 N=N+1
      IF(M .LE. N) GO TO 170
      DO 150 K=1,4
  150 IX(N,K)=IX(N-1,K)+1
      IX(N,5)=IX(N-1,5)
  170 WRITE(6,2002) N,(IX(N,I),I=1,5)
      IF(M .GT. N) GO TO 140
      IF(NEL.GT.N) GO TO 130
C
```

```
C     READ AND PRINT BOUNDARY COORDINATES
C
      READ(5,1006) (XL(I),YL(I),I=1,NLC)
C
      WRITE(6,2008)
      WRITE(6,2012)  (XL(I),YL(I),I=1,NLC)
C
C     READ STRAIN POTENTIAL
C
      WRITE(6,2010)
C
      M = 0
  200 READ(5,1004) N,EP(N)
  201 M= M + 1
      IF(N.LE.M) GO TO 202
      EP(M) = 0.0
  202 WRITE(6,2011) M,EP(M)
      IF(N.GT.M) GO TO 201
      IF(NEL.GT.M) GO TO 200
      IF (KSTART .EQ. 0) GO TO 260
      NT=5
      IF(KSTART .EQ. 2) NT=10
      WRITE(6,3001)
      DO 250 I=1,NEL
      READ(NT,3000) N,XC,YC,(SIGMA(J,N),J=1,3),(STRN(J,N),J=1,3)
      WRITE(6,3010) N,XC,YC,(SIGMA(J,N),J=1,3),(STRN(J,N),J=1,3)
  250 CONTINUE
  260 CONTINUE
C
  300 RETURN
C
 1001 FORMAT(6I5)
 1003 FORMAT(I10,6F10.0/4F10.0)
 1004 FORMAT(I5,F10.0)
 1005 FORMAT(2I5,4F10.0)
 1006 FORMAT(2F10.0)
 2000 FORMAT(1H1,10X,7HELEMENT,13X,7HSIGMA-X,8X,7HSIGMA-Y,9X,6HTAU-XY,
     1          10X,5HEPS-X,10X,5HEPS-Y,9X,6HGAM-XY//)
 2002 FORMAT(I10,3X,4(1X,I5),5X,I5)
 2003 FORMAT(1H0,27X,18HMODULUS PARAMETERS,4X,24HPOISSON RATIO PARAMETER
     1S,10X,19HSTRENGTH PARAMETERS/
     2          1H0,6X,8HMAT. NO.,3X,7HDENSITY,5X,1HK,11X,1HN,8X,1HD,10X,
     3          1HG,9X,1HF,8X,1HC,8X,3HPHI,5X,9HDELTA PHI,5X,2HRF/)
 2004 FORMAT(/8X,I3,4X,10F10.3)
 2005 FORMAT(I12,I10,2F12.2,6X,F12.3,5X,F12.3)
 2006 FORMAT(1H1,8X,4HNODE,6X,4HTYPE,4X,7HX-COORD,5X,7HY-COORD,11X,
     1          7HX-FORCE,10X,7HY-FORCE/)
 2008 FORMAT(1H1,5X,14HBOUNDARY NODES/6X,14H-------------  ///20X,
     1          5HX-ORD,10X,5HY-ORD/)
 2009 FORMAT (26H0NODAL POINT CARD ERROR N= I5)
 2010 FORMAT(1H1,5X,7HELEMENT,10X,16HSTRAIN POTENTIAL/)
 2011 FORMAT(I10,14X,F10.4)
 2012 FORMAT(15X,F10.2,5X,F10.2)
 2013 FORMAT(1H1,5X,7HELEMENT,5X,1HI,5X,1HJ,5X,1HK,5X,1HL,5X,
     1          8HMATERIAL/)
 2014 FORMAT(1H1,5X,37HMATERIAL PROPERTIES BEFORE EARTHQUAKE//)
 2015 FORMAT(1H1,5X,37HMATERIAL PROPERTIES DURING EARTHQUAKE//)
```

```
C
 3000 FORMAT (I5,1X,2F7.1,6E10.3)
 3001 FORMAT(1H1,5X,46HINITIAL STRESSES AND STRAINS BEFORE EARTHQUAKE//
     142X,14HELEMENT STRESS,19X,24HELEMENT STRAIN (PERCENT)/1H ,4HELEM,
     27X,2HXC,9X,2HYC,10X,7HSIGMA X,4X,7HSIGMA Y,5X,6HTAU XY,6X,5HEPS X,
     34X,5HEPS Y,3X,6HGAM XY//)
 3010 FORMAT(I4,2X,2F11.3,2X,3F11.3,2X,3F9.3)
      END



      SUBROUTINE EXEC(IX,BMOD,SIGMA,SIGIT,CODE,X,Y,XLD,YLD,DISP,GAM,
     1                 COEF,EXP,DM,GM,FM,CM,PHI,DPHI,RF,EP,STRN,A,A1,A2,
     2                A3,B,ENF,BINT,SMOD,ETAN,TNU,SL,SIGI3,
     3                 NEL,NDP,MAT,M2,M3,NSB,N2)
C
      COMMON/CONST1/ NLD,VOL,MTYPE,NSTEP,PATM,GAMW,NNN,TIME(3)
      COMMON/CONST2/ ITER,MBAND,NUMBLK,TITLE(8),STAGE,XL(50),YL(50),NLC
      COMMON/CONST3/KPNCH,KSTART,NANA
C
      DIMENSION GAM(MAT),COEF(MAT),EXP(MAT),DM(MAT),GM(MAT),FM(MAT),
     1          CM(MAT),PHI(MAT),DPHI(MAT),RF(MAT)
      DIMENSION IX(NEL,5),EP(NEL),SIGMA(3,NEL),SIGIT(3,NEL),STRN(3,NEL),
     1      BMOD(NEL),SMOD(NEL),ETAN(NEL),TNU(NEL),SL(NEL),SIGI3(NEL)
      DIMENSION X(NDP),Y(NDP),XLD(NDP),YLD(NDP),CODE(NDP),
     1          DISP(NDP,2),ENF(NDP,2),B(N2),BINT(N2)
      DIMENSION A(M2,M3),A1(NSB),A2(NSB),A3(M3)
      DIMENSION P(8),ST(3,8),C(3,3),S(8,8)
C
      INTEGER CODE, STAGE
C
C
C     INITIALIZE DISPLACEMENTS, STRESSES AND STRAINS
C
      DO 10 N = 1,NDP
      DO 10 I = 1,2
   10 DISP(N,I) = 0.0
      DO 20 I = 1,3
      DO 20 J = 1,NEL
      SIGIT(I,J) = 0.0
   20 CONTINUE
C
      IF (KSTART .NE. 0) GO TO 60
      IF(STAGE.EQ.2) GO TO 40
C
C     INITIALIZE STRESSES AND STRAINS (FIRST STAGE ONLY)
C
      DO 30 I = 1,3
      DO 30 J = 1,NEL
      SIGMA(I,J) = 0.0
      STRN(I,J) = 0.0
   30 CONTINUE
C
      GO TO 60
C
```

```
   40 CONTINUE
C
C     CHANGE MATERIAL PROPERTIES FROM PRE-EARTHQUAKE TO EARTHQUAKE VALUE
C
      DO 50 I = 1,MAT
      J = I + MAT
      GAM(I) = GAM(J)
      COEF(I) = COEF(J)
      EXP(I) = EXP(J)
      DM(I) = DM(J)
      GM(I) = GM(J)
      FM(I) = FM(J)
      CM(I) = CM(J)
      PHI(I) = PHI(J)
      DPHI(I) = DPHI(J)
      RF(I) = RF(J)
   50 CONTINUE
C
   60 CONTINUE
C
      NSTEP=1
C
      DO 500 NNN = 1,NLD
C
      ITER=0
      IF(STAGE.EQ.2.AND.NANA.EQ.1) ITER=1
      IF (KSTART .NE. 0) ITER=1
C
   70 CONTINUE
C
      CALL SECOND(T1)
      IF (KSTART .NE. 0) GO TO 100
C
C     GENERATE SIMULTANEOUS EQUATIONS
C
      CALL BLOCK(A,B,BINT,P,ST,IX,X,Y,CODE,XLD,YLD,GAM,CM,PHI,DPHI,COEF,
     1           EXP,DM,GM,FM,RF,ETAN,BMOD,SMOD,TNU,SIGMA,SIGIT,SL,
     2           SIGI3,NEL,NDP,MAT,M2,M3,N2)
C
      CALL SECOND(T2)
C
      TIME(1) = T2 - T1
C
C     SOLVE SIMULTANEOUS EQUATIONS
C
      CALL USOL(A1,A2,A3,MBAND,MBAND,1,NUMBLK,NSB,2,1,8,9,3)
C
      CALL SECOND(T3)
C
      TIME(2) = T3 - T2
C
C     READ DISPLACEMENTS FROM TAPE
C
      REWIND 3
      NQ=MBAND*NUMBLK
      DO 80 I=1,NUMBLK
      JN1=NQ-MBAND+1
```

```
      JN2=JN1+MBAND-1
      READ(3) (B(J),J=JN1,JN2)
      NQ=NQ-MBAND
   80 CONTINUE
C
      IF(ITER.EQ.0) GO TO 100
      IF(STAGE.EQ.1) GO TO 100
C
      WRITE (6,2014) NSTEP
C
      WRITE (6,2022)
C
      DO 90 N = 1,NDP
      DISP(N,1)=DISP(N,1)+B(2*N-1)
      DISP(N,2)=DISP(N,2)+B(2*N)
      WRITE(6,2010) N,B(2*N-1),B(2*N),DISP(N,1),DISP(N,2)
      IF(KPNCH.NE.1) GO TO 90
      IF(NNN.EQ.NLD) WRITE(7,2000) N,X(N),Y(N),DISP(N,1),DISP(N,2)
   90 CONTINUE
C
  100 CONTINUE
C
      IF(ITER.EQ.1) WRITE(6,2030)
C
      CALL SECOND(T4)
C
C     CALCULATE ELEMENT STRESSES AND STRAINS
C
      CALL STRESS(BMOD,SMOD,ETAN,TNU,SL,SIGIT,SIGMA,STRN,EP,
     1            GAM,COEF,EXP,DM,GM,FM,CM,PHI,DPHI,RF,SIGI3,
     2            IX,X,Y,CODE,XLD,YLD,B,ENF,C,ST,S,P,
     3            NEL,NDP,MAT,M2,N2)
C
      IF (KSTART .NE. 0) GO TO 501
      CALL SECOND(T5)
C
      TIME(3) = T5 - T4
      IF(ITER.EQ.2) WRITE (6,2001) (TIME(I),I=1,3)
C
      IF(ITER.EQ.1) GO TO 70
C
      NSTEP=NSTEP+1
C
  500 CONTINUE
  501 KSTART=0
C
C
C
 2000 FORMAT(I5,2F10.2,2F10.5)
 2001 FORMAT    (/20X,28HFORMATION OF K MATRIX       =,F10.3,2X,21HSECONDS
     1 PER ITERATION/
     2            21X,28HSOLUTION OF EQUATIONS       =,F10.3,2X,21HSECONDS
     3 PER ITERATION/
     4            21X,28HCALCULATION OF STRESSES     =,F10.3,2X,21HSECONDS
     5 PER ITERATION)
 2010 FORMAT(3X,I5,12X,F10.3,9X,F10.3,16X,F10.3,8X,F10.3)
 2014 FORMAT(1H1,11HSTEP NUMBER,I3/13H ----------- - /)
```

```
2022 FORMAT(1H0,23X,25HINCREMENTAL DISPLACEMENTS,20X,24HCUMULATIVE DISP
    *LACEMENTS//5X,4HNODE,15X,6HX-DISP,13X,6HY-DISP,20X,6HX-DISP,12X,
    *6HY-DISP//)
2030 FORMAT(1H1)
C
     RETURN
     END




     SUBROUTINE STRESS(BMOD,SMOD,ETAN,TNU,SL,SIGIT,SIGMA,STRN,EP,
    1              GAM,COEF,EXP,DM,GM,FM,CM,PHI,DPHI,RF,SIGI3,
    2              IX,X,Y,CODE,XLD,YLD,B,ENF,C,ST,S,P,
    3              NEL,NDP,MAT,M2,N2)
C
     COMMON/CONST1/ NLD,VOL,MTYPE,NSTEP,PATM,GAMW,NNN,TIME(3)
     COMMON/CONST2/ ITER,MBAND,NUMBLK,TITLE(8),STAGE,XL(50),YL(50),NLC
     COMMON/CONST3/KPNCH,KSTART,NANA
C
     DIMENSION GAM(MAT),COEF(MAT),EXP(MAT),DM(MAT),GM(MAT),FM(MAT),
    *          CM(MAT),PHI(MAT),DPHI(MAT),RF(MAT)
     DIMENSION IX(NEL,5),EP(NEL),SIGMA(3,NEL),SIGIT(3,NEL),STRN(3,NEL),
    1        BMOD(NEL),SMOD(NEL),ETAN(NEL),TNU(NEL),SL(NEL),SIGI3(NEL)
     DIMENSION X(NDP),Y(NDP),CODE(NDP),ENF(NDP,2),B(N2)
     DIMENSION XLD(NDP),YLD(NDP)
     DIMENSION P(8),ST(3,8),C(3,3),S(8,8),D(3,3),SIG(6)
C
     INTEGER STAGE,CODE
C
     REWIND 4
C
     MPRINT=0
C
C    INITIALIZE EQUIVALENT NODAL FORCES
C
     IF(STAGE.NE.1) GO TO 20
     DO 10 I = 1,NDP
     DO 10 J = 1,2
     ENF(I,J) = 0.0
  10 CONTINUE
C
  20 CONTINUE
C
C    START ELEMENT LOOP
C
     DO 300 N = 1,NEL
C
     IX(N,5)= IABS(IX(N,5))
     MTYPE = IX(N,5)
     M = MTYPE
C
     DO 30 I = 1,6
     SIG(I) = 0.0
  30 CONTINUE
C
```

```
      DO 40 I = 1,3
      DO 40 J = 1,8
      ST(I,J) = 0.0
   40 CONTINUE
C
      IF(ITER.EQ.1) GO TO 60
C
      DO 50 I = 1,3
      SIGIT(I,N) = SIGMA(I,N)
   50 CONTINUE
C
   60 CONTINUE
      IF (KSTART .NE. 0) GO TO 95
C
      DO 70 I = 1,4
      II = 2*I
      JJ = 2*IX(N,I)
      P(II-1) = B(JJ-1)
      P(II) = B(JJ)
   70 CONTINUE
C
C     READ ELEMENT STRAIN-DISPLACEMENT RELATIONSHIP FROM TAPE 4
C
      READ(4) ST
C
      DO 80 I = 1,3
      D(I,1) = 0.0
      DO 80 K = 1,8
      D(I,1) = D(I,1) + ST(I,K)*P(K)
   80 CONTINUE
C
C
      C(1,1) = BMOD(N) + SMOD(N)
      C(1,2) = BMOD(N) - SMOD(N)
      C(1,3) = 0.0
      C(2,1) = C(1,2)
      C(2,2) = C(1,1)
      C(2,3) = 0.0
      C(3,1) = 0.0
      C(3,2) = 0.0
      C(3,3) = SMOD(N)
C
      DO 90 I = 1,3
      DO 90 K = 1,3
      SIG(I) = (SIG(I) + C(I,K)*D(K,1))
   90 CONTINUE
C
      IF(ITER.EQ.1) GO TO 110
C
C     AVERAGE STRESSES
C
   95 DO 100 I=1,3
      SIGIT(I,N)=SIGMA(I,N)-0.5*SIG(I)
      SIG(I) = SIGIT(I,N)
  100 CONTINUE
      GO TO 140
C
```

```
  110 CONTINUE
C
C     ADD STRESS INCREMENTS TO PREVIOUS STRESSES
C
      DO 120 I = 1,3
      SIG(I)=(SIGMA(I,N)-SIG(I))
  120 CONTINUE
C
      DO 130 I = 1,3
      SIGMA(I,N) = SIG(I)
  130 CONTINUE
C
C     OUTPUT STRESSES
C
  140 IF(ITER.EQ.0) GO TO 300
C
C     CALCULATE PRINCIPAL STRESSES
C
      CC = (SIG(2)+SIG(1))/2.0
      BB = (SIG(2)-SIG(1))/2.
      CR = SQRT(BB**2+SIG(3)**2)
C
      SIG(4) = 0.0
      IF(SIG(3).EQ.0.0.AND.BB.EQ.0.0) GO TO 150
      SIG(4)=28.648*ATAN2(SIG(3),BB)
  150 CONTINUE
C
      SIG(5) = CC + CR
      SIG(6) = CC - CR
      IF(KSTART.NE.0.OR.STAGE.EQ.1.AND.NSTEP.EQ.NLD.AND.ITER.EQ.1)
     1 SIGI3(N)=SIG(6)
C
      IN = IX(N,1)
      JN = IX(N,2)
      KN = IX(N,3)
      LN = IX(N,4)
      IF (KSTART .NE. 0) GO TO 175
C
      IF(NSTEP.NE.NLD) GO TO 160
C
C     DETERMINE FINAL VALUE OF MODULUS AND POISSONS RATIO
C
      SIGIT(1,N) = SIG(1)
      SIGIT(2,N) = SIG(2)
      SIGIT(3,N) = SIG(3)
C
C
      CALL NONLIN(N,IN,JN,KN,LN,M,ETAN,TNU,BMOD,SMOD,EI,HCS,GAM,COEF,
     1            EXP,DM,GM,FM,CM,PHI,DPHI,RF,SIGIT,SIGMA,SL,X,Y,IX,
     2        SIGI3,NEL,NDP,MAT)
C
C
  160 CONTINUE
C
C     CALCULATE STRAINS (X,Y,XY)
C
      DO 170 I = 1,3
```

```
      STRN(I,N)=STRN(I,N)-D(I,1)*100.0
  170 CONTINUE
C
  175 CONTINUE
      EPSX  = STRN(1,N)
      EPSY  = STRN(2,N)
      GAMXY = STRN(3,N)
C
      IF (MPRINT) 190,180,190
  180 WRITE (6,1002)
 1002 FORMAT(1H1)
      WRITE (6,2014) NSTEP
      WRITE (6,2001)
      MPRINT=50
      IF(NSTEP.EQ.NLD.AND.STAGE.EQ.1) MPRINT=25
  190 MPRINT = MPRINT - 1
      IF(KSTART .NE. 0) GO TO 230
C
      IF(KN.EQ.LN) GO TO 200
      XC = (X(IN)+X(JN)+X(KN)+X(LN))/4.0
      YC = (Y(IN)+Y(JN)+Y(KN)+Y(LN))/4.0
      GO TO 210
  200 XC = (X(IN)+X(JN)+X(KN))/ 3.0
      YC = (Y(IN)+Y(JN)+Y(KN))/ 3.0
  210 CONTINUE
C
C     PRINT MODULUS, STRESSES AND STRAINS
C
      WRITE(6,2002) N,ETAN(N),BMOD(N),SMOD(N),TNU(N),SIG(1),SIG(2),
     1                    SIG(3),EPSX,EPSY,GAMXY,SIG(4),SL(N),N
C
      IF (NSTEP.EQ.NLD.AND.ITER.EQ.1.AND.STAGE.EQ.1)
     1  WRITE(10,2003) N,XC,YC,SIG(1),SIG(2),SIG(3),EPSX,EPSY,GAMXY
      IF(KPNCH.NE.1) GO TO 220
      IF (NSTEP.EQ.NLD.AND.ITER.EQ.1)
     1   WRITE(7,2003) N,XC,YC,SIG(1),SIG(2),SIG(3),EPSX,EPSY,GAMXY
C
  220 CONTINUE
      IF(STAGE.NE.1) GO TO 300
      IF(NSTEP.NE.NLD) GO TO 300
      IF(ITER.NE.1) GO TO 300
  230 CONTINUE
      NM=M+MAT
      CALL NONLIN(N,IN,JN,KN,LN,NM,ETAN,TNU,BMOD,SMOD,EI,HCS,GAM,COEF,
     1              EXP,DM,GM,FM,CM,PHI,DPHI,RF,SIGIT,SIGMA,SL,X,Y,IX,
     2          SIGI3,NEL,NDP,MAT)
C
C     CALCULATE EQUIVALENT NODAL POINT FORCES
C
      IF (EP(N) .LE. 0.0001) GO TO 250
C
      CALL EQUIV(N,EPSX,EPSY,GAMXY,EI,HCS,EP,SIG,IX,ENF,X,
     1                  Y,NEL,NDP,ETAN,TNU,SMOD)
  250 CONTINUE
      WRITE (6,1001) N,ETAN(N),BMOD(N),SMOD(N),TNU(N),SL(N)
 1001 FORMAT (I5,1X,1P3E11.3,0PF8.3,73X,F7.3)
C
```

```
  300 CONTINUE
C
C     TRANSFER EQUIVALENT NODAL POINT FORCES INTO LOAD VECTOR
C
      IF (KSTART .NE. 0) GO TO 305
      IF(STAGE.NE.1) GO TO 410
      IF(NSTEP.NE.NLD) GO TO 410
      IF(ITER.NE.1) GO TO 410
  305 DO 400 I=1,NDP
      XLD(I) = ENF(I,1)
      YLD(I) = ENF(I,2)
      IF(CODE(I) .EQ. 0) GO TO 350
      IF( CODE(I) .EQ. 1) GO TO 310
      IF (CODE(I) .EQ. 2) GO TO 320
  310 XLD(I)=0.0
      IF (CODE(I) .EQ. 3) GO TO 320
      GO TO 350
  320 YLD(I)=0.0
  350 CONTINUE
  400 CONTINUE
C
C     PRINT EQUIVALENT NODAL POINT FORCES
C
      WRITE(6,2005)
      WRITE(6,2006) (N,CODE(N),X(N),Y(N),(ENF(N,L),L=1,2),N=1,NDP)
C
  410 ITER = ITER + 1
C
      RETURN
C
 2001 FORMAT(10X,6HYOUNGS,6X,4HBULK,6X,5HSHEAR,5X,7HPOISSON,11X,
     1        14HELEMENT STRESS,14X,24HELEMENT STRAIN (PERCENT),9X,
     2        6HSTRESS/1H ,4HELEM,4X,7HMODULUS,4X,7HMODULUS,4X,7HMODULUS,
     3        5X,5HRATIO,5X,7HSIGMA X,4X,7HSIGMA Y,5X,6HTAU XY,6X,
     4        5HEPS X,4X,5HEPS Y,3X,6HGAM XY,3X,5HANGLE,3X,5HLEVEL,2X,
     5        4HELEM//)
 2002 FORMAT(I4,2X,1P3E11.3,0PF8.3,2X,3F11.3,2X,3F9.3,2X,F7.1,F7.3,I5)
 2003 FORMAT(I5,1X,2F7.1,  6E10.3)
 2004 FORMAT(2I5,4F10.3)
 2005 FORMAT(1H1,5X,23HEQUIVALENT NODAL FORCES/6X,23H--------
     1----///9X,4HNODE,6X,4HTYPE,4X,7HX-COORD,6X,7HY-COORD,9X,7HX-FORCE,
     110X,7HY-FORCE/)
 2006 FORMAT(I12,I10,2F12.2,6X,F12.3,5X,F12.3)
 2014 FORMAT(1X,11HSTEP NUMBER,I3/)
C
      END




      SUBROUTINE NONLIN(N,I,J,K,L,M,ETAN,TNU,BMOD,SMOD,EI,HCS,GAM,COEF,
     1              EXP,DM,GM,FM,CM,PHI,DPHI,RF,SIGIT,SIGMA,SL,X,Y,IX,
     2              SIGI3,NEL,NDP,MAT)
C
      COMMON/CONST1/ NLD,VOL,MTYPE,NSTEP,PATM,GAMW,NNN,TIME(3)
      COMMON/CONST2/ ITER,MBAND,NUMBLK,TITLE(8),STAGE,XL(50),YL(50),NLC
```

```
      COMMON/CONST3/KPNCH,KSTART,NANA
C
      DIMENSION GAM(MAT),COEF(MAT),EXP(MAT),DM(MAT),GM(MAT),FM(MAT),
     *          CM(MAT),PHI(MAT),DPHI(MAT),RF(MAT)
      DIMENSION IX(NEL,5),SIGMA(3,NEL),SIGIT(3,NEL),SIGI3(NEL),
     *          BMOD(NEL),SMOD(NEL),ETAN(NEL),TNU(NEL),SL(NEL)
      DIMENSION X(NDP),Y(NDP)
C
      INTEGER STAGE
C
      IF(ITER .EQ. 0) GO TO 10
      CC=(SIGIT(2,N)+SIGIT(1,N))/2.
      BB=(SIGIT(2,N)-SIGIT(1,N))/2.
      CR=SQRT(SIGIT(3,N)*SIGIT(3,N)+BB*BB)
      GO TO 40
   10 CONTINUE
C
      IF(STAGE.EQ.2) GO TO 20
C
C     ESTIMATE INITIAL STRESSES FOR FIRST LOAD STEP
C
      IF(NSTEP.EQ.1.AND.ITER.EQ.0)
     *CALL APPROX(N,I,J,K,L,M,SIGMA,X,Y,GM,GAM,NEL,NDP,MAT)
C
   20 CONTINUE
      CC=(SIGMA(2,N)+SIGMA(1,N))/2.0
      BB=(SIGMA(2,N)-SIGMA(1,N))/2.0
      CR=SQRT(SIGMA(3,N)*SIGMA(3,N)+BB*BB)
      IF(NSTEP.NE.1.OR.ITER.NE.0) GO TO 40
      IF(STAGE.EQ.2) GO TO 40
      DO 30 KI = 1,3
      DO 30 KJ = 1,NEL
      SIGMA(KI,KJ) = 0.0
   30 CONTINUE
   40 CONTINUE
      SIG1=CC+CR
      SIG3=CC-CR
      DEV=SIG1-SIG3
      IF(SIG1.LT.0.0) SIG1 = 0.0
      IF(SIG3.LT.0.0) SIG3 = 0.0
      IF(DEV.LT.0.0) DEV = 0.0
      IF(STAGE.EQ.2) GO TO 45
      SIGI3(N)=SIG3
   45 CONTINUE
C
C
C    COMPUTE MODULI
C
C
      SIG3=SIGI3(N)
      IF(SIG3.LE.0.0) GO TO 50
      FI=(PHI(M)-DPHI(M)*ALOG10(SIG3/PATM))/57.28
      GO TO 60
   50 FI = PHI(M)/57.28
   60 CONTINUE
      RCS=2.*(CM(M)*COS(FI)+SIG3*SIN(FI))/(1.0-SIN(FI))
      HCS = RCS/RF(M)
```

```
      F=SIG3/PATM
      IF(RCS.GT.0.0) GO TO 70
      SL(N) = 1.0
      GO TO 80
   70 SL(N) = DEV/RCS
      IF (SL(N) .GT. 1.0 .AND. KSTART .NE.0) SL(N)=1.0
      IF(SL(N).GT.1.0) GO TO 100
   80 CONTINUE
      IF(SIG3.LE.0.0.AND.KSTART.NE.0) GO TO 86
      IF(SIG3.LE.0.0) GO TO 100
   85 CONTINUE
      EI = COEF(M)*(F**EXP(M))*PATM
      ETAN(N) = EI*((1.0 - SL(N)*RF(M))**2)
      GO TO 87
   86 ETAN(N)=0.00001
      EI=COEF(M)*(PATM**EXP(M))*PATM
   87 CONTINUE
C
C     COMPUTE POISSONS RATIO
C
      IF(SIG3 .LE. PATM) SIG3=PATM
      STRAIN=2.0*CR/(EI*(1.0-(2.0*CR/HCS)))
      PRAT=GM(M)-FM(M)*ALOG10(SIG3/PATM)
      TNU(N) =PRAT/(1.0-DM(M)*STRAIN)**2
      IF(TNU(N).GT.0.49) TNU(N) = 0.49
C
      IF(STAGE.EQ.2) GO TO 90
      BMOD(N) = ETAN(N)/(2.0*(1.0+TNU(N))*(1.0-2.0*TNU(N)))
   90 SMOD(N) = ETAN(N)/(2.0*(1.0+TNU(N)))
C
      GO TO 110
C
  100 SMOD(N)=.00001
C
  110 CONTINUE
C
      RETURN
C
      END


      SUBROUTINE BLOCK(A,B,BINT,P,ST,IX,X,Y,CODE,XLD,YLD,GAM,CM,PHI,
     1                 DPHI,COEF,EXP,DM,GM,FM,RF,ETAN,BMOD,SMOD,TNU,
     2                 SIGMA,SIGIT,SL,SIGI3,NEL,NDP,MAT,M2,M3,N2)
C
      COMMON/CONST1/ NLD,VOL,MTYPE,NSTEP,PATM,GAMW,NNN,TIME(3)
      COMMON/CONST2/ ITER,MBAND,NUMBLK,TITLE(8),STAGE,XL(50),YL(50),NLC
      COMMON/CONST3/ KPNCH,KSTART,NANA
C
      DIMENSION GAM(MAT),COEF(MAT),EXP(MAT),DM(MAT),GM(MAT),FM(MAT),
     *          CM(MAT),PHI(MAT),DPHI(MAT),RF(MAT)
      DIMENSION X(NDP),Y(NDP),XLD(NDP),YLD(NDP),CODE(NDP),
     1          B(N2),BINT(N2)
      DIMENSION IX(NEL,5),SIGMA(3,NEL),SIGIT(3,NEL),SIGI3(NEL),
```

```
     *           BMOD(NEL),SMOD(NEL),ETAN(NEL),TNU(NEL),SL(NEL)
      DIMENSION A(M2,M3),P(8),ST(3,8),C(3,3),S(8,8),LM(4)
C
      INTEGER CODE,STAGE
C
C
C     INITIALIZATION
C
C
      REWIND 2
      REWIND 4
      NB = MBAND/2
      ND=2*NB
      ND2=2*ND
      NUMBLK=0
C
      DO 10 N = 1,ND2
      B(N) = 0.0
      DO 10 M = 1,ND
   10 A(N,M) = 0.0
C
C
C     FORM STIFFNESS MATRIX IN BLOCKS
C
C
   30 NUMBLK = NUMBLK+1
      NH = NB*(NUMBLK+1)
      NM = NH-NB
      NL = NM - NB + 1
      KSHIFT = 2*NL - 2
C
C
C     START ELEMENT LOOP
C
C
      DO 210 N = 1,NEL
C
      DO 40 I = 1,3
      DO 40 J = 1,8
   40 ST(I,J) = 0.0
C
      IF (IX(N,5)) 210,210,50
   50 DO 80 I = 1,4
      IF (IX(N,I)-NL) 80,70,70
   70 IF (IX(N,I)-NM) 90,90,80
   80 CONTINUE
      GO TO 210
C
C
   90 CONTINUE
C
      CALL MATRIX(N,GAM,CM,PHI,DPHI,COEF,EXP,DM,GM,FM,RF,ETAN,BMOD,SMOD,
     1         TNU,SL,SIGMA,SIGIT,IX,X,Y,P,C,S,ST,SIGI3,NEL,NDP,MAT)
C
      IF (VOL) 100,100,110
  100 WRITE(6,2003) N
```

```
C
C     ADD ELEMENT STIFFNESS TO TOTAL STIFFNESS
C
C
  110 IX(N,5) = -IX(N,5)
      DO 120 I = 1,4
      LM(I) = 2*IX(N,I) - 2
  120 CONTINUE
C
      DO 130 I = 1,4
      DO 130 K = 1,2
      II = LM(I) + K - KSHIFT
      KK = 2*I - 2 + K
      B(II) = B(II) + P(KK)
      DO 130 J = 1,4
      DO 130 L = 1,2
      JJ = LM(J) + L - II + 1 - KSHIFT
      LL = 2*J - 2 + L
      IF(JJ.LE.0) GO TO 130
      A(II,JJ) = A(II,JJ) + S(KK,LL)
  130 CONTINUE
C
  210 CONTINUE
C
C
C     FORM LOAD VECTOR FOR CURRENT STEP AND BLOCK
C
      DO 240 N=NL,NM
      IF(N.GT.NDP) GO TO 240
      K=N+N-KSHIFT
      IF(ITER.EQ.1.AND.MANA.EQ.2) GO TO 230
      IF(ITER.EQ.1.AND.STAGE.EQ.1) GO TO 230
      BINT(N+N-1) = (B(K-1)+XLD(N))/NLD
      BINT(N+N) = (B(K)+YLD(N))/NLD
  230 B(K) = BINT(N+N)
      B(K-1) = BINT(N+N-1)
  240 CONTINUE
C
C
C     APPLY BOUNDARY CONDITIONS
C
      DO 300 M = NL,NH
      IF(M.GT.NDP) GO TO 300
      MC = CODE(M) + 1
      GO TO (300,250,260,250), MC
  250 R=XLD(M)
      N = 2*M - 1 - KSHIFT
      GO TO 280
  260 R=YLD(M)
      N = 2*M - KSHIFT
      MC = 0
C
  280 CALL BCOND(A,B,ND2,MBAND,N,R,M2,M3,N2)
C
      IF(MC.EQ.4) GO TO 260
  300 CONTINUE
```

```
C     WRITE BLOCK OF EQUATIONS ON TAPE AND SHIFT UP LOWER BLOCK
C
      WRITE(2) ((A(N,M),N=1,ND),M=1,MBAND),(B(N),N=1,ND)
C
      DO 330 N = 1,ND
      K = N + ND
      B(N) = B(K)
      B(K) = 0.0
      DO 330 M = 1,ND
      A(N,M) = A(K,M)
  330 A(K,M) = 0.0
C
C     CHECK FOR LAST BLOCK
C
      IF(NM-NDP) 30,340,340
  340 CONTINUE
C
C
      RETURN
C
 2003 FORMAT (26H0NEGATIVE AREA ELEMENT NO. I4)
C
      END




      SUBROUTINE MATRIX(N,GAM,CM,PHI,DPHI,COEF,EXP,DM,GM,FM,RF,ETAN,
     1             BMOD,SMOD,TNU,SL,SIGMA,SIGIT,IX,X,Y,P,C,S,ST,
     2             SIGI3,NEL,NDP,MAT)
C
      COMMON/CONST1/ NLD,VOL,MTYPE,NSTEP,PATM,GAMW,NNN,TIME(3)
      COMMON/CONST2/ ITER,MBAND,NUMBLK,TITLE(8),STAGE,XL(50),YL(50),NLC
      COMMON/CONST3/KPNCH,KSTART,NANA
C
      DIMENSION GAM(MAT),COEF(MAT),EXP(MAT),DM(MAT),GM(MAT),FM(MAT),
     *          CM(MAT),PHI(MAT),DPHI(MAT),RF(MAT)
      DIMENSION X(NDP),Y(NDP)
      DIMENSION IX(NEL,5),SIGMA(3,NEL),SIGIT(3,NEL),SIGI3(NEL),
     *          BMOD(NEL),SMOD(NEL),ETAN(NEL),TNU(NEL),SL(NEL)
      DIMENSION P(8),ST(3,8),C(3,3),S(3,8)
C
      INTEGER STAGE
C
C
      I = IX(N,1)
      J = IX(N,2)
      K = IX(N,3)
      L = IX(N,4)
      MTYPE = IX(N,5)
      M = MTYPE
      IF(STAGE.EQ.2.AND.NLD.EQ.1.AND.NANA.EQ.1) GO TO 50
C
C          FORM STRESS-STRAIN RELATIONSHIP
C
      CALL NONLIN(N,I,J,K,L,M,ETAN,TNU,BMOD,SMOD,EI,HCS,GAM,COEF,EXP,DM,
```

```
     1              GM,FM,CM,PHI,DPHI,RF,SIGIT,SIGMA,SL,X,Y,IX,
     2              SIGI3,NEL,NDP,MAT)
C
   50 CONTINUE
      C(1,1) = BMOD(N) + SMOD(N)
      C(1,2) = BMOD(N) - SMOD(N)
      C(1,3) = 0.0
      C(2,1) = C(1,2)
      C(2,2) = C(1,1)
      C(2,3) = 0.0
      C(3,1) = 0.0
      C(3,2) = 0.0
       C(3,3) = SMOD(N)
C
C
C     FORM QUADRILATERAL STIFFNESS MATRIX FOR EACH ELEMENT
C
      DO 100 II = 1,8
      P(II) = 0.0
      DO 100 JJ = 1,8
      S(II,JJ) = 0.0
  100 CONTINUE
C
      VOL = 0.0
C
      CALL ELMAT(I,J,K,L,C,S,ST,X,Y,VOL,NDP)
C
C     CALCUATE GRAVITY LOADS
C
      IF(STAGE.EQ.2) GO TO 300
      IF(ITER.NE.0) GO TO 300
C
      W = GAM(M)
C
      FG=-W*VOL
      IF (IX(N,3) .EQ. IX(N,4))  GO TO 150
      FG=FG/4.
      KL=4
      GO TO 160
  150 FG=FG/3.0
      KL=3
  160 CONTINUE
      DO 200 IJ=1,KL
      II=IJ+IJ
      P(II)=P(II)+FG
  200 CONTINUE
C
  300 CONTINUE
C
      RETURN
C
      END
```

```
      SUBROUTINE USOL (A,B,MAXB,NEQB,MB,LL,NBLOCK,NSB,NORG,NBKS,NT1,
     .                                                          NT2,NRST)
C     THIS SUBROUTINE (CODED BY WILSON) USES AN EFFICIENT GAUSSIAN ELIMI
C     TECHNIQUE TO SOLVE THE SIMULTANEOUS EQUATIONS
      DIMENSION A(NSB),B(NSB),MAXB(NEQB)
C
      NC=MB+LL
      NBR=(MB-1)/NEQB+1
      INC=NEQB-1
      NMB=NEQB*MB
      N2=NT2
      N1=NT1
      REWIND NORG
      REWIND NBKS
C
C     REDUCE EQUATIONS BLOCK BY BLOCK
C
      DO 900 N=1,NBLOCK
      IF (N.GT.1.AND.NBR.EQ.1) GO TO 110
      IF (NBR.EQ.1) GO TO 105
      REWIND N1
      REWIND N2
  105 NI=N1
      IF(N.EQ.1) NI=NORG
      READ (NI) A
  110 DO 300 I=1,NEQB
      D=A(I)
      IF(D) 115,300,120
  115 M=NEQB*(N-1)+I
      WRITE (6,116) M,D
  116 FORMAT (33H0SET OF EQUATIONS MAY BE SINGULAR   /
     .  26H DIAGONAL TERM OF EQUATION   I8, 8H  EQUALS   1PE12.4)
      D=-D
  120 D=SQRT(D)
      A(I)=D
C
      II=I
      DO 125 J=2,NC
      II=II+NEQB
  125 A(II)=A(II)/D
C
      DO 130 J=I,NMB,NEQB
      IF (A(J).NE.0.) MAXB(I)=J
  130 CONTINUE
C
      JL=I+1
      IF (JL.GT.NEQB) GO TO 300
      II=I
      DO 200 J=JL,NEQB
      II=II+NEQB
      IF(II.GT.NMB) GO TO 200
      C=A(II)
      IF (C.EQ.0.0) GO TO 200
C
      KK=J
      MAX=MAXB(I)
      DO 150 JJ=II,MAX,NEQB
```

```
      A(KK)=A(KK)-C*A(JJ)
  150 KK=KK+NEQB
C
      KK=J +NMB
      JJ=I+NMB
      DO 175 L=1,LL
      A(KK)=A(KK)-C*A(JJ)
      KK=KK+NEQB
  175 JJ=JJ+NEQB
  200 CONTINUE
  300 CONTINUE
      WRITE (NBKS) A,MAXB
C
C     SUBSTITUTE INTO REMAINING EQUATIONS
C
      DO 800 NN=1,NBR
      IF(N+NN.GT.NBLOCK) GO TO 800
      NI=N1
      IF(N.EQ.1) NI=NORG
      IF(NN.EQ.NBR) NI=NORG
      READ (NI) B
      IL=1+NN*NEQB*NEQB
      DO 700 I=1,NEQB
      II=IL
      DO 690 K=1,NEQB
      IF (II.GT.NMB) GO TO 690
      C=A(II)
      IF (C.EQ.0.0) GO TO 690
      MAX=MAXB(K)
C
      KK=I
      DO 640 JJ=II,MAX,NEQB
      B(KK)=B(KK)-C*A(JJ)
  640 KK=KK+NEQB
C
      KK=I+NMB
      JJ=K+NMB
      DO 650 L=1,LL
      B(KK)=B(KK)-C*A(JJ)
      KK=KK+NEQB
  650 JJ=JJ+NEQB
C
  690 II=II-INC
  700 IL=IL+NEQB
C
      IF(NBR.NE.1) GO TO 750
      DO 740 I=1,NSB
  740 A(I)=B(I)
      GO TO 800
  750 WRITE (N2) B
  800 CONTINUE
C
      M=N1
      N1=N2
  900 N2=M
C
C     BACKSUBSTITUTION - RESULTS ON TAPE NRST
```

```
C
      LS=LL*NEQB
      NEB=NEQB*(NBR+1)
      NUM=NBR*NEQB
      MAX=NEB*LL
      DO 905 I=1,MAX
  905 B(I)=0.
      REWIND NRST
C
      DO 1000 N=1,NBLOCK
      BACKSPACE NBKS
      READ (NBKS) A,MAXB
      BACKSPACE NBKS
      DO 910 L=1,LL
      K=L*NEB
      DO 910 J=1,NUM
      I=K-NEQB
      B(K)=B(I)
  910 K=K-1
C
      I=NMB
      DO 920 L=1,LL
      K=(L-1)*NEB
      DO 920 J=1,NEQB
      I=I+1
      K=K+1
  920 B(K)=A(I)
C
      DO 955 I=1,NEQB
      J=NEQB+1-I
      MAX=MAXB(J)
      IF (A(J).EQ.0.) GO TO 955
      DO 950 L=1,LL
      KK=J+(L-1)*NEB
      JJ=KK+1
      IL=J+NEQB
      C=B(KK)
      DO 940 II=IL,MAX,NEQB
      C=C-A(II)*B(JJ)
  940 JJ=JJ+1
  950 B(KK)=C/A(J)
  955 CONTINUE
C
      I=0
      DO 960 L=1,LL
      K=(L-1)*NEB
      DO 960 J=1,NEQB
      K=K+1
      I=I+1
  960 A(I)=B(K)
C
      WRITE (NRST) (A(I),I=1,LS)
 1000 CONTINUE
C
      RETURN
      END
```

```
      SUBROUTINE BAND(IX,NEL)
C
      COMMON/CONST1/ NLD,VOL,MTYPE,NSTEP,PATM,GAMW,NNN,TIME(3)
      COMMON/CONST2/ ITER,MBAND,NUMBLK,TITLE(8),STAGE,XL(50),YL(50),NLC
C
      DIMENSION IX(NEL,5)
C
C     DETERMINE BAND WIDTH
C
      JDIF = 0
C
      DO 300 N = 1,NEL
      DO 200 I = 1,3
      DO 100 J = 1,3
      L = I + J
      IF(L.GT.4) GO TO 200
      NDIF = IABS(IX(N,I)-IX(N,L))
      IF(NDIF.GT.JDIF) JDIF = NDIF
  100 CONTINUE
  200 CONTINUE
  300 CONTINUE
C
      MBAND = 2*JDIF + 2
C
      WRITE(6,2000) MBAND
C
      RETURN
C
 2000 FORMAT(1H1,////10X,11HBANDWIDTH =,I5)
C
      END



      SUBROUTINE ELMAT (IA,JA,KA,LA,C,S,ST,X,Y,VOL,NDP)
C
C     THIS SUBROUTINE FORMS THE STIFFNESS MATRIX FOR A RECTANGULAR ELEME
C     SUBROUTINE IS A MODIFICATION OF GLST WRITTEN BY A. ALCAIDE (1971)
C
C     VS,VT   LOCAL COORDINATES OF ELEMENT
C     VH      COEFFICIENTS FOR GAUSSIAN INTEGRATION
C     ST      STRAIN-DISPLACEMENT MATRIX AT ELEMENT CENTER
C     AB      STRAIN-DISPLACEMENT MATRIX AT POINT VS,VT
C     S       STIFFNESS MATRIX OF ELEMENT
C     AS      FIRST DIFFERENTIAL OF S AT VS,VT
C     AJ      MATRIX PROPORTIONAL TO INVERTED JACOBIAN MATRIX
C     COMM    VARIABLE PROPORTIONAL TO JACOBIAN DETERMINANT
C
C     THE STRAIN-DISPLACEMENT RELATIONSHIP (ST) FOR EACH ELEMENT IS STOR
C     TAPE 4 FOR LATER USE IN SUBROUTINE STRESS
C
```

```
      DIMENSION X(NDP),Y(NDP)
      DIMENSION C(3,3),ST(3,8),S(8,8)
      DIMENSION VH(6),VS(6),VT(6),AP(2,4),AB(3,8),AS(8,8)
C
      NP1=4
      VH(1)=0.5555555556
      VH(2)=0.8888888889
      VH(3)=VH(1)
      VS(1)=0.7745966692
      VS(2)=0.
      VS(3)=-VS(1)
      VT(1)=VS(1)
      VT(2)=0.
      VT(3)=VS(3)
      VS(NP1)=0.
      VT(NP1)=0.
      VOL=(Y(JA)-Y(LA))*(X(IA)+X(JA)-X(KA)-X(LA))
      VOL=VOL-(X(JA)-X(LA))*(Y(IA)+Y(JA)-Y(KA)-Y(LA))
      VOL=0.5*VOL
      DO 1 I=1,NP1
      DO 1 J=1,NP1
      IF (I.EQ.NP1.AND.J.EQ.NP1) GO TO 10
      IF (I.EQ.NP1) GO TO 1
      IF (J.EQ.NP1) GO TO 1
   10 AP(1,1)=-1.+VT(J)
      AP(2,1)=-1.+VS(I)
      AP(1,2)=1.-VT(J)
      AP(2,2)=-1.-VS(I)
      AP(1,3)=1.+VT(J)
      AP(2,3)=1.+VS(I)
      AP(1,4)=-1.-VT(J)
      AP(2,4)=1.-VS(I)
      AJ1=AP(2,1)*Y(IA)+AP(2,2)*Y(JA)+AP(2,3)*Y(KA)+AP(2,4)*Y(LA)
      AJ2=-AP(1,1)*Y(IA)-AP(1,2)*Y(JA)-AP(1,3)*Y(KA)-AP(1,4)*Y(LA)
      AJ3=-AP(2,1)*X(IA)-AP(2,2)*X(JA)-AP(2,3)*X(KA)-AP(2,4)*X(LA)
      AJ4=AP(1,1)*X(IA)+AP(1,2)*X(JA)+AP(1,3)*X(KA)+AP(1,4)*X(LA)
      COMM=AJ1*AJ4-AJ2*AJ3
      DO 2 K=1,4
      K1=2*K-1
      K2=2*K
      AB(1,K1)=AJ1*AP(1,K)+AJ2*AP(2,K)
      AB(3,K2)=AB(1,K1)
      AB(1,K2)=0.
      AB(2,K2)=AJ3*AP(1,K)+AJ4*AP(2,K)
      AB(3,K1)=AB(2,K2)
    2 AB(2,K1)=0.
      IF (I. EQ.NP1.AND.J.EQ.NP1) GO TO 20
      DO 40 K=1,8
      DO 40 L=1,3
      ST(L,K)=0.
      DO 40 M=1,3
   40 ST(L,K)=ST(L,K)+C(L,M)*AB(M,K)
      DO 41 K=1,8
      DO 41 L=1,8
      AS(K,L)=0.
      DO 41 M=1,3
   41 AS(K,L)=AS(K,L)+AB(M,K)*ST(M,L)
```

```
      DO 5 K=1,8
      DO 5 L=1,8
    5 S(K,L)=S(K,L)+(VH(I)*VH(J)*AS(K,L))/(16.*COMM)
    1 CONTINUE
   20 DO 6 I=1,3
      DO 6 J=1,8
    6 ST(I,J)=AB(I,J)/COMM
C
C     WRITE STRAIN-DISPLACEMENT MATRIX ON TAPE
C
      WRITE(4) ST
C
      RETURN
C
      END



      SUBROUTINE BCOND (A,B,NEQ,MBAND,N,U,M2,M3,N2)
C
C     THIS SUBROUTINE APPLIES THE BOUNDARY CONDITIONS TO THE STRUCTURE S
C     MATRIX
      DIMENSION A(M2,M3),B(N2)
C
      DO 40 M = 2,MBAND
      K = N - M + 1
      IF(K) 20,20,10
   10 B(K) = B(K) - A(K,M)*U
      A(K,M) = 0.0
   20 K = N + M - 1
      IF(NEQ-K) 40,30,30
   30 B(K) = B(K) - A(N,M)*U
      A(N,M) = 0.0
   40 CONTINUE
      A(N,1) = 1.0
      B(N) = U
C
      RETURN
C
      END



      SUBROUTINE APPROX(N,I,J,K,L,M,SIGMA,X,Y,GM,GAM,NEL,NDP,MAT)
C
      COMMON/CONST1/ NLD,VOL,MTYPE,NSTEP,PATM,GAMW,NNN,TIME(3)
      COMMON/CONST2/ ITER,MBAND,NUMBLK,TITLE(8),STAGE,XL(50),YL(50),NLC
C
      DIMENSION SIGMA(3,NEL),X(NDP),Y(NDP),GM(MAT),GAM(MAT)
C
C     COORDINATES OF CENTROID OF ELEMENT
C
      IF (K.EQ.L) GO TO 10
```

```
      XC = (X(I)+X(J)+X(K)+X(L))/4.0
      YC = (Y(I)+Y(J)+Y(K)+Y(L))/4.0
      GO TO 20
   10 XC = (X(I)+X(J)+X(K))/3.0
      YC = (Y(I)+Y(J)+Y(K))/3.0
   20 CONTINUE
C
C     DETERMINE O/B PRESSURE
C
      DO 30 IL = 1,NLC
      IF(XC.LE.XL(IL)) GO TO 40
   30 CONTINUE
C
   40 YD = YL(IL) - YL(IL-1)
      XD = XL(IL) - XL(IL-1)
      YM = YD*(XC-XL(IL-1))/XD
      YH = YL(IL-1) + YM - YC
      ALPHA=ATAN2(YD,XD)
      SIGMA(2,N) = YH*GAM(M)/NLD
      AKO = GM(M)/(1.0-GM(M))
      SIGMA(1,N) = SIGMA(2,N)*AKO
      SIGMA(3,N)=0.5*(SIGMA(2,N)*SIN(ALPHA))
C
      RETURN
C
C
      END



      SUBROUTINE EQUIV(N,EPSX,EPSY,GAMXY,EI,HCS,EP,SIG,IX,ENF,X,
     1                 Y,NEL,NDP,ETAN,TNU,SMOD)
C
C
      COMMON/CONST1/ NLD,VOL,MTYPE,NSTEP,PATM,GAMW,NNN,TIME(3)
      COMMON/CONST2/ ITER,MBAND,NUMBLK,TITLE(8),STAGE,XL(50),YL(50),NLC
      COMMON/CONST3/KPNCH,KSTART,MANA
C
C
      DIMENSION EP(NEL),IX(NEL,5),X(NDP),Y(NDP),ENF(NDP,2),SIG(6)
      DIMENSION ETAN(NEL),TNU(NEL),SMOD(NEL)
C
C
C     CALCULATE STRAIN CORRESPONDING TO INITIAL STRESSES
C
      DEV1=SIG(5)-SIG(6)
      EE=EI*(1.-DEV1/HCS)
      EPS1=DEV1/EE
C
      EPS1F = EPS1 + EP(N)
C
      DEV2 = EPS1F/(1.0/EI + EPS1F/HCS)
C
C     CALCULATE INCREASE IN SHEAR STRESS DUE TO STRAIN POTENTIAL
C
```

```
      DTAU = (DEV2-DEV1)/2.0
      IF(NANA.NE.1) GO TO 100
      ETAN(N)=DTAU*2./EP(N)
      SMOD(N)=ETAN(N)/(2.0*(1.0+TNU(N)))
  100 CONTINUE
C
C     CALCULATE EQUIVALENT NODAL LOADS FOR ELEMENT
C
      I=IX(N,1)
      J=IX(N,2)
      K = IX(N,3)
      L = IX(N,4)
      D=(ABS(X(I)-X(J))+ABS(X(K)-X(L)))*0.5
      DV=(ABS(Y(L)-Y(I))+ABS(Y(K)-Y(J)))*0.5
      TXY = SIG(3)
      F= -SIGN(DTAU,TXY)*D/2.0
      FV=-SIGN(DTAU,TXY)*DV*0.5
      PM=TXY/SIG(2)
      IF(ABS(PM) .LE. 0.001) F=0.
      IF(ABS(PM) .LE. 0.001) FV=0.
C
C     ADD ELEMENT NODAL FORCES TO STRUCTURE NODAL FORCES
C
      ENF(K,1) = ENF(K,1) + F
      ENF(L,1) = ENF(L,1) + F
      ENF(I,1)=ENF(I,1)-F
      ENF(J,1)=ENF(J,1)-F
      ENF(I,2)=ENF(I,2)-FV
      ENF(L,2)=ENF(L,2)-FV
      ENF(J,2)=ENF(J,2)+FV
      ENF(K,2)=ENF(K,2)+FV
C
      RETURN
C
      END
```

EARTHQUAKE ENGINEERING RESEARCH CENTER REPORTS

NOTE: Numbers in parenthesis are Accession Numbers assigned by the National Technical Information Service; these are followed by a price code. Copies of the reports may be ordered from the National Technical Information Service, 5285 Port Royal Road, Springfield, Virginia, 22161. Accession Numbers should be quoted on orders for reports (PB --- ---) and remittance must accompany each order. Reports without this information were not available at time of printing. Upon request, EERC will mail inquirers this information when it becomes available.

EERC 67-1 "Feasibility Study Large-Scale Earthquake Simulator Facility," by J. Penzien, J.G. Bouwkamp, R.W. Clough and D. Rea - 1967 (PB 187 905)A07

EERC 68-1 Unassigned

EERC 68-2 "Inelastic Behavior of Beam-to-Column Subassemblages Under Repeated Loading," by V.V. Bertero - 1968 (PB 184 888)A05

EERC 68-3 "A Graphical Method for Solving the Wave Reflection-Refraction Problem," by H.D. McNiven and Y. Mengi - 1968 (PB 187 943)A03

EERC 68-4 "Dynamic Properties of McKinley School Buildings," by D. Rea, J.G. Bouwkamp and R.W. Clough - 1968 (PB 187 902)A07

EERC 68-5 "Characteristics of Rock Motions During Earthquakes," by H.B. Seed, I.M. Idriss and F.W. Kiefer - 1968 (PB 188 338)A03

EERC 69-1 "Earthquake Engineering Research at Berkeley," - 1969 (PB 187 906)A11

EERC 69-2 "Nonlinear Seismic Response of Earth Structures," by M. Dibaj and J. Penzien - 1969 (PB 187 904)A08

EERC 69-3 "Probabilistic Study of the Behavior of Structures During Earthquakes," by R. Ruiz and J. Penzien - 1969 (PB 187 886)A06

EERC 69-4 "Numerical Solution of Boundary Value Problems in Structural Mechanics by Reduction to an Initial Value Formulation," by N. Distefano and J. Schujman - 1969 (PB 187 942)A02

EERC 69-5 "Dynamic Programming and the Solution of the Biharmonic Equation," by N. Distefano - 1969 (PB 187 941)A03

EERC 69-6 "Stochastic Analysis of Offshore Tower Structures," by A.K. Malhotra and J. Penzien - 1969 (PB 187 903)A09

EERC 69-7 "Rock Motion Accelerograms for High Magnitude Earthquakes," by H.B. Seed and I.M. Idriss - 1969 (PB 187 940)A02

EERC 69-8 "Structural Dynamics Testing Facilities at the University of California, Berkeley," by R.M. Stephen, J.G. Bouwkamp, R.W. Clough and J. Penzien - 1969 (PB 189 111)A04

EERC 69-9 "Seismic Response of Soil Deposits Underlain by Sloping Rock Boundaries," by H. Dezfulian and H.B. Seed 1969 (PB 189 114)A03

EERC 69-10 "Dynamic Stress Analysis of Axisymmetric Structures Under Arbitrary Loading," by S. Ghosh and E.L. Wilson 1969 (PB 189 026)A10

EERC 69-11 "Seismic Behavior of Multistory Frames Designed by Different Philosophies," by J.C. Anderson and V. V. Bertero - 1969 (PB 190 662)A10

EERC 69-12 "Stiffness Degradation of Reinforcing Concrete Members Subjected to Cyclic Flexural Moments," by V.V. Bertero, B. Bresler and H. Ming Liao - 1969 (PB 202 942)A07

EERC 69-13 "Response of Non-Uniform Soil Deposits to Travelling Seismic Waves," by H. Dezfulian and H.B. Seed - 1969 (PB 191 023)A03

EERC 69-14 "Damping Capacity of a Model Steel Structure," by D. Rea, R.W. Clough and J.G. Bouwkamp - 1969 (PB 190 663)A06

EERC 69-15 "Influence of Local Soil Conditions on Building Damage Potential during Earthquakes," by H.B. Seed and I.M. Idriss - 1969 (PB 191 036)A03

EERC 69-16 "The Behavior of Sands Under Seismic Loading Conditions," by M.L. Silver and H.B. Seed - 1969 (AD 714 982)A07

EERC 70-1 "Earthquake Response of Gravity Dams," by A.K. Chopra - 1970 (AD 709 640)A03

EERC 70-2 "Relationships between Soil Conditions and Building Damage in the Caracas Earthquake of July 29, 1967," by H.B. Seed, I.M. Idriss and H. Dezfulian - 1970 (PB 195 762)A05

EERC 70-3 "Cyclic Loading of Full Size Steel Connections," by E.P. Popov and R.M. Stephen - 1970 (PB 213 545)A04

EERC 70-4 "Seismic Analysis of the Charaima Building, Caraballeda, Venezuela," by Subcommittee of the SEAONC Research Committee: V.V. Bertero, P.F. Fratessa, S.A. Mahin, J.H. Sexton, A.C. Scordelis, E.L. Wilson, L.A. Wyllie, H.B. Seed and J. Penzien, Chairman - 1970 (PB 201 455)A06

EERC 70-5 "A Computer Program for Earthquake Analysis of Dams," by A.K. Chopra and P. Chakrabarti - 1970 (AD 723 994)A05

EERC 70-6 "The Propagation of Love Waves Across Non-Horizontally Layered Structures," by J. Lysmer and L.A. Drake 1970 (PB 197 896)A03

EERC 70-7 "Influence of Base Rock Characteristics on Ground Response," by J. Lysmer, H.B. Seed and P.B. Schnabel 1970 (PB 197 897)A03

EERC 70-8 "Applicability of Laboratory Test Procedures for Measuring Soil Liquefaction Characteristics under Cyclic Loading," by H.B. Seed and W.H. Peacock - 1970 (PB 198 016)A03

EERC 70-9 "A Simplified Procedure for Evaluating Soil Liquefaction Potential," by H.B. Seed and I.M. Idriss - 1970 (PB 198 009)A03

EERC 70-10 "Soil Moduli and Damping Factors for Dynamic Response Analysis," by H.B. Seed and I.M. Idriss - 1970 (PB 197 869)A03

EERC 71-1 "Koyna Earthquake of December 11, 1967 and the Performance of Koyna Dam," by A.K. Chopra and P. Chakrabarti 1971 (AD 731 496)A06

EERC 71-2 "Preliminary In-Situ Measurements of Anelastic Absorption in Soils Using a Prototype Earthquake Simulator," by R.D. Borcherdt and P.W. Rodgers - 1971 (PB 201 454)A03

EERC 71-3 "Static and Dynamic Analysis of Inelastic Frame Structures," by F.L. Porter and G.H. Powell - 1971 (PB 210 135)A06

EERC 71-4 "Research Needs in Limit Design of Reinforced Concrete Structures," by V.V. Bertero - 1971 (PB 202 943)A04

EERC 71-5 "Dynamic Behavior of a High-Rise Diagonally Braced Steel Building," by D. Rea, A.A. Shah and J.G. Bouwkamp 1971 (PB 203 584)A06

EERC 71-6 "Dynamic Stress Analysis of Porous Elastic Solids Saturated with Compressible Fluids," by J. Ghaboussi and E. L. Wilson - 1971 (PB 211 396)A06

EERC 71-7 "Inelastic Behavior of Steel Beam-to-Column Subassemblages," by H. Krawinkler, V.V. Bertero and E.P. Popov 1971 (PB 211 335)A14

EERC 71-8 "Modification of Seismograph Records for Effects of Local Soil Conditions," by P. Schnabel, H.B. Seed and J. Lysmer - 1971 (PB 214 450)A03

EERC 72-1 "Static and Earthquake Analysis of Three Dimensional Frame and Shear Wall Buildings," by E.L. Wilson and H.H. Dovey - 1972 (PB 212 904)A05

EERC 72-2 "Accelerations in Rock for Earthquakes in the Western United States," by P.B. Schnabel and H.B. Seed - 1972 (PB 213 100)A03

EERC 72-3 "Elastic-Plastic Earthquake Response of Soil-Building Systems," by T. Minami - 1972 (PB 214 868)A08

EERC 72-4 "Stochastic Inelastic Response of Offshore Towers to Strong Motion Earthquakes," by M.K. Kaul - 1972 (PB 215 713)A05

EERC 72-5 "Cyclic Behavior of Three Reinforced Concrete Flexural Members with High Shear," by E.P. Popov, V.V. Bertero and H. Krawinkler - 1972 (PB 214 555)A05

EERC 72-6 "Earthquake Response of Gravity Dams Including Reservoir Interaction Effects," by P. Chakrabarti and A.K. Chopra - 1972 (AD 762 330)A08

EERC 72-7 "Dynamic Properties of Pine Flat Dam," by D. Rea, C.Y. Liaw and A.K. Chopra - 1972 (AD 763 928)A05

EERC 72-8 "Three Dimensional Analysis of Building Systems," by E.L. Wilson and H.H. Dovey - 1972 (PB 222 438)A06

EERC 72-9 "Rate of Loading Effects on Uncracked and Repaired Reinforced Concrete Members," by S. Mahin, V.V. Bertero, D. Rea and M. Atalay - 1972 (PB 224 520)A08

EERC 72-10 "Computer Program for Static and Dynamic Analysis of Linear Structural Systems," by E.L. Wilson, K.-J. Bathe, J.E. Peterson and H.H.Dovey - 1972 (PB 220 437)A04

EERC 72-11 "Literature Survey - Seismic Effects on Highway Bridges," by T. Iwasaki, J. Penzien and R.W. Clough - 1972 (PB 215 613)A19

EERC 72-12 "SHAKE-A Computer Program for Earthquake Response Analysis of Horizontally Layered Sites," by P.B. Schnabel and J. Lysmer - 1972 (PB 220 207)A06

EERC 73-1 "Optimal Seismic Design of Multistory Frames," by V.V. Bertero and H. Kamil - 1973

EERC 73-2 "Analysis of the Slides in the San Fernando Dams During the Earthquake of February 9, 1971," by H.B. Seed, K.L. Lee, I.M. Idriss and F. Makdisi - 1973 (PB 223 402)A14

EERC 73-3 "Computer Aided Ultimate Load Design of Unbraced Multistory Steel Frames," by M.B. El-Hafez and G.H. Powell 1973 (PB 248 315)A09

EERC 73-4 "Experimental Investigation into the Seismic Behavior of Critical Regions of Reinforced Concrete Components as Influenced by Moment and Shear," by M. Celebi and J. Penzien - 1973 (PB 215 884)A09

EERC 73-5 "Hysteretic Behavior of Epoxy-Repaired Reinforced Concrete Beams," by M. Celebi and J. Penzien - 1973 (PB 239 568)A03

EERC 73-6 "General Purpose Computer Program for Inelastic Dynamic Response of Plane Structures," by A. Kanaan and G.H. Powell - 1973 (PB 221 260)A08

EERC 73-7 "A Computer Program for Earthquake Analysis of Gravity Dams Including Reservoir Interaction," by P. Chakrabarti and A.K. Chopra - 1973 (AD 766 271)A04

EERC 73-8 "Behavior of Reinforced Concrete Deep Beam-Column Subassemblages Under Cyclic Loads," by O. Küstü and J.G. Bouwkamp - 1973 (PB 246 117)A12

EERC 73-9 "Earthquake Analysis of Structure-Foundation Systems," by A.K. Vaish and A.K. Chopra - 1973 (AD 766 272)A07

EERC 73-10 "Deconvolution of Seismic Response for Linear Systems," by R.B. Reimer - 1973 (PB 227 179)A08

EERC 73-11 "SAP IV: A Structural Analysis Program for Static and Dynamic Response of Linear Systems," by K.-J. Bathe, E.L. Wilson and F.E. Peterson - 1973 (PB 221 967)A09

EERC 73-12 "Analytical Investigations of the Seismic Response of Long, Multiple Span Highway Bridges," by W.S. Tseng and J. Penzien - 1973 (PB 227 816)A10

EERC 73-13 "Earthquake Analysis of Multi-Story Buildings Including Foundation Interaction," by A.K. Chopra and J.A. Gutierrez - 1973 (PB 222 970)A03

EERC 73-14 "ADAP: A Computer Program for Static and Dynamic Analysis of Arch Dams," by R.W. Clough, J.M. Raphael and S. Mojtahedi - 1973 (PB 223 763)A09

EERC 73-15 "Cyclic Plastic Analysis of Structural Steel Joints," by R.B. Pinkney and R.W. Clough - 1973 (PB 226 843)A08

EERC 73-16 "QUAD-4: A Computer Program for Evaluating the Seismic Response of Soil Structures by Variable Damping Finite Element Procedures," by I.M. Idriss, J. Lysmer, R. Hwang and H.B. Seed - 1973 (PB 229 424)A05

EERC 73-17 "Dynamic Behavior of a Multi-Story Pyramid Shaped Building," by R.M. Stephen, J.P. Hollings and J.G. Bouwkamp - 1973 (PB 240 718)A06

EERC 73-18 "Effect of Different Types of Reinforcing on Seismic Behavior of Short Concrete Columns," by V.V. Bertero, J. Hollings, O. Küstü, R.M. Stephen and J.G. Bouwkamp - 1973

EERC 73-19 "Olive View Medical Center Materials Studies, Phase I," by B. Bresler and V.V. Bertero - 1973 (PB 235 986)A06

EERC 73-20 "Linear and Nonlinear Seismic Analysis Computer Programs for Long Multiple-Span Highway Bridges," by W.S. Tseng and J. Penzien - 1973

EERC 73-21 "Constitutive Models for Cyclic Plastic Deformation of Engineering Materials," by J.M. Kelly and P.P. Gillis 1973 (PB 226 024)A03

EERC 73-22 "DRAIN - 2D User's Guide," by G.H. Powell - 1973 (PB 227 016)A05

EERC 73-23 "Earthquake Engineering at Berkeley - 1973," (PB 226 033)A11

EERC 73-24 Unassigned

EERC 73-25 "Earthquake Response of Axisymmetric Tower Structures Surrounded by Water," by C.Y. Liaw and A.K. Chopra 1973 (AD 773 052)A09

EERC 73-26 "Investigation of the Failures of the Olive View Stairtowers During the San Fernando Earthquake and Their Implications on Seismic Design," by V.V. Bertero and R.G. Collins - 1973 (PB 235 106)A13

EERC 73-27 "Further Studies on Seismic Behavior of Steel Beam-Column Subassemblages," by V.V. Bertero, H. Krawinkler and E.P. Popov - 1973 (PB 234 172)A06

EERC 74-1 "Seismic Risk Analysis," by C.S. Oliveira - 1974 (PB 235 920)A06

EERC 74-2 "Settlement and Liquefaction of Sands Under Multi-Directional Shaking," by R. Pyke, C.K. Chan and H.B. Seed 1974

EERC 74-3 "Optimum Design of Earthquake Resistant Shear Buildings," by D. Ray, K.S. Pister and A.K. Chopra - 1974 (PB 231 172)A06

EERC 74-4 "LUSH - A Computer Program for Complex Response Analysis of Soil-Structure Systems," by J. Lysmer, T. Udaka, H.B. Seed and R. Hwang - 1974 (PB 236 796)A05

EERC 74-5 "Sensitivity Analysis for Hysteretic Dynamic Systems: Applications to Earthquake Engineering," by D. Ray 1974 (PB 233 213)A06

EERC 74-6 "Soil Structure Interaction Analyses for Evaluating Seismic Response," by H.B. Seed, J. Lysmer and R. Hwang 1974 (PB 236 519)A04

EERC 74-7 Unassigned

EERC 74-8 "Shaking Table Tests of a Steel Frame - A Progress Report," by R.W. Clough and D. Tang - 1974 (PB 240 869)A03

EERC 74-9 "Hysteretic Behavior of Reinforced Concrete Flexural Members with Special Web Reinforcement," by V.V. Bertero, E.P. Popov and T.Y. Wang - 1974 (PB 236 797)A07

EERC 74-10 "Applications of Reliability-Based, Global Cost Optimization to Design of Earthquake Resistant Structures," by E. Vitiello and K.S. Pister - 1974 (PB 237 231)A06

EERC 74-11 "Liquefaction of Gravelly Soils Under Cyclic Loading Conditions," by R.T. Wong, H.B. Seed and C.K. Chan 1974 (PB 242 042)A03

EERC 74-12 "Site-Dependent Spectra for Earthquake-Resistant Design," by H.B. Seed, C. Ugas and J. Lysmer - 1974 (PB 240 953)A03

EERC 74-13 "Earthquake Simulator Study of a Reinforced Concrete Frame," by P. Hidalgo and R.W. Clough - 1974 (PB 241 944)A13

EERC 74-14 "Nonlinear Earthquake Response of Concrete Gravity Dams," by N. Pal - 1974 (AD/A 006 583)A06

EERC 74-15 "Modeling and Identification in Nonlinear Structural Dynamics - I. One Degree of Freedom Models," by N. Distefano and A. Rath - 1974 (PB 241 548)A06

EERC 75-1 "Determination of Seismic Design Criteria for the Dumbarton Bridge Replacement Structure, Vol. I: Description, Theory and Analytical Modeling of Bridge and Parameters," by F. Baron and S.-H. Pang - 1975 (PB 259 407)A15

EERC 75-2 "Determination of Seismic Design Criteria for the Dumbarton Bridge Replacement Structure, Vol. II: Numerical Studies and Establishment of Seismic Design Criteria," by F. Baron and S.-H. Pang - 1975 (PB 259 408)A11 (For set of EERC 75-1 and 75-2 (PB 259 406))

EERC 75-3 "Seismic Risk Analysis for a Site and a Metropolitan Area," by C.S. Oliveira - 1975 (PB 248 134)A09

EERC 75-4 "Analytical Investigations of Seismic Response of Short, Single or Multiple-Span Highway Bridges," by M.-C. Chen and J. Penzien - 1975 (PB 241 454)A09

EERC 75-5 "An Evaluation of Some Methods for Predicting Seismic Behavior of Reinforced Concrete Buildings," by S.A. Mahin and V.V. Bertero - 1975 (PB 246 306)A16

EERC 75-6 "Earthquake Simulator Study of a Steel Frame Structure, Vol. I: Experimental Results," by R.W. Clough and D.T. Tang - 1975 (PB 243 981)A13

EERC 75-7 "Dynamic Properties of San Bernardino Intake Tower," by D. Rea, C.-Y. Liaw and A.K. Chopra - 1975 (AD/A008 406) A05

EERC 75-8 "Seismic Studies of the Articulation for the Dumbarton Bridge Replacement Structure, Vol. I: Description, Theory and Analytical Modeling of Bridge Components," by F. Baron and R.E. Hamati - 1975 (PB 251 539)A07

EERC 75-9 "Seismic Studies of the Articulation for the Dumbarton Bridge Replacement Structure, Vol. 2: Numerical Studies of Steel and Concrete Girder Alternates," by F. Baron and R.E. Hamati - 1975 (PB 251 540)A10

EERC 75-10 "Static and Dynamic Analysis of Nonlinear Structures," by D.P. Mondkar and G.H. Powell - 1975 (PB 242 434)A08

EERC 75-11 "Hysteretic Behavior of Steel Columns," by E.P. Popov, V.V. Bertero and S. Chandramouli - 1975 (PB 252 365)A11

EERC 75-12 "Earthquake Engineering Research Center Library Printed Catalog," - 1975 (PB 243 711)A26

EERC 75-13 "Three Dimensional Analysis of Building Systems (Extended Version)," by E.L. Wilson, J.P. Hollings and H.H. Dovey - 1975 (PB 243 989)A07

EERC 75-14 "Determination of Soil Liquefaction Characteristics by Large-Scale Laboratory Tests," by P. De Alba, C.K. Chan and H.B. Seed - 1975 (NUREG 0027)A08

EERC 75-15 "A Literature Survey - Compressive, Tensile, Bond and Shear Strength of Masonry," by R.L. Mayes and R.W. Clough - 1975 (PB 246 292)A10

EERC 75-16 "Hysteretic Behavior of Ductile Moment Resisting Reinforced Concrete Frame Components," by V.V. Bertero and E.P. Popov - 1975 (PB 246 388)A05

EERC 75-17 "Relationships Between Maximum Acceleration, Maximum Velocity, Distance from Source, Local Site Conditions for Moderately Strong Earthquakes," by H.B. Seed, R. Murarka, J. Lysmer and I.M. Idriss - 1975 (PB 248 172)A03

EERC 75-18 "The Effects of Method of Sample Preparation on the Cyclic Stress-Strain Behavior of Sands," by J. Mulilis, C.K. Chan and H.B. Seed - 1975 (Summarized in EERC 75-28)

EERC 75-19 "The Seismic Behavior of Critical Regions of Reinforced Concrete Components as Influenced by Moment, Shear and Axial Force," by M.B. Atalay and J. Penzien - 1975 (PB 258 842)A11

EERC 75-20 "Dynamic Properties of an Eleven Story Masonry Building," by R.M. Stephen, J.P. Hollings, J.G. Bouwkamp and D. Jurukovski - 1975 (PB 246 945)A04

EERC 75-21 "State-of-the-Art in Seismic Strength of Masonry - An Evaluation and Review," by R.L. Mayes and R.W. Clough 1975 (PB 249 040)A07

EERC 75-22 "Frequency Dependent Stiffness Matrices for Viscoelastic Half-Plane Foundations," by A.K. Chopra, P. Chakrabarti and G. Dasgupta - 1975 (PB 248 121)A07

EERC 75-23 "Hysteretic Behavior of Reinforced Concrete Framed Walls," by T.Y. Wong, V.V. Bertero and E.P. Popov - 1975

EERC 75-24 "Testing Facility for Subassemblages of Frame-Wall Structural Systems," by V.V. Bertero, E.P. Popov and T. Endo - 1975

EERC 75-25 "Influence of Seismic History on the Liquefaction Characteristics of Sands," by H.B. Seed, K. Mori and C.K. Chan - 1975 (Summarized in EERC 75-28)

EERC 75-26 "The Generation and Dissipation of Pore Water Pressures during Soil Liquefaction," by H.B. Seed, P.P. Martin and J. Lysmer - 1975 (PB 252 648)A03

EERC 75-27 "Identification of Research Needs for Improving Aseismic Design of Building Structures," by V.V. Bertero 1975 (PB 248 136)A05

EERC 75-28 "Evaluation of Soil Liquefaction Potential during Earthquakes," by H.B. Seed, I. Arango and C.K. Chan - 1975 (NUREG 0026)A13

EERC 75-29 "Representation of Irregular Stress Time Histories by Equivalent Uniform Stress Series in Liquefaction Analyses," by H.B. Seed, I.M. Idriss, F. Makdisi and N. Banerjee - 1975 (PB 252 635)A03

EERC 75-30 "FLUSH - A Computer Program for Approximate 3-D Analysis of Soil-Structure Interaction Problems," by J. Lysmer, T. Udaka, C.-F. Tsai and H.B. Seed - 1975 (PB 259 332)A07

EERC 75-31 "ALUSH - A Computer Program for Seismic Response Analysis of Axisymmetric Soil-Structure Systems," by E. Berger, J. Lysmer and H.B. Seed - 1975

EERC 75-32 "TRIP and TRAVEL - Computer Programs for Soil-Structure Interaction Analysis with Horizontally Travelling Waves," by T. Udaka, J. Lysmer and H.B. Seed - 1975

EERC 75-33 "Predicting the Performance of Structures in Regions of High Seismicity," by J. Penzien - 1975 (PB 248 130)A03

EERC 75-34 "Efficient Finite Element Analysis of Seismic Structure - Soil - Direction," by J. Lysmer, H.B. Seed, T. Udaka, R.N. Hwang and C.-F. Tsai - 1975 (PB 253 570)A03

EERC 75-35 "The Dynamic Behavior of a First Story Girder of a Three-Story Steel Frame Subjected to Earthquake Loading," by R.W. Clough and L.-Y. Li - 1975 (PB 248 841)A05

EERC 75-36 "Earthquake Simulator Study of a Steel Frame Structure, Volume II - Analytical Results," by D.T. Tang - 1975 (PB 252 926)A10

EERC 75-37 "ANSR-I General Purpose Computer Program for Analysis of Non-Linear Structural Response," by D.P. Mondkar and G.H. Powell - 1975 (PB 252 386)A08

EERC 75-38 "Nonlinear Response Spectra for Probabilistic Seismic Design and Damage Assessment of Reinforced Concrete Structures," by M. Murakami and J. Penzien - 1975 (PB 259 530)A05

EERC 75-39 "Study of a Method of Feasible Directions for Optimal Elastic Design of Frame Structures Subjected to Earthquake Loading," by N.D. Walker and K.S. Pister - 1975 (PB 257 781)A06

EERC 75-40 "An Alternative Representation of the Elastic-Viscoelastic Analogy," by G. Dasgupta and J.L. Sackman - 1975 (PB 252 173)A03

EERC 75-41 "Effect of Multi-Directional Shaking on Liquefaction of Sands," by H.B. Seed, R. Pyke and G.R. Martin - 1975 (PB 258 781)A03

EERC 76-1 "Strength and Ductility Evaluation of Existing Low-Rise Reinforced Concrete Buildings - Screening Method," by T. Okada and B. Bresler - 1976 (PB 257 906)A11

EERC 76-2 "Experimental and Analytical Studies on the Hysteretic Behavior of Reinforced Concrete Rectangular and T-Beams," by S.-Y.M. Ma, E.P. Popov and V.V. Bertero - 1976 (PB 260 843)A12

EERC 76-3 "Dynamic Behavior of a Multistory Triangular-Shaped Building," by J. Petrovski, R.M. Stephen, E. Gartenbaum and J.G. Bouwkamp - 1976

EERC 76-4 "Earthquake Induced Deformations of Earth Dams," by N. Serff and H.B. Seed - 1976

EERC 76-5 "Analysis and Design of Tube-Type Tall Building Structures," by H. de Clercq and G.H. Powell - 1976 (PB 252 220) A10

EERC 76-6 "Time and Frequency Domain Analysis of Three-Dimensional Ground Motions, San Fernando Earthquake," by T. Kubo and J. Penzien (PB 260 556)A11

EERC 76-7 "Expected Performance of Uniform Building Code Design Masonry Structures," by R.L. Mayes, Y. Omote, S.W. Chen and R.W. Clough - 1976

EERC 76-8 "Cyclic Shear Tests on Concrete Masonry Piers," Part I - Test Results," by R.L. Mayes, Y. Omote and R.W. Clough - 1976 (PB 264 424)A06

EERC 76-9 "A Substructure Method for Earthquake Analysis of Structure - Soil Interaction," by J.A. Gutierrez and A.K. Chopra - 1976 (PB 257 783)A08

EERC 76-10 "Stabilization of Potentially Liquefiable Sand Deposits using Gravel Drain Systems," by H.B. Seed and J.R. Booker - 1976 (PB 258 820)A04

EERC 76-11 "Influence of Design and Analysis Assumptions on Computed Inelastic Response of Moderately Tall Frames," by G.H. Powell and D.G. Row - 1976

EERC 76-12 "Sensitivity Analysis for Hysteretic Dynamic Systems: Theory and Applications," by D. Ray, K.S. Pister and E. Polak - 1976 (PB 262 859)A04

EERC 76-13 "Coupled Lateral Torsional Response of Buildings to Ground Shaking," by C.L. Kan and A.K. Chopra - 1976 (PB 257 907)A09

EERC 76-14 "Seismic Analyses of the Banco de America," by V.V. Bertero, S.A. Mahin and J.A. Hollings - 1976

EERC 76-15 "Reinforced Concrete Frame 2: Seismic Testing and Analytical Correlation," by R.W. Clough and J. Gidwani - 1976 (PB 261 323)A08

EERC 76-16 "Cyclic Shear Tests on Masonry Piers, Part II - Analysis of Test Results," by R.L. Mayes, Y. Omote and R.W. Clough - 1976

EERC 76-17 "Structural Steel Bracing Systems: Behavior Under Cyclic Loading," by E.P. Popov, K. Takanashi and C.W. Roeder - 1976 (PB 260 715)A05

EERC 76-18 "Experimental Model Studies on Seismic Response of High Curved Overcrossings," by D. Williams and W.G. Godden - 1976

EERC 76-19 "Effects of Non-Uniform Seismic Disturbances on the Dumbarton Bridge Replacement Structure," by F. Baron and R.E. Hamati - 1976

EERC 76-20 "Investigation of the Inelastic Characteristics of a Single Story Steel Structure Using System Identification and Shaking Table Experiments," by V.C. Matzen and H.D. McNiven - 1976 (PB 258 453)A07

EERC 76-21 "Capacity of Columns with Splice Imperfections," by E.P. Popov, R.M. Stephen and R. Philbrick - 1976 (PB 260 378)A04

EERC 76-22 "Response of the Olive View Hospital Main Building during the San Fernando Earthquake," by S. A. Mahin, R. Collins, A.K. Chopra and V.V. Bertero - 1976

EERC 76-23 "A Study on the Major Factors Influencing the Strength of Masonry Prisms," by N.M. Mostaghel, R.L. Mayes, R. W. Clough and S.W. Chen - 1976

EERC 76-24 "GADFLEA - A Computer Program for the Analysis of Pore Pressure Generation and Dissipation during Cyclic or Earthquake Loading," by J.R. Booker, M.S. Rahman and H.B. Seed - 1976 (PB 263 947)A04

EERC 76-25 "Rehabilitation of an Existing Building: A Case Study," by B. Bresler and J. Axley - 1976

EERC 76-26 "Correlative Investigations on Theoretical and Experimental Dynamic Behavior of a Model Bridge Structure," by K. Kawashima and J. Penzien - 1976 (PB 263 388)A11

EERC 76-27 "Earthquake Response of Coupled Shear Wall Buildings," by T. Srichatrapimuk - 1976 (PB 265 157)A07

EERC 76-28 "Tensile Capacity of Partial Penetration Welds," by E.P. Popov and R.M. Stephen - 1976 (PB 262 899)A03

EERC 76-29 "Analysis and Design of Numerical Integration Methods in Structural Dynamics," by H.M. Hilber - 1976 (PB 264 410)A06

EERC 76-30 "Contribution of a Floor System to the Dynamic Characteristics of Reinforced Concrete Buildings," by L.J. Edgar and V.V. Bertero - 1976

EERC 76-31 "The Effects of Seismic Disturbances on the Golden Gate Bridge," by F. Baron, M. Arikan and R.E. Hamati - 1976

EERC 76-32 "Infilled Frames in Earthquake Resistant Construction," by R.E. Klingner and V.V. Bertero - 1976 (PB 265 892)A13

UCB/EERC-77/01 "PLUSH - A Computer Program for Probabilistic Finite Element Analysis of Seismic Soil-Structure Interaction," by M.P. Romo Organista, J. Lysmer and H.B. Seed - 1977

UCB/EERC-77/02 "Soil Structure Interaction Effects at the Humboldt Bay Power Plant in the Ferndale Earthquake of June 7, 1975," by J.E. Valera, H.B. Seed, C.F. Tsai and J. Lysmer - 1975

UCB/EERC-77/03 "Influence of Sample Disturbance on Sand Response to Cyclic Loading," by K. Mori, H.B. Seed and C.K. Chan - 1977 (PB 267 352)A04

UCB/EERC-77/04 "Seismological Studies of Strong Motion Records," by J. Shoja-Taheri - 1977 (PB 269 655)A10

UCB/EERC-77/05 "Testing Facility for Coupled-Shear Walls," by L. Li-Hyung, V.V. Bertero and E.P. Popov - 1977

UCB/EERC-77/06 "Developing Methodologies for Evaluating the Earthquake Safety of Existing Buildings," No. 1 - B. Bresler; No. 2 - B. Bresler, T. Okada and D. Zisling; No. 3 - T. Okada and B. Bresler; No. 4 - V.V. Bertero and B. Bresler - 1977 (PB 267 354)A08

UCB/EERC-77/07 "A Literature Survey - Transverse Strength of Masonry Walls," by Y. Omote, R.L. Mayes, S.W. Chen and R.W. Clough 1977

UCB/EERC-77/08 "DRAIN-TABS: A Computer Program for Inelastic Earthquake Response of Three Dimensional Buildings," by R. Guendelman-Israel and G.H. Powell - 1977

UCB/EERC-77/09 "SUBWALL: A Special Purpose Finite Element Computer Program for Practical Elastic Analysis and Design of Structural Walls with Substructure Option," by D.Q. Le, H. Peterson and E.P. Popov - 1977

UCB/EERC-77/10 "Experimental Evaluation of Seismic Design Methods for Broad Cylindrical Tanks," by D.P. Clough - 1977

UCB/EERC-77/11 "Earthquake Engineering Research at Berkeley - 1976," - 1977

UCB/EERC-77/12 "Automated Design of Earthquake Resistant Multistory Steel Building Frames," by N.D. Walker, Jr. - 1977

UCB/EERC-77/13 "Concrete Confined by Rectangular Hoops Subjected to Axial Loads," by D. Zallnas, V.V. Bertero and E.P. Popov - 1977

UCB/EERC-77/14 "Seismic Strain Induced in the Ground During Earthquakes," by Y. Sugimura - 1977

UCB/EERC-77/15 "Bond Deterioration under Generalized Loading," by V.V. Bertero, E.P. Popov and S. Viwathanatepa - 1977

UCB/EERC-77/16 "Computer Aided Optimum Design of Ductile Reinforced Concrete Moment Resisting Frames," by S.W. Zagajeski and V.V. Bertero - 1977

UCB/EERC-77/17 "Earthquake Simulation Testing of a Stepping Frame with Energy-Absorbing Devices," by J.M. Kelly and D.F. Tsztoo 1977

UCB/EERC-77/18 "Inelastic Behavior of Eccentrically Braced Steel Frames under Cyclic Loadings," by C.W. Roeder and E.P. Popov 1977

UCB/EERC-77/19 "A Simplified Procedure for Estimating Earthquake-Induced Deformations in Dams and Inbankments, by F.I. Makdisi and H.B. Seed - 1977

UCB/EERC-77/20 "The Performance of Earth Dams during Earthquakes," by H.B. Seed, F. I. Makdisi and P. de Alba - 1977

UCB/EERC-77/21 "Dynamic Plastic Analysis Using Stress Resultant Finite Element Formulation," by P. Lukkunapvasit and J.M. Kelly 1977

UCB/EERC-77/22 "Preliminary Experimental Study of Seismic Uplift of a Steel Frame," by R.W. Clough and A.A. Huckelbridge - 1977

UCB/EERC-77/23 "Earthquake Simulator Tests of a Nine-Story Steel Frame with Columns Allowed to Uplift," by A.A. Huckelbridge - 1977

UCB/EERC-77/24 "Nonlinear Soil-Structure Interaction of Skew Highway Bridges," by M.-C. Chen and Joseph Penzien - 1977

UCB/EERC-77/25 "Seismic Analysis of an Offshore Structure Supported on Pile Foundations," by D.D.-N. Liou - 1977

UCB/EERC-77/26 "Dynamic Stiffness Matrices for Homogeneous Viscoelastic Half-Planes," by G. Dasgupta and A.K. Chopra - 1977

UCB/EERC-77/27 "A Practical Soft Story Earthquake Isolation System," by J.M. Kelly and J.M. Eidinger - 1977

UCB/EERC-77/28 "Seismic Safety of Existing Buildings and Incentives for Hazard Mitigation in San Francisco: An Exploratory Study," by A.J. Meltsner - 1977

UCB/EERC-77/29 "Dynamic Analysis of Electrohydraulic Shaking Tables," by D. Rea, S. Abedi-Hayati and Y. Takahashi - 1977

UCB/EERC-77/30 "An Approach for Improving Seismic-Resistant Behavior of Reinforced Concrete Interior Joints," by B. Galunic, V.V. Bertero and E.P. Popov - 1977

UCB/EERC-78/01 "The Development of Energy-Absorbing Devices for Aseismic Base Isolation Systems," by J. M. Kelly and D.F. Tsztoo - 1978

UCB/EERC-78/02 "Effect of Tensile Prestrain on the Cyclic Response of Structural Steel Connections," by J.G. Bouwkamp and A. Mukhopadhyay - 1978

UCB/EERC-78/03 "Experimental Results of an Earthquake Isolation System using Natural Rubber Bearings," by J.M. Eidinger and J.M. Kelly - 1978

UCB/EERC-78/04 "Seismic Behavior of Tall Liquid Storage Tanks," by A. Niwa - 1978

UCB/EERC-78/05 "Hysteretic Behavior of Reinforced Concrete Columns Subjected to High Axial and Cyclic Shear Forces," by S.W. Zagajeski, V.V. Bertero and J.G. Bouwkamp - 1978

UCB/EERC-78/06 "Inelastic Beam-Column Elements for the ANSR-I Program," by A. Riahi, D.G. Row and G.H. Powell - 1978

UCB/EERC-78/07 "Studies of Structural Response to Earthquake Ground Motion," by O. A. Lopez and A.K. Chopra - 1978

UCB/EERC-78/08 "A Laboratory Study of the Fluid-Structure Interaction of Submerged Tanks and Caissons in Earthquakes," by R.C. Byrd - 1978

UCB/EERC-78/09 "Models for Evaluating Damageability of Structures," by I. Sakamoto and B. Bresler - 1978

UCB/EERC-78/10 "Seismic Performance of Secondary Structural Elements," by I. Sakamoto - 1978

UCB/EERC-78/11 Case Study--Seismic Safety Evaluation of a Reinforced Concrete School Building," by J.Axley and B. Bresler - 1978

UCB/EERC-78/12 "Potential Damageability in Existing Buildings," by T. Blejwas and B. Bresler - 1978

UCB/EERC-78/13 "Dynamic Behavior of a Pedestal Base Multistory Building," by R. M. Stephen, E. L. Wilson, J.G. Bouwkamp and M. Button - 1978

UCB/EERC-78/14 "Seismic Response of Bridges - Case Studies," by R.A. Imbsen, V. Nutt and J. Penzien - 1978

UCB/EERC-78/15 "A Substructure Technique for Nonlinear Static and Dynamic Analysis," by D.G. Row and G.H. Powell - 1978

UCB/EERC-78/16 "Seismic Performance of Nonstructural and Secondary Structural Elements," by Isao Sakamoto - 1978

UCB/EERC-78/17 "Model for Evaluating Damageability of Structures," by Isao Sakamoto and B. Bresler - 1978

UCB/EERC-78/18 "Response of K-Braced Steel Frame Models to Lateral Loads," by J. G. Bouwkamp, R. M. Stephen and E. P. Popov - 1978

UCB/EERC-78/19 "Rational Design Methods for Light Equipment in Structures Subjected to Ground Motion," by J. L. Sackman and J. M. Kelly - 1978

UCB/EERC-78/20 "Testing of a Wind Restraint for Aseismic Base Isolation," by J. M. Kelly and D. E. Chitty - 1978

UCB/EERC-78/21 "APOLLO: A Computer Program for the Analysis of Pore Pressure Generation and Dissipation in Horizontal Sand Layers During Cyclic or Earthquake Loading," by Philippe P. Martin and H. Bolton Seed - 1978

UCB/EERC-78/22 "Optimal Design of an Earthquake Isolation System," by M. A. Bhatti, K. S. Pister and E. Polak - 1978

UCB/EERC-78/23 "MASH: A Computer Program for the Non-Linear Analysis of Vertically Propagating Shear Waves in Horizontally Layered Deposits," by Philippe P. Martin and H. Bolton Seed - 1978